

Optimization of long-term quarry production planning to supply raw
materials for cement plants

To the Faculty of Geosciences, Geoengineering and Mining
of the Technische Universität Bergakademie Freiberg
approved

THESIS

to attain the academic degree of
Doctor of Engineering
(Dr.-Ing)

Submitted

by M.Sc. Dinh Trong Vu

born on the 02.06.1986 in Quang Ninh, Vietnam

Reviewers: Prof. Dr. Carsten Drebenstedt (TU Bergakademie Freiberg)
Prof. Dr. Xuan Nam Bui (Hanoi University of Mining and Geology)
Prof. Dr. Peter Moser (Montanuniversität Leoben)

Date of the award: 21.12.2021

Declaration

I hereby declare that I completed this work without any improper help from a third party and without using any aids other than those cited. All ideas derived directly or indirectly from other sources are identified as such.

In the selection and in the use of materials, and in the writing of the manuscript, I received support from the following persons:

Prof. Dr. Carsten Drebenstedt

Persons other than those above did not contribute to the writing of this thesis. I did not seek the help of a professional doctorate-consultant. Only persons identified as having done so received any financial payment from me for any work done for me.

This thesis has not previously been submitted to another examination authority in the same or similar form in Germany or abroad.

Signature:

Date:

To my parents, my wife Khanh Luan, my two little boys Duc&Hieu
for their love, support and patience

Acknowledgements

I would like to express my very great appreciation to Prof. Dr Carsten Drebenstedt, my research supervisor, for his valuable and constructive suggestions and guidance during the planning and development of this thesis.

I would also like to thank my colleagues in Vietnam and Germany for their help in collecting data and discussions for this research.

My grateful thanks are also extended to the following organizations for funding this research:

- Vietnam International Education Development (VIED)
- Quang Ninh University of Industry, Vietnam
- DAAD STIBET-Doktoranden program, Germany

As the world faces a global pandemic, I wish to thank the doctors, nurses, medical personnel teams and all healthcare heroes who are on the frontline of the war against Covid-19.

Finally, I wish to thank my lovely family for their support and encouragement throughout my study.

Publications during candidature

1. Vu T, Bao T, Drebenstedt C, Pham H, Nguyen H, Nguyen D. Optimisation of long-term quarry production scheduling under geological uncertainty to supply raw materials to a cement plant. *Mining Technology*. 2021 Mar 4:1-3. <https://doi.org/10.1080/25726668.2021.1894398>
2. Vu T, Drebenstedt C, Bao T. Assessing geological uncertainty of a cement raw material deposit, southern Vietnam, based on hierarchical simulation. *International Journal of Mining Science and Technology*. 2020 Nov 1;30(6):819-37. <https://doi.org/10.1016/j.ijmst.2020.05.022>
3. Bao TD, Thang HH, Vu T. An Introduction of New Simulation and Optimization Software Application for Long-Term Limestone Quarry Production Planning. *Inżynieria Mineralna*. 2020.
4. Tran BD, Vu TD, Pham VV, Nguyen TA, Nguyen AD, Le GH. Developing a mathematical model to optimize long-term quarrying planning for limestone quarries producing cement in Vietnam. *Journal of Mining and Earth Sciences*. 2020;61(5):58-70.
5. Vu T, Drebenstedt C. Optimization model for long-term cement quarry production scheduling. In *Scientific and Practical Studies of Raw Material Issues*. 2019 Nov 7:219. ISBN: 978-0-367-86153-7
6. Trong Vu, Drebenstedt C. (2018), Selection of quality estimation methods for cement limestone deposits. In: *Scientific reports on Resource Issues*, TU Bergakademie Freiberg, ISSN 2190-555X
7. Vu T, Bao TD, Fomin SI. Ordinary kriging comparison and inverse distance weighting for quality assessment of Vietnam cement limestone deposits. *International Multidisciplinary Scientific GeoConference: SGEM*. 2017;17:61-8. DOI:10.5593/sgem2017H/63

Abstract

The success of a cement production project depends on the raw material supply. Long-term quarry production planning (LTQPP) is essential to maintain the supply to the cement plant. The quarry manager usually attempts to fulfil the complicated calculations, ensuring a consistent supply of raw materials to the cement plant while guaranteeing technical and operational parameters in mining. Modern quarry management relies on block models and mathematical algorithms integrated into the software to optimize the LTQPP. However, this method is potentially sensitive to geological uncertainty in resource estimation, resulting in the deviation of the supply production of raw materials. More importantly, quarry managers lack the means to deal with these requirements of LTQPP.

This research develops a stochastic optimization framework based on the combination of geostatistical simulation, clustering, and optimization techniques to optimize the LTQPP. In this framework, geostatistical simulation techniques aim to model the quarry deposit while capturing the geological uncertainty in resource estimation. The clustering techniques are to aggregate blocks into selective mining cuts that reduce the optimization problem size and generate solutions in a practical timeframe. Optimization techniques were deployed to develop a new mathematical model to minimize the cost of producing the raw mix for the cement plant and mitigate the impact of geological uncertainty on the raw material supply. Matlab programming platform was chosen for implementing the clustering and optimization techniques and creating the software application.

A case study of a limestone deposit in Southern Vietnam was carried out to verify the proposed framework and optimization models. Geostatistical simulation is applied to capture and transfer geological uncertainty into the optimization process. The optimization model size decreases significantly using the block clustering techniques and allowing generate solutions in a reasonable timeframe on ordinary computers. By considering mining and blending simultaneously, the optimization model minimizes the additive purchases to meet blending requirements and the amount of material sent to the waste dump. The experiments are also compared with the traditional optimization

framework currently used for the deposit. The comparisons show a higher chance of ensuring a consistent supply of raw materials to the cement plant with a lower cost in the proposed framework. These results proved that the proposed framework provides a powerful tool for planners to optimize the LTQPP while securing the raw material supply in cement operations under geological uncertainty.

Table of contents

Title page.....	i
Declaration	ii
Acknowledgements	i
Publications during candidature.....	ii
Abstract	iii
Table of contents	v
List of figures	viii
List of tables	xi
List of abbreviations.....	xii
Chapter 1 . Introduction	1
1.1 Background	1
1.2 Statement of the problem	2
1.3 Research aims and objectives.....	3
1.4 Scope of research.....	4
1.5 Research methodology	4
1.6 Significance of the research.....	5
1.7 Organization of thesis.....	6
Chapter 2 . Literature review	8
2.1 Introduction	8
2.2 Cement raw materials.....	8
2.3 Cement production process	8
2.3.1 Raw material recovery.....	9
2.3.2 Raw material processing.....	10
2.4 Impact of raw materials on the cement production process	12
2.5 Quarry planning and optimization.....	13
2.6 Long-term production planning (LTPP) problem	14
2.6.1 Deterministic approaches to solve the LTPP problem.....	15
2.6.2 Stochastic approaches for solving the LTPP problem.....	21
2.7 Conclusion.....	26

Chapter 3 . A stochastic optimization framework for LTQPP problem	28
3.1 Introduction	28
3.2 Deposit simulation.....	29
3.2.1 Simulating the rock type domains using SIS	30
3.2.2 Simulating the chemical grades within each domain conditionally to rock type domains, using SGS.....	30
3.3 Block clustering.....	31
3.4 The mathematical formulation for the LTQPP problem	32
3.4.1 Notation	34
3.4.2 Mathematical formulation.....	36
3.5 Numerical modelling.....	39
3.5.1 Clustering.....	39
3.5.2 SMIP formulation	41
3.6 Conclusion.....	47
Chapter 4 . Hierarchical simulation of cement raw material deposit.....	49
4.1 Introduction	49
4.2 Research area.....	50
4.2.1 General description	50
4.2.2. Data set	50
4.3. Application of hierarchical simulation	53
4.3.1 Rock-type simulation.....	53
4.3.2 Grade simulation.....	60
4.4. Discussion	73
4.5. Conclusion.....	76
Chapter 5 . Application of the stochastic optimization framework	77
5.1 Introduction	77
5.2 Implementation of KHRA	77
5.3 Implementation of the SMIP model	78
5.3.1 Sensitivity of the penalty cost.....	80
5.3.2 The effectiveness of the SMIP model.....	82
5.4 Risk mitigation	85

5.5 Conclusion.....	87
Chapter 6 . Conclusions and future works	89
6.1 Conclusions	89
6.2 Future works.....	91
References	93
Appendix I. Software Application	100
A.I.1 Introduction	100
A.I.2 Input preparation	101
A.I.2.1 Format of block model input	101
A.I.2.2 Import block model input	102
A.I.2.2 Cost assignment.....	104
A.I.2.3 Size reduction	107
A.I.3 Optimization.....	110
A.I.3.1 Destination.....	110
A.I.3.2 Production capacity	111
A.I.3.3 Additive purchase.....	111
A.I.3.4 Pit slopes.....	111
A.I.3.5 Optimization	112
A.I.4 Visualization of optimization results	112

List of figures

Figure 2.1 General cement manufacturing process.....	9
Figure 2.2 Cost for correcting or mitigating quality deviations at different stages of cement production between quarry and market [10].....	12
Figure 2.3 An example of a 3D block model	15
Figure 3.1 Three stages of the proposed risk-based framework for the LTQP problem .	29
Figure 3.2 Determination of block precedence using slope angle and block coordinates	45
Figure 4.1 Locations of the research area and exploratory drill holes	50
Figure 4.2 A perspective view showing the composites of rock-type composites in the research area.....	51
Figure 4.3 A perspective view showing composites of CaO, SiO ₂ , Al ₂ O ₃ , Fe ₂ O ₃ , MgO, and LOI grades in the research area.....	51
Figure 4.4 Histogram of the six chemical grades.....	52
Figure 4.5 Rock-type proportion along the upward direction (right); Example of reproduced trend (right) of rock-type domains on a realization	53
Figure 4.6 Variogram maps of Soil (a), Clay (b), Laterite (c), and Limestone (d). The red lines show the direction of maximum continuity in composited rock-type data	54
Figure 4.7 Experimental variograms and their suitable models of limestone in the horizontal and vertical directions.....	55
Figure 4.8 Perspective view (left), cross-section (easting = 548110 m) (middle), and horizontal section (elevation= 32.2 m) (right) of rock-type realization #1	57
Figure 4.9 Probabilities of occurrence of four rock types, obtained from a set of 20 conditional realizations on 3D block model (left), cross-section (easting = 548110 m) (middle), and horizontal section (elevation= 32.2 m) (right).....	58
Figure 4.10 Comparison of histograms of rock types between composited data (left) and Realization #1 (right)	59
Figure 4.11 Reproduced variograms of four rock types	60
Figure 4.12 Variogram maps of the six chemical grades within domain 1. The red lines show the direction of maximum continuity in composited grade data	62

Figure 4.13 Variogram maps of the six chemical grades within domain 2. The red lines show the direction of maximum continuity in composited grade data	63
Figure 4.14 Experimental variograms and their fitting models of the six chemical grades in the horizontal plane within domain 1.....	66
Figure 4.15 Experimental variograms and their fitting models of the six chemical grades in the horizontal plane within domain 2.....	67
Figure 4.16 Example of the spatial distribution of SiO ₂ , CaO, Al ₂ O ₃ , Fe ₂ O ₃ and MgO grades generated on rock-type realization #1 on 3D block model (left), cross-section (easting = 548110 m) (middle), and horizontal section (elevation= 32.2 m) (right)	68
Figure 4.17 Variogram reproduction in the main direction of the six chemical grades within Domain 1 and Domain 2	69
Figure 4.18 Histogram reproductions of the six chemical grades in Domain 1.....	70
Figure 4.19 Histogram reproductions of the six chemical grades in Domain 2.....	71
Figure 4.20 Q-Q plot of the six simulated grades versus their declustered data in Domain 1 and 2	72
Figure 4.21 Perspective view (left), cross-section (easting = 548110 m) (middle), and horizontal section (elevation= 32.2 m) (right) of the expected CaO grade (calculated by averaging the 20 realizations of chemical grades), obtained without rock-type modeling (a, b, c), with deterministic rock-type modeling (d, e, f), and stochastic rock-type modeling (g, h, k).....	74
Figure 4.22 Box plot of the limestone tonnage above CaO cut-off of 36%, calculated over 20 realizations using stochastic, and deterministic rock-type modelling approaches	75
Figure 5.1 Clustering scheme on bench +32.2 m.....	78
Figure 5.2 Three-dimensional plan view (a), cross-section looking North (b) and West (c) generated by SMIP model	82
Figure 5.3 Expected composition of the raw mix suggested by SMIP model	83
Figure 5.4 Deviations from quarry (left) and raw mix (right) production targets generated by the SMIP model.....	83
Figure 5.5 Deviations of waste dump production, additive purchases, and raw mix quality targets suggested by the SMIP model.....	84

Figure 5.6 Deviations from quarry (left) and raw mix (right) production targets generated by the DMIP mode	85
Figure 5.7 Deviations of waste dump production, additive purchases, and raw mix quality targets suggested by the DMIP model	86
Figure 5.8 Cumulative raw material supply and cost per ton comparison between SMIP and DMIP model.....	87
Figure A.0.1 The workflow of the developed software	100
Figure A.0.2 Three main menus of the developed software (<i>a – Input; b – Optimization; c – Visualization</i>)	101
Figure A.0.3 Example of block model input.....	102
Figure A.0.4 Import block model menu.....	103
Figure A.0.5 An example of visualization of the block model input.....	104
Figure A.0.6 Import from block model file.....	104
Figure A.0.7 An example of mining cost import using MCAF by a range function	105
Figure A.0.8 An example of using the line of best fit with the equation.....	106
Figure A.0.9 An example of mining cost import using MCAF by a range equation.....	106
Figure A.0.10 An example of mining cost import using rock type and elevation	107
Figure A.0.11 An example of the definition of block sizes using the reblocking technique	107
Figure A.0.12 Block clustering menu	108
Figure A.0.13 An example of visualization of a clustering scheme	109
Figure A.0.14 Definition of destinations.....	110
Figure A.0.15 Production capacity set up	111
Figure A.0.16 An example of additive purchase input	111
Figure A.0.17 Pit slope input	112
Figure A.0.18 Optimization input parameters.....	112
Figure A.0.19 Numerical results of optimization results recorded in an Excel file.....	113
Figure A.0.20 Example of 3D quarry extraction schedule	113
Figure A.0.21 Example of a 3D quarry extraction schedule on a cross-section	113
Figure A.0.22 An example of ultimate topography after finishing all mining periods..	114
Figure A.0.23 Deviations of the quarry production target along with their probability	114

List of tables

Table 2.1 The raw materials for Portland cement manufacture	8
Table 2.2 Limiting values of the chemical compositions of cement raw material	10
Table 2.3 The differences in production planning problem between metal mining and cement raw material mining.....	14
Table 3.1 Pseudo code of KHRA.....	32
Table 4.1 Relationships between the rock-type domains and average grades	53
Table 4.2 Indicator variogram parameters for each rock type	56
Table 4.3 Mean value of chemical grades before and after declustering.....	61
Table 4.4 Fitting parameters of variogram models for each Gaussian grades in domain 1	64
Table 4.5 Fitting parameters of variogram models for each Gaussian grades in domain 1	65
Table 5.1 Clustering input parameters	77
Table 5.2 The sensitivity of the clustering schemes	78
Table 5.3 Quality and cost of purchased additive materials	79
Table 5.4 Production target parameters	79
Table 5.5 Summary of four different SMIP schedules with different <i>low_dr</i>	81
Table 5.6 Summary of expected production and quality of the raw mix in each period ..	82
Table A.I.1 An example of mining cost and MCAF distribution	105

List of abbreviations

CaO	Lime or calcium oxide
SiO ₂	Silica
Al ₂ O ₃	Alumina
Fe ₂ O ₃	Iron oxide
MgO	Magnesium oxide
LOI	Loss on ignition
SR	Silica ratio
AM	Alumina ratio
LSF	Lime saturation factor
LTPP	Long-term production planning
LTQPP	Long-term quarry production planning
CAD	Computer-aided design
IP	Integer programming
LP	Linear programming
MIP	Mixed-integer linear programming
SIP	Stochastic integer programming
SMIP	Stochastic mixed-integer programming
DMIP	Deterministic mixed-integer programming
2D	Two dimensional
3D	Three dimensional
SIS	Sequential indicator simulation
SGS	Sequential gaussian simulation
AHCA	Agglomerative hierarchical clustering algorithm
KHRA	K-means and hierarchical realization aggregation
LVM	Locally variance mean
Eq	Equation
t	Ton unit
Mt	Million ton

Chapter 1. Introduction

1.1 Background

Cement is used worldwide as an essential binding agent in concrete. Cement is manufactured by blending different raw materials and burning them at a high temperature to achieve the desired chemical proportions of four principal oxides: lime or calcium oxide (CaO), silica (SiO_2), alumina (Al_2O_3), and iron oxide (Fe_2O_3) in the finished product, known as cement clinker. Cement manufacturing uses high calcium limestone (or its calcareous raw materials) to meet the calcium requirement and clay, mudstone, or shale for silica and alumina. Generally, cement production includes several subsequent processes. These consist of quarry raw material extraction, raw material blending and burning processes, cement clinker grinding process, and packaging process. As an initial process, quarry extraction contributes directly to the quality and production of cement clinker. Proper management at the quarry is the key to handling the raw material issue in cement production.

Controlling the raw material quality at the quarry is not an easy task. Quarry planners usually struggle with the calculations required to blend the chemical characteristics and mining parameters to maintain a consistent supply of raw materials. Additive materials such as high-grade limestone, bauxite, iron ore, and sand are often required to modify the raw mix quality. The calculations are frequently done on a spreadsheet or by trial and error procedure, resulting in high additive cost and increased product variability. These methods are locked into short-term practice and ignore global objectives. Therefore, mining intelligently raw material is crucial and an increasing issue in the cement industry.

Subsequent steps, including exploration, modelling, and planning, are employed to handle this modern cement raw material management issue. The exploration step generates necessary information for planning, such as grades, density, lithology, to integrate into 3D arrays of rectangular units called block model. Typically, each block is assigned attributes that are interpolated, usually from exploration drilling information by geostatistical estimation approaches. It should be noted that modelling is an uncertain process because it depends significantly on input data, applied estimation approach, and

sometimes modelling experts' experience. The block model is the input for the optimization and scheduling of the quarry production. There is much effortless focusing on developing algorithms and software applications to optimize mine planning in the mining industry. In mining metallic ores, mine planners must answer two questions about which blocks to remove and when to remove them to maximize the profit. Those questions could not be easy to answer globally because of the large size of the mathematical optimization problem in the real world, despite the advances in computer and software technology throughout many decades. The most common approach to the problem is decomposing it into three stages: the ultimate pit limit, pushback design to answer the first question (which), and production schedules to answer the second question (when). However, optimization techniques in open pit mine planning are still not widely used in mining cement raw materials, and the market of available applications and software for them is restricted.

1.2 Statement of the problem

This research aims to deal with three critical problems related to LTQPP, as follows:

- The objective of the LTQPP problem

Applications of operations research to mine planning have a long history, starting from the 1960s [1] when the first attempts were made using mathematical algorithms and computers based on block models. Since that time, many research works and software have been introduced and applied to various mine planning problems. However, the applications are primarily applicable to metallic ore mining, which have different optimization objectives and starting input than cement raw materials mining. While metal production planning is driving NPV, quarry planning drives the cost to maximize quarry lifetime to generate the highest possible return from the investment of the cement plant. Thus, the application of available software and algorithms in quarry planning for cement production is much more limited.

- Geological uncertainty in resource estimation

Optimization of the LTQPP problem is based on block models mainly constructed using geostatistical or estimation techniques. The estimation of a deposit is uncertain due to sparse geological data. If this propagates to production, it can lead to a severe of not meeting production expectations and project failures [2]–[4]. When the raw material

supply is at risk, cement operations traditionally deploy a range of tactics, including sourcing like purchasing additive materials from outside sources, changing input mixtures, and maintaining minimum long-term reserve levels. Thus, a new method that can cope directly with geological uncertainty is needed.

- The size of the LTQPP problem in optimization

One of the essential criteria to evaluate the success of operations research techniques in solving real-life mine planning problems is obtaining the solution within the practical timeframe. Since the optimization problem size with the original block model is often too large to be solved using conventional solvers, block aggregation or clustering techniques are traditional approaches for dealing with this challenge. However, either is integrated into a stochastic framework to consider geological uncertainty.

In response to these problems, this research focuses on developing a new solution specific to the LTQPP problem. A stochastic optimization framework is developed based on stochastic techniques, including simulation, clustering, and optimization, to address the above issues. The software application was also designed with a graphical interface and based on the developed framework to enable quarry managers and planners to produce an optimal quarry production plan.

1.3 Research aims and objectives

The aims of this research are twofold: First, developing a stochastic optimization framework to optimize LTQPP for consistent supply of raw materials to the cement plant; second, creating a software application as a tool to serve quarry manager to figure out the optimal quarry production plan: a plan that is reliable, feasible and meets all production requirements.

Based on the aims, the objectives of this research consist of:

- i. Analyze the entire cement raw material management process to provide a theoretical framework for developing the optimization process.
- ii. Review and compare the most remarkable deposit simulation and optimization techniques used in open pit mining production planning and quarry production planning to propose a practical simulation and optimization framework.
- iii. Examine geostatistical simulation application in a limestone deposit to produce a source of geological uncertainty for the optimization process.

iv. Examine the application of the block clustering technique in a limestone deposit to create selective mining cuts for the optimization process.

v. Develop a new Stochastic Mixed Integer Programming (SMIP) optimization model to address the LTQPP problem. The objective of the proposed model does minimize the cost of raw material supply and the deviation of production targets due to the uncertainty of geological data.

vi. Develop a computer code/numerical modelling and software as a tool to implement and verify the proposed framework and model on a practical case study.

1.4 Scope of research

This research focuses on applying geostatistical, clustering, and optimization techniques in mine planning to generate an optimal LTQPP. For short-term planning, where the optimization objective and constraints are the same, the research application can be available. The research applies a series of theories from resource estimation, Monte Carlo simulation, clustering, and mine production scheduling in terms of methodology.

The case study on the cement raw material extraction in Vietnam where the quarry uses waste dump and blending stockpile as destinations for raw materials after extracting from the quarry.

1.5 Research methodology

LTQPP plays a vital role in the cement manufacturing process. However, providing an optimal plan is never an easy task for mine planners due to the complexity of production and quality requirements, geological, financial uncertainty, et cetera. This research aims to develop a stochastic optimization framework for a software application as a solution tool for mine planners to provide an optimal LTQPP.

The first part of this research involved reviewing the cement production processes' literature, particularly quarry raw material extraction, deposit modelling and simulation techniques, mathematical programming, and their implementation on open pit and quarry production planning problems. Subsequently, a set of exploration drill hole data from a quarry in the south of Vietnam was analyzed using Matlab software [5] for modelling and deposit simulation. A series of equally probable models of the deposit were prepared using the hierarchical simulation method to capture the geological

uncertainty of the deposit. The hierarchical simulation method first applied Sequential Indicator Simulation (SIS) to simulate rock type distribution of the deposit. Then, it used Sequential Gaussian Simulation (SGS) to simulate the grade distribution of the deposit based on the generated rock-type layouts. Both tasks were implemented on the GSLIB software [6]. A stochastic optimization framework was developed in the forward steps using the hybrid clustering approach to reduce the size of the LTQPP problem and the SMIP model to generate the quarry extraction schedule. Matlab software [5] was used as the programming platform for both block clustering and SMIP optimization. CPLEX solver [7] was employed to solve the SMIP model. Finally, the proposed framework was integrated into a software application with a graphical user interface.

The proposed framework and mathematical model were implemented and verified on limestone deposit datasets to supply raw materials for a nearby cement plant. The experiments tested four capacities of the proposed framework, including (i) generating solution in a reasonable timeframe; (ii) consistent supply of raw materials to the cement plant at minimum cost; (iii) integrating geological uncertainty into quarry extraction schedules; (iv) mitigating the impact of geological uncertainty on the long-term supply of raw materials to the cement plant. The results were compared to the deterministic framework model to highlight the proposed framework and software's capacities. Furthermore, the sensitivity of some important optimization parameters was performed explicitly.

1.6 Significance of the research

In terms of scientific contribution, the research provides as follows:

i) A new optimization framework to integrate the LTQPP and cement manufacturing process. It can generate extraction plans that comply with the quality targets of the raw mix while minimizing additive purchase and maintaining mining parameters.

ii) A new SMIP model for the LTQPP problem to capture the geological uncertainty and simultaneously reduce the deviations of the production targets. The model quantifies the risk of a given schedule or chooses the schedules that operate well under geological uncertainty.

iii) A new method to solve large-scale production planning problem under the consideration of geological uncertainty. The solution time of the SMIP model decreases considerably, making it possible to integrate uncertainty factors or evaluate different scenarios.

In terms of industrial contribution, the research provides as follows:

i) An introduction of optimization framework and mathematical models into mining cement raw materials. Optimization techniques were used many years ago, and since then, most metallic ore mining has been applied to these techniques. This optimization framework and models highlight their applications to improve quarry extraction management in the cement manufacturing process.

ii) A software application as a digital tool assisting mine planners and managers in figuring out an optimal or feasible quarry production plan. The software supports the quarry managers at three different levels: i) understand the geological characteristics of the deposit; ii) understand the optimal feasible production plan; iii) simulate and access the risk of supplying raw materials to the cement plant; iv) have a tool to mitigate and control the geological risk.

1.7 Organization of thesis

Chapter 1 describes the general overview of the research, including background, problem statements, research aims and objectives, the scope of research, proposed methodology, and significance of the research.

Chapter 2 provides literature reviews related to this research. The review starts by looking into the cement manufacturing process and the impact of raw materials on it. The review discusses the past and recent developments in the optimization and scheduling algorithms used for open-pit mining and cement raw materials mining. Some methods used to solve the mine planning problems are reviewed as well.

Chapter 3 presents a stochastic optimization framework using geostatistical simulation, block clustering technique, and SMIP model. The numerical modelling for the clustering algorithms and models for software development are also presented in this chapter.

Chapter 4 discusses the application of hierarchical simulation for raw material deposits. A case study in a limestone deposit to prepare the input for the optimization process is the main content of this chapter.

Chapter 5 presents the application of the stochastic optimization framework in the limestone deposit in Chapter 4. Comparisons and discussions of the results are also presented here.

Chapter 6 concludes the research and recommends future works.

Chapter 2. Literature review

2.1 Introduction

This chapter first looks at the raw material quality management in the cement production process. It considers the cement manufacturing process and the impact of raw materials. Then, there will be discussions of past and recent developments in the optimization and scheduling algorithms used for open-pit mining and cement raw materials mining. Some methods used to solve the production planning and scheduling problems are reviewed as well.

2.2 Cement raw materials

The ideal raw materials for cement manufacture are rocks that contain suitable composition and proportions to produce cement clinker at the required quality. Also, they should be pure with uniform quality and available in abundance to supply and blend. In practice, these raw materials are exceedingly rare, and the blending of various raw materials is binding.

Generally, cement manufacturing's primary raw materials should contain CaO , SiO_2 , Al_2O_3 , and Fe_2O_3 and can be classified into two types of calcareous materials and argillaceous materials. Table 2.1 shows the classification of raw materials for Portland cement manufacture.

Table 2.1 The raw materials for Portland cement manufacture [8]

Calcareous material	Argillaceous material		
Calcium	Silicon	Aluminium	Iron
Limestone	Clay	Clay	Clay
Marl	Marl	Shale	Iron ore
Calcite	Sand	Fly ash	Mill scale
Aragonite	Shale	Aluminium ore refuse	Shale
Shale	Fly ash		Blast furnace dust
Seashells	Rice hull ash		
Cement kiln dust	Slag		

2.3 Cement production process

Generally, a simple layout of the cement production process consists of two significant steps: raw material recovery and raw material processing. The first step consists of

mining (quarrying) and crushing raw material. The second step consists of blending raw materials to develop an acceptable raw mix, burning the raw mix in a cement kiln to produce a new product: clinker, and grinding clinker to make the final cement product. Figure 2.1 describes a simple layout of the cement manufacturing process. The detailed processes are discussed below.

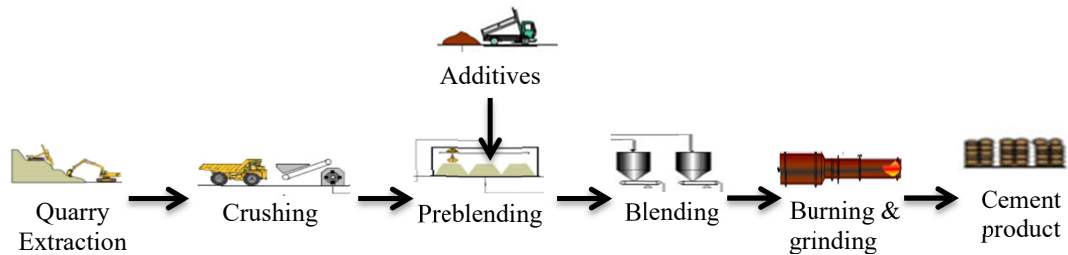


Figure 2.1 General cement manufacturing process

2.3.1 Raw material recovery

2.3.1.1 Quarrying

Raw materials for the cement industry are usually extracted by large-scale surface mining or quarrying operations. Quarries may operate with several million tons annually, depending on the required clinker capacity of cement plants. The conventional benching technique is the most widely used in quarries, in which the deposit is extracted in several benches. In some cases where the raw material deposits are located below the cement works level, the hillside quarrying technique is a more favourable technique in which gravity can move the materials to the haulage level after blasting.

A layer of overburden usually covers raw material deposits. Cleaning operations must excavate the overburden and transport it to the disposal area or storage if its chemical composition could fit the development of the raw mix. Introducing the overburden in the raw mix can reduce the stripping ratio in many quarries. However, the usage of overburden requires more investment in exploration as well as storage activity. Drilling and blasting are needed in limestone quarries to break up hard rock into acceptable sizes. In some quarries where the rock is soft, ripping can be replaced by drilling and blasting. The machines are used for loading in quarries are various, including cable-operated excavators, hydraulic excavators, wheel loaders, and crawler

loaders. Simultaneously, dump trucks and belt conveyors are the most common means to transport fragmented materials from the loading point to the crushing plant.

2.3.1.2 Crushing and sizing

Crushing and sizing in the cement manufacturing process aims to enhance the recovery of raw materials by reducing the raw material itself as quickly and economically as possible. In some cases, the goal of crushing and sizing is to consider the community environment where the use of explosives is limited by safety, noise, and vibration standards. Various types of crushing machines can be found in crushing areas. Typically, a primary crusher includes a screen to determine the crusher-run size and a secondary crusher to generate the final product that meets the mills' desired size.

2.3.2 Raw material processing

2.3.2.1 Pre-blending and milling

Pre-blending raw materials in the form of a raw mix stockpile play an essential role in maintaining a consistent supply of materials for cement production processing. It allows better recovery of inhomogeneous raw material deposits, pre-blending of various material components, and better uniformity of raw material to produce a consistent quality for cement products. The stockpile can be designed as longitudinal or circular beds. A blending bed may consist of two stockpiles in which one is to reclaim, and the other is to supply the grinding units. Table 2.2 presents the limiting values of the chemical composition of cement raw material (after ignition), which can help determine the quality requirements of raw mix.

Table 2.2 Limiting values of the chemical compositions of cement raw material [9]

Oxide	Limiting value (%)	Content (%)
CaO	58 - 69	65
SiO ₂	18 - 24	21
Al ₂ O ₃	4 - 8	6
Fe ₂ O ₃	1 - 8	3
MgO	< 5,0	2
K ₂ O, Na ₂ O	< 2,0	1
SO ₃	< 3,0	1

For practical purposes, the composition of oxides needs to be balanced using the indices of silica ratio (SR), lime saturation factor (LSF), and alumina ratio (AM). In industrial cement, SR, LSF, and AM are generally between 1 to 3, 0.845 to 1, 1 to 3, respectively [9]. They are expressed as follows [9]:

$$LSF = \frac{CaO}{2.8SiO_2 + 1.18Al_2O_3 + 0.65Fe_2O_3} \quad (2.1)$$

$$SR = \frac{SiO_2}{Al_2O_3 + Fe_2O_3} \quad (2.2)$$

$$AM = \frac{Al_2O_3}{Fe_2O_3} \quad (2.3)$$

The desired raw mix is then ground again using a ball mill or tube mill, or both to get fine particles. Now, these powdered materials are blended to adjust their compositions and kept ready for the burning process. Based on the mixing procedure, the cement production process can be divided into two methods:

- (i) The dry process refers to grinding raw materials and feeding them into the kiln in dry powder.
- (ii) The wet process refers to grinding raw materials and feeding them into the kiln in the form of a slurry.

2.3.2.2 Burning

The previous processes make the physical changes of raw materials, including size reduction and proper blending. The burning process conducts the chemical shifts of raw materials by heating them to a sintering temperature as high as 1450⁰C in a cement kiln. In this process, the raw materials' chemical proportions are broken down and recombined into new compounds called clinker. For instance, the Portland cement requires four compounds formed during the burning process, including tricalcium C₃S (3CaO.SiO₂), dicalcium silicate C₂S (2CaO.SiO₂), tricalcium aluminate C₃A (3CaO.Al₂O₃), and tetra calcium aluminoferrite C₄AF (4CaO. Al₂O₃. Fe₂O₃). The burning process is implemented in the rotary kiln, which often uses fuel such as coal, oil, natural gas, or wastes to burn the raw mill. Because the kiln's clinkers are very hot, the air is admitted to the kiln to cool down the temperature of clinkers.

2.3.2.3 Grinding of clinkers

The cooled clinkers are ground finely into powder using the ball mill or tube mill. Gypsum is commonly added during grinding to provide the desired setting time for concrete made with the finished cement. The ground cement is stored in silos, sampled, and verified by quality, from which it is marketed either in bags or container load.

2.4 Impact of raw materials on the cement production process

The success of cement plants depends much on the reliable supply of raw materials from quarry extraction. Failure to obtain the raw materials at an economical cost and desired quality may adversely impact cement product cost and quality. Raw material extraction is the first process in a series of connected processes in cement manufacturing. For that reason, the impact of raw material extraction at quarries can spread out the whole cement production process. For instance, insufficient and variable quality of raw materials at the raw mix blending process can require high electrical energy to homogenize the raw materials or a large amount of additive to correct the raw mix quality.

Figure 2.2 demonstrates the cost of remedying quality deviations at various stages of the cement production process. The latter the correction of quality deviations, the higher the cost is.

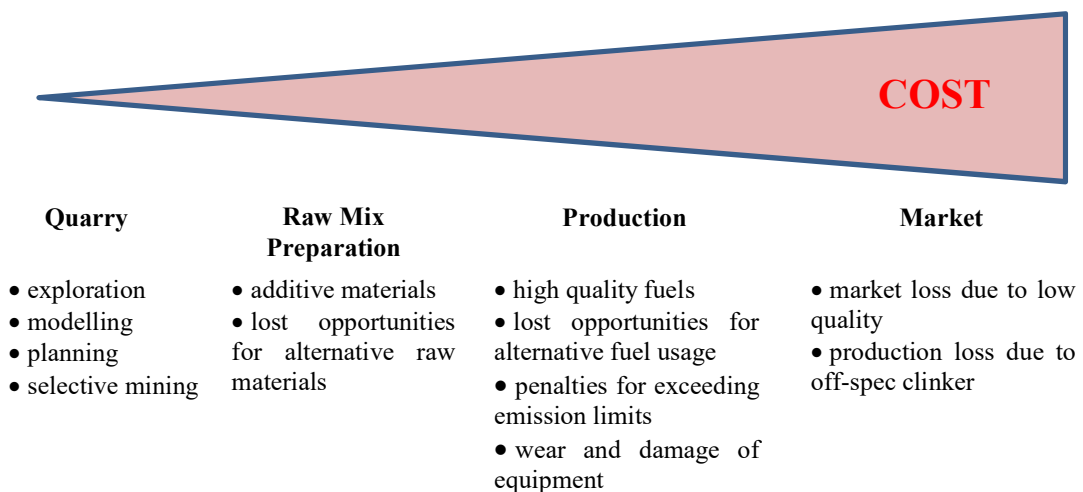


Figure 2.2 Cost for correcting or mitigating quality deviations at different stages of cement production between quarry and market [10]

Therefore, obtaining an acceptable quality of raw mix at the quarrying stage is the key to reducing cement manufacturing cost. Raw material accounts for 28% of the production cost of cement [11]. Production of one ton of cement requires approximately 1.6 tons of raw materials [12], [13]. Therefore, minimizing the cost of supplying raw material contributes significantly to the cost of the cement product.

2.5 Quarry planning and optimization

As analyzed above, quality management at the quarry is the key to ensuring the operation of a cement production project. Generally, it consists of three subsequent steps: exploration, modelling, and planning. The exploration step supplies data for the modelling step, possibly including core data available from a limited number of exploratory drill holes or sometimes from rig drilling. The modelling step employs the resulting data to conduct a geological model represented by 2D cross-sections or 3D block models. Based on the geological model, production planning and raw material blending can be implemented using manual or optimization methods. The manual method generates planning based on 2D cross-sections using trial and error or a spreadsheet calculation. Although this method can be supported by computer-aided design (CAD), it is human dependencies and unable to find an optimum solution for quarry production planning.

The optimization method can eliminate the disadvantages of the manual method. It uses geological block models, 3D arrays of rectangular cubes to formulate the quarry planning problem. With significant developments in operations research techniques in recent years, finding a feasible solution for the problem is not difficult. However, the optimization method in cement raw material mining is still much more limited than metal mining. Furthermore, the implementation of production planning for the mining of cement raw materials is different from metal mining. Table 2.3 summarizes the differences between them.

Table 2.3 The differences in production planning problem between metal mining and cement raw material mining

	Metal mining	Cement raw material mining
Block value	Determined based on the price of the metal	Unable to determine, depends on blending opportunities with other blocks and additive materials
Cut-off grade	Determined to classify ore and waste	Unable to determine
Optimization objective	Maximize net present value or discounted benefit, which means the highest grade mined first	Maximize the life of the quarry, which keeps a constant supply of raw materials as long as possible

These differences require the cement industry to develop a unique planning tool to address cement production requirements. The first software specialized for cement raw material mining is QSO Expert (Quarry Scheduling and Optimization), developed and used internally at Holderbank (now LafargeHolcim) in the 1980s. Several authors have been proposed approaches to the quarry planning problem. Rehman and Asad [14], [15] applied mixed-integer linear programming (MIP) to formulate the blending problem for an existing cement manufacturing operation in Pakistan. The blending model demonstrates its ability to generate an optimum schedule in cost savings compared to the manual schedule. For LTPP, Asad [16] presented the sequencing algorithm to find a set of solutions that satisfies block precedence and quarry production capacity constraints and then choose the best feasible solution ensuring the quality and quantity constraints of the cement manufacturing process. Joshi [17] also developed a long-term production planning model based on the block clustering method to assess quarry life. Both approaches can generate a feasible solution for LTQPP but do not ensure the optimality of the solution.

2.6 Long-term production planning (LTPP) problem

Mine planning is hierarchy works from long-term to short- term depending on the time range from several years to months. Amongst those types of production planning, the

LTPP is critical and determines the cash flow and the feasibility of the project and guides the medium and short-term planning. In practice, the number of blocks within a resource model is too large to solve the entire LTPP problem directly. Hence, the LTPP process consists of three consecutive stages: ultimate pit limit, pushback design, and production scheduling [18], [19]. At the first stage, the ultimate pit limit is evaluated to specify the deposit's minable part. The second stage decomposes the ultimate pit limit into smaller sequencing nested pits, namely pushbacks. Finally, a long-term production schedule is determined within pushbacks to decide which blocks should be mined in a particular production period. Recent research for solving the LTPP problems in literature has been developed along with two main areas: the deterministic and stochastic approaches [20].

2.6.1 Deterministic approaches to solve the LTPP problem

2.6.1.1 Deposit modelling

Standard input for LTPP problems is a block model that consists of a series or collection of cubes covering the entire reserve area. Each cube has specific attributes of quantity and quality characteristics assigned using available estimation techniques such as inverse distance weighted or Kriging. Figure 2.3 illustrates an example of the 3D block model. These estimation techniques use data collected from the exploratory drill holes or rig drilling and construct a single estimated ore body model.

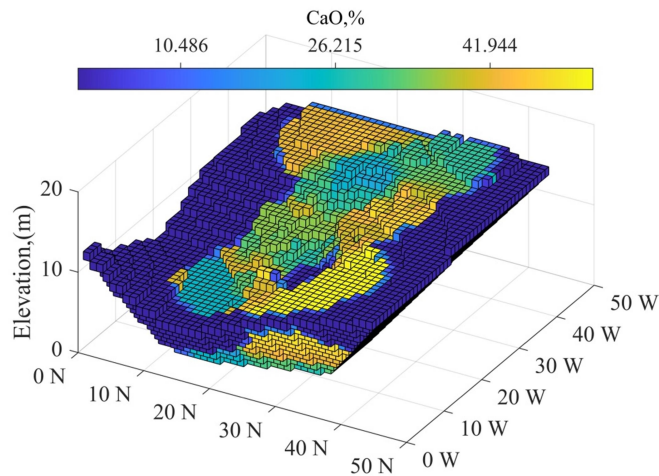


Figure 2.3 An example of a 3D block model

2.6.1.2 Ultimate pit limit problem

The ultimate pit limit problem aims to define the final pit contour so that the total profit when extracting this pit is maximum. Hochbaum and Chen [21] described this problem using an integer programming (IP) algorithm. The mathematical model of the algorithm can be represented as follows:

$$\text{Max} \quad \sum_{i \in N} V_i x_i \quad (2.4)$$

$$\text{Subject to:} \quad x_j - x_i \leq 0 \quad \forall i, j \in N \quad (2.5)$$

$$x_i \in \{0, 1\} \quad \forall i \in N \quad (2.6)$$

Where: V_i is the economic value of block i ; x_i is the binary value which equals *one* if the block being extracted and 0 otherwise.

The objective in Eq 2.4 is to maximize the undiscounted value of extracted blocks while satisfies the precedence constraint (Eq 2.5). Graph theory provides an effective way to solve this problem. First, it considers blocks as vertices associated with weights representing the block economic value and the sequencing relationship between two blocks as an arc. The Lerch-Grossmann algorithm can then be applied to maximize the objective (Eq.2.4) by finding the maximum closure of a given graph [22]. Many commercial software packages, such as Vulcan or Whittle, currently apply this algorithm. Several authors, such as Zhao [23] and Hochbaum [24], developed their new graph theory to improve the Lerch-Grossmann algorithm's computational efficiency. Detailed discussion on the improvement can be found at [25] and [26].

2.6.1.3 Pushback design problem

The first method employs the parameterization process, which varies the input parameters' value in the ultimate pit limit algorithm to generate pushbacks. For instance, Whittle [19] produced pushbacks by changing the ratio of metal price to mining cost in the Lerch-Grossmann algorithm. This method has been available in Whittle software until nowadays. Seymour [27] relied on pit volume to eliminate the gap between consecutive pushbacks generated by the Whittle method. Ramazan and Dagdele [28]

recognized the impact stripping ratio on generating pushbacks so that they used it and extended Seymour's algorithm [27] to develop a new pushback algorithm.

The second method to generate pushbacks is to apply operations research techniques. Dagdelen [29] introduced a Linear Programming (LP) model to address the generation of pushbacks as follows:

$$\text{Max} \quad \sum_{i \in N} V_i x_i \quad (2.7)$$

$$\text{Subject to:} \quad x_j - x_i \leq 0 \quad \forall i, j \in N \quad (2.8)$$

$$\sum_{i \in N} x_i = b \quad (2.9)$$

$$x_i \in [0,1] \quad \forall i \in N \quad (2.10)$$

In this model, the objective function (Eq 2.7) and precedence constraints (Eq 2.8) are identical to the ultimate pit limit problem. In contrast, the constraint (Eq 2.9) enforces the desired size of the pushback b , and the constraint (Eq 2.10) defines the decision variables as continuous variables. Lagrangian relaxation can be deployed to solve this model. Meagher [30] expanded this LP model to an IP model to avoid generating fractional pushbacks. This IP model's application on a copper deposit produced an unsuitable schedule when mostly waste tonnage is extracted in early periods.

2.6.1.4 Production scheduling problem

The production scheduling problem has been a significant research area for many years attracting and attracted huge attractions from many researchers. It aims to determine when and which blocks inside the ultimate pit limit should be extracted and where these blocks should come (which destinations) to maximize the NPV of the project. Unlike the ultimate pit limit problem, the production scheduling problem accounts for the time value of money in the form of the discounted value of blocks. Various operational constraints, such as mining and processing capacity, grade blending, are considered to guarantee the practicality of the schedule. Three typical types of mathematical formulations for the production scheduling problem, including LP, IP, and MIP, are discussed in this section.

a. Linear programming

T.B.Johnson [31] developed the LP model to optimize production scheduling. The LP model can be described as follows:

$$\text{Max} \quad \sum_{t \in T} \sum_{m \in M} \sum_{i \in N} V_i C_{im}^t x_{im}^t \quad (2.11)$$

$$\text{Subject to:} \quad P_{\min k}^t \leq \sum_{m \in M} \sum_{i \in N} V_i x_{im}^t \leq P_{\max k}^t \quad \forall t \in T, \forall k \in K \quad (2.12)$$

$$\sum_{t' \in T} x_{jm}^{t'} - x_{im}^t \geq 0 \quad \forall (i, j) \in N, \forall t \in T \quad (2.13)$$

$$\sum_{t \in T} \sum_{m \in M} x_{im}^t = 1 \quad \forall i \in N \quad (2.14)$$

$$x_{im}^t \in [0, 1] \quad \forall i \in N, \forall t \in T, \forall m \in M \quad (2.15)$$

Where: T is the number of scheduling periods; N is the number of blocks to be scheduled; i is the block index ($i=1, 2, \dots, N$); M is the set of material types available within the deposit; K is the set of production targets; V_i is the total tonnage of block i ; C_{im}^t is expected NPV resulting from extracting material m , within block i , during period t ; x_{im}^t is a linear variable which controls the proportion of material m in block i being removed during period t ; $P_{\min k}^t$ and $P_{\max k}^t$ are the minimum and maximum capacity of production target k in period t , respectively.

The objective function (Eq 2.11) is constructed to maximize the NPV of blocks mined over the life of the mine. Constraints (Eq 2.12) are the minimum and maximum capacity of the corresponding production targets for the material m in period t . Whereas constraints (Eq 2.13) govern the relationship of block extraction, requiring the set of the immediate predecessor of block i must be extracted before it. Finally, constraints (Eq 2.14) enforce the extraction of block i to be completed within the life of mine if it is removed. Constraints (Eq 2.15) define the decision variable x_{im}^t , which is continuously linear from 0 to 1.

Using commercial solvers such as CPLEX [7] or Gurobi [32], one can find the solution for the LP model in a reasonable time. The main drawback of the LP model is

its solution can violate the slope constraints due to the decision variable for block extraction is linear, causing some portions of a block extracted. At the same time, its predecessors have not been mined. Nevertheless, the LP model is relatively helpful in producing an initial scheduling solution to the master problem. Lamghari [33], for instance, used a variable neighbourhood descent algorithm to improve an LP initial solution. The case study on MineLib data [34] demonstrated that the proposed method could generate the solution in a reasonable time.

b. Integer programming

The general mathematical form of the IP model for the production scheduling problem is as follows:

$$\text{Max } \sum_{i \in N} \sum_{t \in T} C_i^t x_i^t \quad (2.16)$$

$$\text{Subject to: } P_{\min k}^t \leq \sum_{i \in N} V_i x_i^t \leq P_{\max k}^t \quad \forall t \in T, \forall k \in K \quad (2.17)$$

$$\sum_{t' \in T} x_j^{t'} - x_i^t \geq 0 \quad \forall (i, j) \in N, \forall t \in T \quad (2.18)$$

$$\sum_{t \in T} x_i^t \leq 1 \quad \forall i \in N \quad (2.19)$$

$$x_i^t \in \{0, 1\} \quad \forall i \in N, \forall t \in T \quad (2.20)$$

Where: T is the maximum number of scheduling periods; N is the number of blocks to be scheduled; i is the block index ($i=1, 2, \dots, N$); K is the set of production targets; V_i is the total tonnage of block i ; C_i^t is expected NPV resulting from extracting block i during period t ; x_i^t is a binary variable which equals one when block i is removed in period t and zeros otherwise; $P_{\min k}^t$ and $P_{\max k}^t$ are the minimum and maximum production target k in period t , respectively.

The description of the IP model is the same as the LP model. The difference between them is that the IP model specifies the decision variable as an integer variable (Eq 2.18) to avoid providing the fractional extraction of blocks (Eq 2.20). Nevertheless, the number of binary variables within the IP model is too large to find even a feasible

solution, causing it not to be applied in large deposits. Reducing the number of binary variables is complicated such as generate pushback before scheduling [35]. Detailed discussions of the IP model can be found in Caccetta and Giannini [36] and Chicoisne *et al.* [37].

c. Mixed Integer Programming

The IP model can be converted into the MIP model to reduce the number of binary variables as follows [38]:

$$\text{Max } \sum_{i \in N} \sum_{t \in T} \sum_{d \in D} c_{id}^t y_{id}^t \quad (2.21)$$

$$\text{Subject to: } P_{\min k}^t \leq \sum_{i \in N} V_i y_{id}^t \leq P_{\max k}^t \quad \forall t \in T, \forall k \in K, \forall d \in D \quad (2.22)$$

$$\sum_{t' \in T} x_j^{t'} - x_i^t \geq 0 \quad \forall (i, j) \in N, \forall t \in T \quad (2.23)$$

$$x_i^t = \sum_{d \in D} y_{id}^t \quad \forall i \in N, \forall t \in T \quad (2.24)$$

$$\sum_{t \in T} x_i^t \leq 1 \quad \forall i \in N \quad (2.25)$$

$$x_i^t \in \{0, 1\}, y_{id}^t \in [0, 1] \quad \forall i \in N, \forall t \in T, \forall d \in D \quad (2.26)$$

The key to this formulation is adding the linear variable y_{id}^t . This variable allows for fractional blocks to be extracted after all its entire predecessor blocks have been removed. The interpretation of the objective and constraints of the MIP model is the same as the IP model. The MIP model's main disadvantage is its inability to tackle the large problem with many binary variables using commercial solvers. Hence, the central attempts in some recent works are to reduce the number of binary variables. Ramazan and Dimatrakopoulos [39] defined the variables representing ore blocks as binary and the remaining variables as linear. The proposed MIP model was found to decrease the solution time and the gap of feasible solutions, but finding exact optimal solutions is difficult.

Aggregation and disaggregation techniques are commonly used to improve the solution time in solving the MIP model. The most straightforward technique is to reduce

the resolution of the block model by decreasing its block sizes. Although the problem's desired size can be easy to achieve, the scheduling solution's quality declines accordingly. Nevertheless, reblocking is still a standard option to deal with large deposits in many commercial software packages such as Minemax [40] or MineSched [41]. Ramazan et al. [35] and Ramazan [42] developed a new algorithm termed Fundamental Tree Algorithm based on block aggregation to reduce the number of binary variables and constraints required within the MIP formulation. The slope angle is ensured during the aggregation process. A popular in-house mine planning tool of BHP Billiton, called Blasor, applies this approach to group blocks into cone-shaped clumps. Despite the success of the approach in reducing the number of binary variables, its implementation is too complicated. Another combination of MIP models and aggregation techniques was also found in the research work by Askari-Nasab et al. [43] when they clustered blocks in the same bench into mining cuts and formulated them using the MIP formulation. The MIP model can be solved using the exact method within the CPLEX environment [7]. This aggregation technique is now available in MineMax software [40].

In contrast to aggregation techniques, Whittle strategic mine planning software [44] decomposes the scheduling problems into pushbacks based on the nested pit approach. It subsequently considers each pushback as a particular MIP problem. This approach can decrease the solution time but does not guarantee a global optimum solution to the problem. Various commercial software now uses the MIP model to tackle the LTPP problem, such as MineMax [40], Blasor [45], or Prober [46].

Metaheuristic algorithms are efficient alternative approaches to solve the large-scale MIP model within a reasonable timeframe. These algorithms can generate a near-optimal solution but do not guarantee the optimality of the solution. Several works based on the MIP model applied the family of metaheuristics successfully and showed promising results, such as Tabu search [47], [48], Simulated annealing [49], [50], Genetic algorithm [51], or Ant colony optimization [52].

2.6.2 Stochastic approaches for solving the LTPP problem

As reviewed above, the deterministic algorithms consider a single estimated orebody model as an input to solve the LTPP problem. Generally, the attribute of each unsampled

block receives a mean value estimated from the surrounding sampling points. It does not consider the in-situ variability or the error associated with it. Mishandling such a significant source of risk and uncertainty in mine planning models may result in unrealistic production expectations [2]–[4], [53].

In this section, the stochastic approaches, including geostatistical simulation to transfer the geological uncertainty of the deposit, the mathematical model algorithms for assessing, mitigating, and taking advantage of the geological uncertainty in the LTPP problem, are discussed.

2.6.2.1 Transfer geological uncertainty

Geostatistical simulation is considered the best method to characterize the risk of geological uncertainty by generating a series of probable geological outcomes or realizations of orebody models with an equal chance to occur in practice. The basic principle of geostatistical simulation is developed based on the spatial random field and Monte Carlo simulation. Each attribute of deposit, such as grade, rock type, is considered regionalized variables, assumed to be the realization of a spatial random field characterized by samples' spatial distribution. Once the spatial random field is determined, the Monte Carlo simulation can draw different realizations or outcomes. If the simulations honour the known values at sampling locations, they are 'conditional simulation.' John Vann *et al.* [54] produced a detailed overview of geostatistical simulation.

It is prevalent to construct geological variables that are facies or rock types before evaluating mineral resources and ore reserves since the relationships between rock types and metallurgical properties. Traditionally, geological models can be obtained by interpreting geological variables on cross-sections or planning maps, where the uncertainty of geological models is not involved. Various simulation approaches have been proposed to quantify the joint uncertainty between grades and rock type domains [55]–[58]. For instance, Roldão *et al.* [57] combined SIS and SGS showing promising results compared to the traditional block model in evaluating the impact of lithological and grade simulation in the economic study of iron ore deposit in Brazil. Talebi *et al.* [58] and Mery *et al.* [59] simulated the geological domains using plurigaussian model and generating the grade simulation within each rock type. The

studies show the ability to improve the accuracy of expected grades when validating the realizations against production data.

2.6.2.2 Integration of geological uncertainty into LTPP problem

The initial idea to integrate geological uncertainty into the LTPP problem is to feed orebody realizations sequentially into deterministic scheduling models and generate multiple schedules showing the impact of geological uncertainty on a project [60]–[62]. However, this method does not suggest an optimal scheduling solution in the presence of geological uncertainty. Godoy and Dimatrakopoulos [63] and Leite and Dimatrakopoulos [64] proposed a new risk-inclusive LTPP approach based on simulated annealing to process the separate schedules yielded by the deterministic scheduling models to extract a single schedule. Nevertheless, the optimality of the solution is not guaranteed. Also, the implementation of the approach is complicated and needs many parameters to gain consistent results.

SIP, an extension of MIP, has gained much more attention in integrating geological uncertainty in recent years. Ramazan and Dimatrakopoulos [65] presented the SIP model to generate optimum long-term production schedules for open-pit mines. The objective function of the SIP model maximizes the total expected NPV under geological uncertainty. It is represented as follows:

$$Max \sum_{t \in T} \left[\underbrace{\sum_{i \in N} C_i^t x_i^t}_{\text{Part 1}} - \underbrace{\sum_{s \in S} (C_u^{tk} d_{su}^{tk} + C_l^{tk} d_{sl}^{tk})}_{\text{Part 2}} \right] \quad (2.27)$$

Where: T is the maximum number of scheduling periods; N is the number of blocks to be scheduled; i is the block index ($i=1,2, \dots, N$); S is the set of orebody realization; C_i^t is discounted NPV of block i during period t resulting from all considered orebody simulations; x_i^t is a binary variable which equals one when block i is extracted in period t and zeros otherwise; d_{su}^{tk} and d_{sl}^{tk} are the amount of upper and lower deviations from production target k in period t on realization s , respectively; and C_u^{tk} C_l^{tk} are the cost unit to penalize the upper and lower deviations from production target k in period t on realization s , respectively.

The objective function is subject to a list of soft constraints and consists of two parts. Part 1 is to maximize the total discounted economic value, while part 2 is to quantify the risk of not meeting production targets by penalizing these deviations. The SIP models are not only proven the capacity to integrate geological uncertainty and mitigate its potential risks [65], [66] but also to have significant economic benefits compared with the deterministic model [67]–[69]. For instance, Dimatrakopoulos and Ramazan [67] tested the SIP model in two cases: a gold and a copper deposit, showing a significantly higher NPV of 10 and 25% projects, respectively, than the deterministic models using a single estimated orebody model. Leite and Dimatrakopoulos [69] report 26% NPV higher than that of the deterministic model in a copper deposit case study. Mai et al. [68] implemented the SIP model in an iron ore deposit in Western Australia, generating a 2.28% higher NPV result than the deterministic model.

Similar to the deterministic models developed based on integer variables, the biggest challenge in solving the SIP models is problem size which can be caused by the number of blocks in the deposit model or the number of constraints. Metaheuristic and block aggregation (clustering) approaches are efficient in overcoming this challenge. Lamghari and Dimatrakopoulos [47] and Lamghari et al. [70] presented two metaheuristic solution approaches based on the Tabu search and neighbourhood descent algorithm, respectively, to solve large-scale SIP models producing reasonable solutions in relatively short computational times. Mai et al. [68] proposed a new risk-based optimization method for the LTPP problem using TopCone Algorithm [68] and SIP. Meanwhile, Behrang et al. [71] applied the clustering algorithm [48] to aggregate the blocks into mining cuts and formulated them into the SIP model. Both proposed models based on clustering methods were proven to reduce the size of the SIP models significantly.

2.6.3 Clustering algorithms

Clustering is the work of grouping similar objects into some groups or clusters using similarity and dissimilarity measures. There are two categories of clustering: hierarchical and partitional clustering.

Hierarchical clustering is an algorithm that creates a hierarchy of objects in the form of a cluster tree. This tree can be constructed using agglomerative and divisive

methods. The former method considers each object as a cluster and groups them into a larger one. The latter method assigns whole objects into one cluster and separates them into smaller clusters.

The partitional clustering algorithms decompose the set of objects into a set of disjoint clusters using iterative processes. One of the famous examples of the partitional clustering algorithms is k-means clustering, which works in five steps: choosing a desired number of clusters, randomly assigning each data point to a cluster, computing cluster centroid, assigning each point to the closest cluster centroid, and re-computing cluster centroids.

In the scheduling model, each mining cut is considered as a mining unit. Grouping blocks into mining cut reduces the size of the scheduling model. Tabesh et al.[48], [71] implemented a variation of the agglomerative hierarchical clustering algorithm (AHCA) and combined it with shape and size control. AHCA works based on the similarity index, which is calculated using four attributes of blocks, including location, grade, rock type, and beneath cluster. The quality of the clustering scheme quality is quantified using two factors: rock unity and the average variation of grades in each mining cut. The general procedure of AHCA is performed as follows:

- (i) Start by considering each block as a cluster and compute the similarity matrix over all blocks on the same bench;

- (ii) Find the most similar adjacent blocks and merge them into a single cluster until the desired number of blocks per cluster or the average number of clusters is reached.

- (iii) Remove narrow corners of the clusters and improve the clusters with an irregular shape to be minable while preserving the similarity between clusters.

The generated block clusters are consequently used as selective mining cuts in the scheduling model. The size of the mining cuts influences the quality of the scheduling solution. Generally speaking, increasing the number of blocks per mining cut results in better NPV but higher computational time.

In Tabesh et al.'s works [48], [71], ACHA was implemented on a single estimated orebody model. However, applying ACHA in a set of orebody realizations is different, requiring dealing with geological uncertainty of rock type and grades. In a forward step, Tabesh and Askari-Nasab [72] proposed four different clustering algorithms, including expected value algorithm, simple realization algorithm, hierarchical realization aggregation, and k-means with hierarchical realization aggregation. The hybrid algorithm using k-means and hierarchical realization aggregation (KHRA) shows its ability to implement real-scale block models in a reasonable computation time to create reliable clustering schemes while considering the geological uncertainty.

2.7 Conclusion

Raw material extraction is an essential component of cement manufacturing operations, contributing significantly to the cement production cost and quality. Ensuring a consistent supply of raw materials is critical for the success of a cement manufacturing project. A little effort in quarry management can generate much higher benefits further down the line. Quarry planning and optimization are pre-requisites for sound and scientific quarry management practices that ensure the consistent supply of raw materials with low cost and maximize deposit life longevity.

Various optimization algorithms and commercially available software packages have been developed to tackle the LTPP problem. Despite the progress made to date, some limitations still exist to the current LTPP problem.

(i) Current best software packages in mine planning have not been integrating explicitly uncertainties, especially geological uncertainty. Scheduling for a single estimated orebody model will result in a suboptimal mine plan.

(ii) The scheduling methods are unable to deal with large-scale industrial problems. In the case of integrating uncertainty in production scheduling, most researchers must deploy heuristics/metaheuristics to obtain a good solution. Clustering techniques seem to be producing more promising results but need to extend to be used in stochastic optimization models.

(iii) Most optimization models and available software encompass maximizing the NPV of the project rather than securing the consistent supply of run-of-mine products and conserving resources like cement manufacturing operations.

These limitations emphasize the need for an optimization tool that can incorporate geological uncertainty, provide optimum solutions in reasonable computation time, and be specialized for cement raw material mining. In the next chapter, the working framework and mathematical model of that optimization tool are presented.

Chapter 3. A stochastic optimization framework for LTQPP problem

3.1 Introduction

LTQPP is an essential component of the cement production process. Optimization of LTQPP deals with the requirement of a consistent supply of an adequate amount of raw materials at the desired quality as long as possible to generate the highest possible return from investment in cement plants. The optimization process begins with a resource model representing a mineral deposit in 3D space. Geostatistical estimation methods have long been applied to model the spatial distribution of attributes of interest within resource models. However, the inferred data is sparse relative to the interest region, and hence, geological uncertainty is inevitable in estimation. For many decades, the traditional or deterministic optimization framework has been developed using a single estimated resource model to optimize the mine planning and assess mining projects. Mishandling the geological uncertainty in traditional frameworks can result in a severe risk of not meeting production expectations and project failures [2], [4], [16], [53], [73].

In recent years, several stochastic or risk-based optimization frameworks have been introduced using a set of equally probable resource models to transfer geological uncertainty into mine planning and proving many advantages in many aspects in comparison with the deterministic framework. Nevertheless, these frameworks are still comparatively new and expose several drawbacks. Most of the proposed frameworks integrate geological uncertainty into the optimization process. However, they do not suggest a method to mitigate the risks of geological uncertainty. Furthermore, the practical size of mining problems is one of the main obstacles that need to overcome to be applicable in practice. Although there is no doubt about the benefits of stochastic frameworks in some specific cases, they still need to be verified when applied to different types of deposits.

This chapter presents a new stochastic optimization framework for LTQPP using geostatistical simulation, clustering approach KHRA, and SMIP model. Based on a series of equally probable models of the deposit, the ultimate goal of stochastic mine planning is to provide an optimal and unique schedule respecting geological uncertainty. The optimization framework can be depicted in Figure 3.1.

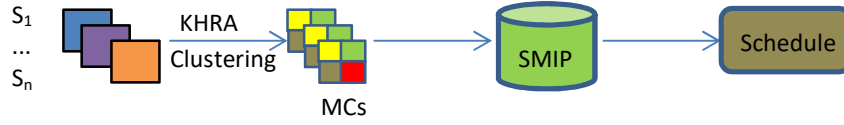


Figure 3.1 Three stages of the proposed risk-based framework for the LTQP problem

The proposed stochastic optimization framework consists of three main stages, as follows:

Stage 1: construct a series of deposit realizations using geostatistical simulation to capture and provide geological uncertainty for the optimization process

Stage 2: aggregate blocks into mining cuts using clustering approach KHRA to reduce the size of LTQPP problem

Stage 3: generate the production schedule using the SMIP model based on the simulated values of mining cuts

This proposed framework was integrated into a software application providing a digital tool for quarry planners (see Appendix I). More detailed discussions on this framework will be presented in the next sections below.

3.2 Deposit simulation

The success of a cement production project depends on the raw material supply. LTQPP, based on resource models, is essential to maintain the consistency of this supply to the cement plant. Therefore, resource modelling plays a crucial role in raw material quality management for cement manufacturing. Geological uncertainty is inherent due to sparse exploratory information in resource models and significant risk factors for not achieving production targets.

Conditional simulation algorithms such as SIS and SGS, standard in the geostatistical method, are considered the best method to characterize geological uncertainty risks. They can generate a series of probable geological outcomes or realizations of orebody models with an equal chance to occur in practice. The limestone deposit in the case study contains four primary rock types, controlling the occurrence of chemical grades and spatial distribution. Hence, the proposed approach is hierarchical, combining SIS and SGS techniques, a common strategy in quantifying the joint

uncertainty between grades and rock type domains [55]–[58]. A brief explanation of two techniques are as follows:

3.2.1 Simulating the rock type domains using SIS

SIS is a widely used technique to model categorical or rock type variables. Consider different mutually exclusive categories of rock types. SIS can be performed through the following steps:

1. Transform a particular rock type at a particular location into binary variables: *one* if the rock type is present, and *zero* otherwise;
2. Assign transformed data into the simulation grid;
3. Visit each grid node in random order;
4. Construct the conditional distribution by indicator kriging, that is, generate the probability of each rock type being available at the current location;
5. Draw a simulated rock type from the set of probabilities using the Monte Carlo simulation;
6. Assign the newly simulated value as a part of the conditioning data;
7. Repeat steps (3) to (4) until all grid nodes are visited.

3.2.2 Simulating the chemical grades within each domain conditionally to rock type domains, using SGS

SGS now has a long history and is an efficient method in the mining industry [2], [74]–[76]. One can perform the SGS through the following steps:

1. Transform the grade data into normal scores;
2. Assign transformed data into the simulation grid;
3. Visit each grid node in random order;
4. Perform kriging to estimate a mean and variance at that node, using the transformed data and the already simulated data;
5. Draw a random value from a Gaussian distribution with a mean and a variance equal to the mean and variance estimated by the kriging method and set the node value to that drawn value;
6. Repeat steps (3) to (5) until all grid nodes are visited;
7. Back-transform the simulated values into the original grade space.

The application of these techniques to the case study is described in Chapter 4.

3.3 Block clustering

Like other integer-based models, these SMIP model size is often too large to be solved using conventional solvers. One of the efficient ways to deal with this challenge is by applying clustering or aggregation techniques. In this research, the KHRA algorithm proposed by Tabesh and Askari-Nasad [72] was used to aggregate the blocks into the minable mining cuts. The objective of KHRA is to create homogeneous mining cuts to be used in the planning optimization stage. KHRA algorithm combines two clustering algorithms: k-means and AHCA [48], [77]. K-means is a built-in function in Matlab [5]. Whereas AHCA consists of two steps: (i) aggregating blocks on the same bench iteratively into clusters until meeting the required number of blocks per cluster, based on a similarity matrix; (ii) improving the cluster shape to be minable in practice.

KHRA aggregates blocks on each bench, from bottom to top, considering all R realizations of deposit block models. The KHRA creates the feature matrix incorporating the block information of coordinates, primary element grade, and rock types. Then, k-means is performed to obtain an initial clustering scheme for each realization k . Next, the common cluster matrix (C_{ij}^k) and the frequency of two blocks i and j being in the same cluster (F_{ij}) are calculated as Eqs 3.1 and 3.2, respectively.

$$C_{ij}^k = \begin{cases} 1 & \text{if block } i \text{ and } j \text{ are from the same cluster} \\ 0 & \text{otherwise} \end{cases} \quad (3.1)$$

$$F_{ij} = \frac{\sum_{k=1}^R C_{ij}^k}{R} \quad (3.2)$$

Finally, the AHCA [48], [77], is performed to form the final clustering scheme. AHCA uses F_{ij} values as indices in the similarity matrix. In this research, the beneath clustering penalty values are calculated for this matrix to improve the solution time of the SMIP model [48]. These penalty values are computed in Eq 3.3.

$$C_{ij} = \begin{cases} 1 & \text{if block } i \text{ and } j \text{ are above the same cluster} \\ c & \text{otherwise} \end{cases} \quad c \in [0, 1] \quad (3.3)$$

Tabesh and Askari-Nasad [72] presented the pseudo-code of KRHA, as in Table 3.1.

Table 3.1 Pseudo code of KHRA

```

Function KRHA(Blocks)
For each  $k$  in Realizations
     $S^k = \text{BuildFeatureMatrix}(\text{Blocks}, k); \text{Cluster}^k = \text{Kmeans}(S^k);$ 
    For each  $i$  in Blocks
        For each  $j$  in Blocks
             $C_{ij}^k = \begin{cases} 1 & \text{if block } i \text{ and } j \text{ are from the same cluster} \\ 0 & \text{otherwise} \end{cases}$ 
        Next
    Next
    For each  $i$  in Blocks
        For each  $j$  in Blocks
            
$$F_{ij} = \frac{\sum_{k=1}^R C_{ij}^k}{R}$$

        Next
    Next
    Clusters=Clustering(F,A)
Return
Function BuildFeatureMatrix(Blocks,k)
For each  $j$  in Rocktypes
     $M_{i1} = X_i; M_{i2} = Y_i; M_{i3} = G_j^k;$ 
    For each  $j$  in Rocktypes
        If  $R_i^k = j$ 
             $M_{i(j+3)} = r$ 
        Else
             $M_{i(j+3)} = 0$ 
        EndIf
    Next
Next
Return M
Function Kmeans(S)
    * Built-in k-means function in Matlab

```

3.4 The mathematical formulation for the LTQPP problem

Two main approaches to the mathematical formulation for the LTQPP problem, including a deterministic MIP (DMIP) model and a SMIP model, are discussed in this section. They were expanded from the MIP model proposed by Askari-Nasab et al. [43], [78], which is widely accepted. Although formulating the SMIP model is the main

objective of this research, the DMIP model was formulated to compare and highlight the capacity of the SMIP.

In the scheduling model, each cluster is considered as a mining unit. The cost, grades, and material tonnage of a mining cut are computed by summing up its member blocks' corresponding values. The chemical grades and rock type of a mining cut are assumed to be homogeneous by the clustering approach. In both models, each mining cut is considered as a selective mining unit that can be extracted fractionally at any production period. The reason for fractional extraction of a mining cut is that the solver has more freedom to converge to a smaller cost value than the case extracting an entire mining cut in a period.

The SMIP model was formulated based on the DMIP model [43], [78]. The DMIP model optimizes the LTQPP problem using a single geological realization (E-type model). In contrast, the SMIP model takes all possible geological realizations. The DMIP model is formulated in subsection 3.4.2.1 for the LTQPP problem to highlight the effectiveness of the SMIP model.

Cement manufacturing generally requires stockpiles to develop a raw mix that blends the raw materials from the quarry and the additive materials from outside to ensure the supply. Hence, the objective is to minimize the total cost of supplying raw materials from two primary sources: quarry and additives. At the same time, the constraints are to satisfy the blending and other operational requirements. The optimization models were designed to follow the general layout of cement manufacturing which uses a blending stockpile for developing raw mix and a waste dump for disposing of unused materials.

The CPLEX solver was deployed to generate the final production schedule. The solver takes two steps to solve the problem. First, it relaxes and solves the linear model and then using the branch and cut algorithm to find a feasible integer solution. The MIP gap (EPGAP), an absolute tolerance of the gap between the best integer objective and the best node remaining, was used to control the solver. When the gap falls below the MIP gap, the solver is terminated. In this research, Matlab (2007) [5] was employed to run the clustering algorithms, formulate the SMIP model, and call CPLEX solver.

3.4.1 Notation

a. Indices and Sets:

$i \in I$ is set of mining cuts for extraction

$j \in J_i$ is immediate predecessors for mining cuts i

$t, t' \in T$ are production periods

$a \in A$ is set of additive materials purchased from outside sources ($a = 1$: Clay, $a = 2$: Laterite, $a = 3$: Limestone, $a = 4$: Iron ore)

$k \in K$ is set of quality targets ($k = 1$: CaO, $k = 2$: SiO₂, $k = 3$: Al₂O₃, $k = 4$: Fe₂O₃, $k = 5$: MgO, $k = 6$: SR, $k = 7$: LSF, $k = 8$: AM)

$s \in S$ is set of realizations

b. Parameters:

P_i is the number of mining cuts that must be extracted before mining cut i

o_{is} is the tonnage of materials that can be sent to the blending stockpile, in mining cut i , on realization s , (tons)

w_{is} is the tonnage of materials that can be sent to the waste dump, in mining cut i , on realization s , (tons)

\bar{o}_i is the average tonnage of materials that can be sent to the blending stockpile, in mining cut i , averaged from all geological realizations (tons)

\bar{w}_i is the average tonnage of materials that can be sent to the waste dump, in mining cut i , averaged from all geological realizations (tons)

\bar{co}_i is the average cost of extracting and sending materials within mining cut i to the blending stockpile, averaged from all geological realizations, (\$)

\bar{cw}_i is the average cost of extracting and sending materials in mining cut i to the waste dump, averaged from all geological realizations, (\$)

c_a is the unit cost of purchasing additive material a , (\$/t)

\bar{g}_{ki} is the average content of chemical k in mining cut i , averaged from all geological realizations, (%)

g_{kis} is the content of chemical k in mining cut i , on realization s , (%)

g_{ka} is the content of chemical k in additive a , (%)

max_g_k / min_g_k is the maximum /minimum allowable content of chemical k in the raw mix, (%)

max_m_t / min_m_t is the maximum /minimum mining production in period t , (tons)

max_r_t / min_r_t is the maximum /minimum raw mix production in period t , (tons)

up_dm / low_dm is the penalty cost of upper/lower deviation from the mining production targets (\$/t)

up_dr / low_dr is the penalty cost of upper/lower deviation from the raw mix production targets (\$/t)

r is the discount rate, %

Linear variables:

up_qm_{st} / low_qm_{st} is the amount of upper/lower deviation from the mining production targets in consideration of realization s , in period t

up_qr_{st} / low_qr_{st} is the amount of upper/lower deviation from the raw mix production targets in consideration of realization s , in period t

q_{at} is the amount of additive a from outside sources needed to complete the blending requirements at the raw mix in period t

q_{ast} is the amount of additive a from external sources needed to complete the blending requirements in consideration of realization s in period t

$x_{it} \in [0,1]$ is the portion of mining cut i extracted and processed as a raw material in cement production, in period t

$y_{it} \in [0,1]$ is the portion of mining cut i extracted and sent to the waste dump, in period t

Binary variables:

$v_{it} \in \{0,1\}$ is the binary variable controlling the precedence of extraction of mining cut s (equals one if mining cut i is scheduled in period t ; zeros otherwise)

3.4.2 Mathematical formulation

3.4.2.1 DMIP model

a. Objective function

$$\min \sum_{t \in T} \left[\frac{1}{\left(1 + \frac{r}{100}\right)^t} \left(\underbrace{\sum_{i \in I} (\bar{c}o_i x_{it} + \bar{c}w_i y_{it})}_{\text{Part 1}} + \underbrace{\sum_{a \in A} c_a q_{at}}_{\text{Part 2}} \right) \right] \quad (3.4)$$

b. Constraints

Quarry production capacity constraints:

$$\min_m_t \leq \sum_{i \in I} \bar{o}_i x_{it} + \sum_{i \in I} \bar{w}_i y_{it} \leq \max_m_t \quad \forall t \in T \quad (3.5)$$

Raw mix quality constraints:

$$\min_r_t \leq \sum_{i \in I} \bar{o}_{it} x_{it} + \sum_{a \in A} q_{at} \leq \max_r_t \quad \forall t \in T \quad (3.6)$$

Raw mix quality constraints:

$$\text{Lower bound: } \sum_{i \in I} (\bar{g}_{ki} - \min_g_k) \bar{o}_i x_{it} + \sum_{a \in A} (g_{ka} - \min_g_k) q_{at} \geq 0 \quad \forall k \in K; \forall t \in T \quad (3.7)$$

$$\text{Upper bound: } \sum_{i \in I} (\bar{g}_{ki} - \max_g_k) \bar{o}_i x_{it} + \sum_{a \in A} (g_{ka} - \max_g_k) q_{at} \leq 0 \quad \forall k \in K; \forall t \in T \quad (3.8)$$

Sequencing constraints:

$$P_i \times v_{it} - \sum_{j \in J_i} \sum_{t' \in T; t' \leq t} (x_{it} + y_{it}) \leq 0 \quad \forall i \in I; \forall t \in T \quad (3.9)$$

$$\sum_{t' \in t, t' \leq t} (x_{it} + y_{it}) - v_{it} \leq 0 \quad \forall i \in I; \forall t \in T \quad (3.10)$$

$$v_{it} - v_{i,t+1} \leq 0 \quad \forall i \in I; \forall t \in T \quad (3.11)$$

Reserve constraint:

$$\sum_{t \in T} (x_{it} + y_{it}) \leq 1 \quad \text{or} \quad \sum_{t \in T} (x_{it} + y_{it}) = 1 \quad \forall i \in I \quad (3.12)$$

Variable definition constraints:

$$x_{it} \in [0, 1]; y_{it} \in [0, 1]; v_{it} \in \{0, 1\} \quad \forall t \in T; \forall i \in I \quad (3.13)$$

The objective function in Eq 3.4 consists of two parts that minimize the cost of supplying the raw materials to the cement plant. It includes the cost of extracting and sending the materials to the blending stockpile and the waste dump and the cost of additive purchases from outside sources. The discount rate considers the time value of the cost over the periods.

The objective function of the DMIP model is subject to a list of hard constraints. Eqs 3.5-3.6 limit quarry and raw mix production capacity in each period. Eqs 3.7-3.8 are to satisfy the grade and the cement modulus requirements commonly used in cement manufacturing to balance the principal oxides. The moduli can be expressed in Eqs 2.1, 2.2, and 2.3 (see Chapter 2).

Eqs 3.9-3.11 implement the sequencing relationship in extracting mining cuts. The binary controller variable v_{it} is to control the sequencing relationship and to ensure the slope constraints. Eq 3.9 forces the variable v_{it} to be equal to 0 until all the predecessors of a mining cut i have been wholly mined. Eq 3.10 ensures that a mining cut can not be extracted unless the variable v_{it} is equal to 1. Also, v_{it} is set to 1 if it has been set to 1 in an earlier period, as shown in Eq 3.11. The reserve constraint presented by Eq 3.12 ensures that the sum of the extraction fractions of a mining cut is not going to exceed one. The second form of Eq 3.12 can be used to ensure that all the materials within the ultimate pit limit are extracted over all periods if the sum equals one. The constraint in Eq 3.13 guarantees the integrality and non-negativity of the decision variables.

3.4.2.1 SMIP model

a. Objective function

$$\min \sum_{t \in T} \left[\frac{1}{\left(1 + \frac{r}{100}\right)^t} \left(\underbrace{\sum_{i \in I} (\overline{co}_i x_{it} + \overline{cw}_i y_{it})}_{\text{Part 1}} + \underbrace{\sum_{s \in S} \sum_{a \in A} c_a q_{ast}}_{\text{Part 2}} + \underbrace{\sum_{s \in S} \left(\begin{array}{l} up_qm_{st} up_dm + low_qm_{st} low_dm + \\ up_qr_{st} up_dr + low_qr_{st} low_dr \end{array} \right)}_{\text{Part 3}} \right) \right] \quad (3.14)$$

b. Constraints

Quarry production capacity constraints:

$$\text{Lower bound: } \min_m_t \leq \sum_{i \in I} o_{is} x_{it} + \sum_{i \in I} w_{is} y_{it} + \text{low_} qm_{st} \quad \forall s \in S; \forall t \in T \quad (3.15)$$

$$\text{Upper bound: } \sum_{i \in I} o_{is} x_{it} + \sum_{i \in I} w_{is} y_{it} + \text{up_} qm_{st} \leq \max_m_t \quad \forall s \in S; \forall t \in T \quad (3.16)$$

Raw mix production capacity constraints:

$$\text{Lower bound: } \min_r_{st} \leq \sum_{i \in I} o_{is} x_{it} + \sum_{s \in S} \sum_{a \in A} q_{ast} + \text{low_} qr_{st} \quad \forall s \in S; \forall t \in T \quad (3.17)$$

$$\text{Upper bound: } \sum_{i \in I} o_{is} x_{it} + \sum_{s \in S} \sum_{a \in A} q_{ast} + \text{up_} qr_{st} \leq \max_r_t \quad \forall s \in S; \forall t \in T \quad (3.18)$$

Raw mix quality constraints:

$$\text{Lower bound: } \sum_{i \in I} (g_{kis} - \min_g_k) o_{is} x_{it} + \sum_{s \in S} \sum_{a \in A} (g_{ka} - \min_g_k) q_{ast} \geq 0 \quad \forall k \in K; \forall t \in T; \forall s \in S \quad (3.19)$$

$$\text{Upper bound: } \sum_{i \in I} (g_{kis} - \max_g_k) o_{is} x_{it} + \sum_{s \in S} \sum_{a \in A} (g_{ka} - \max_g_k) q_{ast} \leq 0 \quad \forall k \in K; \forall t \in T; \forall s \in S \quad (3.20)$$

Sequencing constraints:

$$P_i \times v_{it} - \sum_{j \in J_i} \sum_{t' \in T; t' \leq t} (x_{it} + y_{it}) \leq 0 \quad \forall i \in I; \forall t \in T \quad (3.21)$$

$$\sum_{t' \in T, t' \leq t} (x_{it} + y_{it}) - v_{it} \leq 0 \quad \forall i \in I; \forall t \in T \quad (3.22)$$

$$v_{it} - v_{i,t+1} \leq 0 \quad \forall i \in I; \forall t \in T \quad (3.23)$$

Reserve constraint:

$$\sum_{t \in T} (x_{it} + y_{it}) \leq 1 \quad \text{or} \quad \sum_{t \in T} (x_{it} + y_{it}) = 1 \quad \forall i \in I \quad (3.24)$$

Variable definition constraints:

$$x_{it} \in [0, 1]; y_{it} \in [0, 1]; v_{it} \in \{0, 1\} \quad \forall t \in T; \forall i \in I \quad (3.25)$$

The objective function of the proposed SMIP model consists of three parts, as shown in Eq 3.14. Like the DMIP model, Part 1 minimises the cost of extracting raw materials in the quarry sent to the blending stockpile and the waste dump. Part 2 minimises the purchase of additive materials. Besides, Part 3 is introduced to minimise the deviations of quarry and raw mix production targets due to the impact of geological uncertainty. The penalty costs are multiplied by their corresponding amount of deviation

to control the risk of deviations due to geological uncertainty. By applying the discount rate on the ultimate value of the objective function, the penalty cost is higher in the earlier periods generating a lower deviation of production targets. Simultaneously, the penalty cost is decreased and brings more deviation of production targets in the later periods. As a result, the generated plan tends to extract less uncertain parts of the deposit in earlier periods and defer more uncertain parts for later periods. In general, the geological uncertainty could be reduced when future geological information arrives during the mining process.

Unlike the DMIP model, the objective function of the SMIP model is subject to a list of stochastic and hard constraints, generating a unique solution that is feasible for any value of the decision variables (continuous and binary variables). Eqs 3.15-3.18 are stochastic constraints to govern feasible scheduling solutions for each geological realizations in each planning period. These constraints allow the quarry and raw mix production to deviate from their predefined lower and upper bounds as recorded by linear variables up_qm_{st} , low_qm_{st} , up_qr_{st} , and low_qr_{st} , respectively. The raw mix quality constraints in Eqs 3.19-3.20 are suggested to be implemented as a hard constraint since a typical purchase of additive materials in the cement industry adjusts the raw mix when quarry extracting efforts do not help. The other remaining constraints are similar to the DMIP model.

3.5 Numerical modelling

This section presents the numerical modelling technique for the block clustering algorithms and the SMIP model in sections 3.3 and 3.4. The numerical modelling of the DMIP model was implemented in the same technique used for the SMIP model. The numerical modelling results build a complete software application for the defined problem in this research (see Appendix I).

3.5.1 Clustering

In the first step, the k-means function, which is available in Matlab [5], was deployed and run on a feature matrix, to create the initial clustering scheme for each realization. The first feature matrix was calculated using Eq 3.1. This section will use the horizontal matrix concatenation operator, $'$, and vertical matrix concatenation operator, $;$ to

simplify the notation. These operators construct a matrix or vector by concatenating them along the horizontal or vertical dimension of the matrix or vector. Besides, the weights were used to control the importance of factors (location, grade, and rock type) in generating clustering schemes. Eq 3.26 illustrates the structure of the matrix input for the k-means clustering.

$$S^{N \times (3+r)} = [\bar{X}, \bar{Y}, \bar{G}, R] \quad (3.26)$$

Where:

- \bar{X}/\bar{Y} is the $N \times 1$ vector representing the normalized coordinates of N blocks (\bar{X}_i, \bar{Y}_i) powered to the distance weight (W_d) and normalized by dividing all values by the maximum value of each vector, as shown in Eqs.3.27-3.28:

$$\bar{X}_i = \frac{X_i W_d}{\max(X_i)} \quad (3.27)$$

$$\bar{Y}_i = \frac{Y_i W_d}{\max(Y_i)} \quad (3.28)$$

- \bar{G} is the $N \times 1$ vector representing the normalized values of the primary grade (G_i), powered to the grade weight (W_g) and normalized by dividing all values by the maximum value of that grade, as shown in Eq.3.29:

$$\bar{G}_i = \frac{G_i W_g}{\max(G_i)} \quad (3.29)$$

- R is the $N \times e$ matrix representing the similarity of r rock types. If a block is of rock type e , the e^{th} column in this vector will get a value of $1-r$ (one minus rock type penalty), ($r \in [0,1]$)

In the second step, the second feature matrix continues to be built to perform ACHA. Eq 3.30 shows its structure as:

$$S^{3 \times N} = [F \times AD \times B] \quad (3.30)$$

Where:

- F is the $N \times N$ matrix representing the frequency of two blocks being in the same cluster. This frequency was calculated by constructing the common cluster matrix C_{ij}^s for every realization clustering scheme generated in the first step and then summing up these values over all realizations, as shown in Eqs 3.31-3.32:

$$C_{ij}^s = \begin{cases} 1 & \text{if block } i \text{ and } j \text{ in the same cluster} \\ 0 & \text{otherwise} \end{cases} \quad (3.31); \quad F_{ij} = \frac{\sum_{s=1}^S C_{ij}^s}{S} \quad (3.32)$$

- AD is the $N \times N$ matrix determining the adjacency between the blocks by evaluating the normalized distance ($\overline{D_{ij}}$) as in Eq 3.33 and an adjacency threshold (ADT) as in Eq 3.34 to avoid forming fragmented clusters:

$$\overline{D_{ij}} = \frac{D_{ij}}{\max(D_{ij})} \quad (3.33); \quad AD_{ij} = \begin{cases} 1 & \text{if } AD_{ij} < ADT \\ 0 & \text{otherwise} \end{cases} \quad (3.34)$$

- B is the $N \times N$ matrix representing the beneath cluster factor, which is calculated by using a penalty value $c \in [0,1]$ as a difference of two blocks on the same X, Y coordinates but located on two different clusters on two subsequent benches. Eq 3.35 represents this:

$$B_{ij} = \begin{cases} 1 & \text{if block } i \text{ and } j \text{ are above the same cluster} \\ c & \text{otherwise} \end{cases} \quad (3.35)$$

3.5.2 SMIP formulation

3.5.2.1 General formulation in CPLEX

The general formulation in CPLEX [7] for a MIP problem can be expressed as follows:

$$\text{Min.} \quad f = c.z \quad (3.36)$$

$$\text{Subject.} \quad lb \leq z \leq ub \quad (3.37)$$

$$A.z \leq b \quad (3.38)$$

Where:

- f is the $v \times 1$ Matlab double vector containing the objective function coefficients with K is the number of considered production targets
- z is the $v \times 1$ Matlab double vector containing the decision variables of the MIP formulation
- A is the $v \times h$ Matlab double matrix, representing the constraints of the MIP formulation
- b is the $v \times 1$ Matlab double vector defining the upper limit condition of the MIP constraints

- lb / ub is the $v \times I$ Matlab double vector defining the lower and upper limit of decision variables

3.5.2.2 Objective function

The objective function of the SMIP model in Eq 3.14 was constructed following the general format of MIP formulation in CPLEX [7] as given in Eq 3.36. The objective function coefficient has a size of $(3M+SA+2K)T \times I$ and is created following Eq 3.39 below.

$$c^{(3M+SA+2K)T \times I} = [0; p; w; ad; u] \quad (3.39)$$

Where:

- 0 is the $MT \times I$ vector containing zero elements, where M is the number of mining cuts and T is the number of production periods
- p is the $MT \times I$ vector holding the expected discounted mining costs of materials used as raw materials in the raw mix
- w is the $MT \times I$ vector holding the expected discounted mining costs of materials sent to the waste dump
- ad is the $SAT \times I$ vector holding the discounted costs of additive materials, where A is the number of available additives and S is the number of realizations of the quarry deposit
- u is the $2KT \times I$ vector holding the discounted uncertainty costs of not meeting the production targets, where K is the number of considered production targets

The coefficients in Eq 3.39 is multiplied to the decision variables constructed using $(3M+SA+2K)T \times I$ vector in Eq 3.40.

$$z^{(3M+SA+2K)T \times I} = [z0; zp; zw; zad; zu] \quad (3.40)$$

Where:

- $z0$ the $MT \times I$ vector holding the binary variables a_m^t
- zp is the $MT \times I$ vector holding the continuous variables x_m^t
- zw is the $MT \times I$ vector holding the continuous variables y_m^t
- zad is the $SAT \times I$ vector holding the continuous variables Q_{as}^t

- zu is the $2KT \times I$ vector holding the continuous variables Q_{us}^{kt} and Q_{ls}^{kt}

The constraints in the SMIP model are constructed as follows:

3.5.2.3 Constraints

a. Raw mix production capacity constraints

$$A_1 z \leq b_1 \quad (3.41) \quad A_1^{2TS \times (3M+SA+2K)T} = \begin{bmatrix} 0_1 & A_p & 0_1 & A_{ad} & A_{up} \\ 0_1 & -A_p & 0_1 & A_{ad} & A_{up} \end{bmatrix} \quad (3.42)$$

$$b_1^{2ST \times 1} = \begin{bmatrix} R_u \\ R_l \end{bmatrix} \quad (3.43)$$

Where:

- A_p is the $TS \times TM$ matrix holding the total tonnage of materials used as a raw material in the raw mix in each period on each realization within each mining cut
- R_u/R_l is the $TS \times I$ vector of upper/lower limit of raw mix production capacity
- A_{ad} is the $TS \times SAT$ vector holding the available amount of additive materials in each period
- A_{up} is the $TS \times 2KT$ matrix holding the upper and lower deviations of raw mix production in each period
- 0_1 is the $TS \times TM$ zero matrix

b. Raw mix quality constraints

$$A_2 z \leq b_2 \quad (3.44) \quad A_2^{2TSG \times (3M+SA+2K)T} = \begin{bmatrix} 0_1 & A_{gq} & 0_1 & A_{gad} & 0_2 \\ 0_1 & -A_{gq} & 0_1 & A_{gad} & 0_2 \end{bmatrix} \quad (3.45)$$

$$b_2^{2STG \times 1} = \begin{bmatrix} G_u \\ G_l \end{bmatrix} \quad (3.46)$$

Where:

- G is the number of elements of interest
- A_{gq} is the $TSG \times MT$ matrix of the grade of each element of interest in each mining cut on each realization
- G_u/G_l is the $TSG \times I$ vector representing the upper/lower required quality of each element of interest

- A_{gad} is the $TS \times SAT$ matrix of the grade of elements of interest available in additive materials in consideration of realization s
- 0_2 is the $TS \times 2KT$ zero matrix

c. Quarry production capacity constraints

$$A_3 z \leq b_3 \quad (3.47) \quad A_3^{2TS \times (3M+SA+2K)T} = \begin{bmatrix} 0_1 & 0_1 & A_q & 0_3 & A_{uq} \\ 0_1 & 0_1 & A_q & 0_3 & A_{uq} \end{bmatrix} \quad (3.48)$$

$$b_3^{2ST \times 1} = \begin{bmatrix} Q_u \\ Q_l \end{bmatrix} \quad (3.49)$$

Where:

- A_q is the $TS \times MT$ matrix holding the total tonnage of materials within each mining cut extracted at the quarry on each realization
- Q_u/Q_l is the $TS \times 1$ vector of upper/lower limit of quarry production capacity
- A_{uq} is the $TS \times 2KT$ matrix holding the upper and lower deviations of quarry production in each period
- 0_3 is the $TS \times SAT$ zero matrix

d. Sequencing constraints

The sequencing constraint in Eq 3.21 is to enforce the quarry slope not exceeding a predetermined threshold or a safety slope (α). The traditional rule to perform this constraint using block models is several immediate overlying blocks or predecessor blocks must be removed to extract a given one. Approximation [30], [33], and exact methods [79], [80] are two standard techniques, which have been applied in research works and software. For the first method, the sequencing constraint is implemented by removing a certain number of predecessor blocks, such as 5:1 or 9:1. This method is robust but only efficient with a 45 or 26.5 degrees slope angle in all directions. The extract method based on block coordinates and slope angle are chosen to implement the sequencing constraint in this research due to its capacity to be applied on different block sizes and slope angles. Eq 3.50 and Figure 3.2 demonstrate the rule of sequencing constraint using the extract method.

$$\sqrt{(x_i - x_j)^2 + (y_i - y_j)^2} \leq (z_i - z_j) \tan \alpha \quad (3.50)$$

Where:

- (x_i, y_i, z_i) and (x_j, y_j, z_j) are the coordinates of centroids of blocks i and j , respectively
- α is the safety slope applied on the centroid of block i

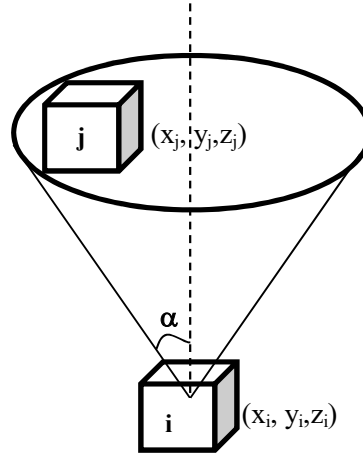


Figure 3.2 Determination of block precedence using slope angle and block coordinates

The sequencing constraint to mining cuts is based on block sequencing in which the predecessors for each block within a given mining cut m are determined. Consequently, the mining cut that the block predecessors belong will be the predecessor of mining cut m . The beneath clustering penalty (Eq 3.3) is used to control the number of predecessors of a mining cut in the clustering process. The numerical modelling of sequencing constraint (Eq 3.22) can be expressed as follows:

$$A_4 z \leq b_4 \quad (3.51)$$

$$A_4^{MT \times (3M+SA+2K)^T} = [A_{se} \quad 0_5 \quad 0_6] \quad (3.52)$$

$$A_{se}^{MT \times MT} = \begin{bmatrix} A_{se1} & 0_4 & \cdots & 0_4 \\ A_{se2} & \ddots & \ddots & \vdots \\ \vdots & \ddots & \ddots & 0_4 \\ A_{se2} & \cdots & A_{se2} & A_{se1} \end{bmatrix} \quad (3.53)$$

Where:

- A_{se1} is the $M \times M$ matrix whose each row contains the total number of predecessors of mining cut m at column m and the values -1 at column m' indicating the predecessors of mining cut m
- A_{se2} is the $M \times M$ matrix whose each row contains the values -1 at column m' indicating the predecessors of mining cut m
- 0_4 is the $M \times M$ zero matrix
- 0_5 is the $MT \times SAT$ zero matrix
- 0_6 is the $MT \times 2KT$ zero matrix
- b_4 is the $MT \times 1$ zero matrix

Whereas, the numerical modelling of Eq 3.23 can be expressed as follows:

$$A_5 z \leq b_5 \quad (3.56) \quad A_5^{MT \times (3M+SA+2K)T} = [A_{se3} \quad A_{se4} \quad A_{se4} \quad 0_5 \quad 0_6] \quad (3.57)$$

$$A_{se3}^{MT \times MT} = \begin{bmatrix} -A_{se5} & 0_4 & \cdots & 0_4 \\ 0_4 & \ddots & \ddots & \vdots \\ \vdots & \ddots & \ddots & 0_4 \\ 0_4 & \cdots & 0_4 & -A_{se5} \end{bmatrix} \quad (3.56) \quad A_{se4}^{MT \times MT} = \begin{bmatrix} A_{se5} & 0_4 & \cdots & 0_4 \\ A_{se5} & \ddots & \ddots & \vdots \\ \vdots & \ddots & \ddots & 0_4 \\ A_{se5} & \cdots & A_{se5} & A_{se5} \end{bmatrix} \quad (3.57)$$

Where:

- A_{se5} is the $M \times M$ matrix whose each row contains the values *one* at column m , indicating the extraction or extraction fraction of mining cut m
- b_4 is the $MT \times 1$ zero matrix

Finally, the numerical modelling of Eq 3.24 can be demonstrated as follows:

$$A_6 z \leq b_6 \quad (3.58) \quad A_6^{M(T-1) \times (3M+SA+2K)T} = [A_{se6} \quad 0_1 \quad 0_1 \quad 0_5 \quad 0_6] \quad (3.59)$$

$$A_{se6}^{M(T-1) \times MT} = \begin{bmatrix} A_{se5} & -A_{se5} & 0_4 & \cdots & \cdots & 0_4 \\ \vdots & A_{se5} & -A_{se5} & \ddots & \ddots & \vdots \\ \vdots & \ddots & \ddots & \ddots & \ddots & \vdots \\ \vdots & \ddots & \ddots & A_{se5} & -A_{se5} & 0_4 \\ 0_4 & \cdots & \cdots & \cdots & A_{se5} & -A_{se5} \end{bmatrix} \quad (3.60)$$

Where:

- b_6 is the $M(T-1) \times 1$ zero matrix

e. Reserve constraint

The reserve constraint in Eq 3.24 is constructed in the form of matrices, as follows:

$$A_7 z \leq b_7 \quad (3.61) \quad A_7^{MT \times (3M+SA+2K)T} = [0_7 \quad A_{re} \quad A_{re} \quad 0_8 \quad 0_9] \quad (3.62)$$

$$A_{re}^{MT \times MT} = \begin{bmatrix} A_{se5} & 0_4 & \cdots & 0_4 \\ A_{se5} & \ddots & \ddots & \vdots \\ \vdots & \ddots & \ddots & 0_4 \\ A_{se5} & \cdots & A_{se5} & A_{se5} \end{bmatrix} \quad (3.63)$$

Where:

- 0_7 is the $MT \times MT$ zero matrix
- 0_8 is the $MT \times SAT$ zero matrix
- 0_9 is the $MT \times 2kT$ zero matrix
- b_7 is the $MT \times 1$ zero matrix

Finally, all matrices and vectors are concentrated to form a coefficient matrix A with a size of $2TS(G+2)+M(4T-1) \times (3M+SA+2K)T$ and a boundary as shown in Eq 3.25 and an upper limit condition vector with a size of $(3M+SA+2K)T \times 1$. The concentration is illustrated as follows:

$$A^{2TS(G+2)+M(4T-1) \times (3M+SA+2K)T} = [A_1; A_2; A_3; A_4; A_5; A_6; A_7] \quad (3.64)$$

$$b^{(3M+SA+2K)T \times 1} = [b_1; b_2; b_3; b_4; b_5; b_6; b_7] \quad (3.65)$$

3.6 Conclusion

This chapter presents a stochastic optimization framework for the LTQPP problem, using geostatistical simulation techniques, the block clustering approach KHRA, and the SMIP model. In this framework, geostatistical simulation is initially deployed to implement the resource simulation using the hierarchical approach to capture the geological uncertainty of rock types and chemical grades. Subsequently, the clustering stage applies the KHRA to aggregate blocks into mining cuts to reduce the SMIP formulation size, which allows generating solutions in a reasonable timeframe. KHRA could improve the optimization problem's objective value since it avoids aggregate the low uncertainty blocks with high uncertainty blocks into a mining cut. A new SMIP model was formulated that takes mining cuts as input data to find an optimal production schedule in the final stage with two objectives: to minimize the raw mix cost and

minimize the risk of not meeting production targets. This model was expanded from the DMIP model, which was also introduced in this chapter.

Numerical modelling of the clustering approach and the SMIP model was performed to formulate the proposed framework into the Matlab environment. The numerical results are a series of matrices and vectors in a form that the CPLEX solver recognises. GUIDE function in Matlab employs these matrices and vectors to create a software application (see Appendix I).

Chapter 4. Hierarchical simulation of cement raw material deposit

4.1 Introduction

A cement production starts at the raw material deposit. Thus, raw material quality management plays a crucial role in cement manufacturing. Exploration, modelling, and planning are three necessary steps to raw material quality management in cement manufacturing. The exploration step supplies data for the modelling stage, possible including core data available from a limited number of exploratory drill holes or sometimes from rig drilling. The main characteristic of the data is sparse relative to the region that must be modelled, and hence, uncertainty is inevitable in estimation and commonly referred to as geological uncertainty. Geological uncertainty can be transferred into raw material extraction planning, resulting in discrepancies between planning expectations and actual production [79]. Understanding the geological uncertainty and associated risk in resource modelling is very important to future extraction planning and cement plant operations.

This chapter examines an application of geostatistical simulation for assessing the mineral resources and quantifying the geological uncertainty through a case study on the Ta Thiet deposit, located in Southern Vietnam. The main results of this chapter were published in [80]. The deposit has four primary facies or rock types, including soil, clay, laterite, and limestone, which control mineral grade occurrence and spatial distribution. For example, CaO grade is averagely high in limestone and low in soil, clay, laterite. Hence, the risk due to the uncertainty of rock-type domains is essential. The traditional method to integrate the uncertainty of rock types relies on the subjective or deterministic interpretation of geological domains. Subsequently, one can predict the mineral grades within each domain. However, this method reveals only one scenario of rock type domains and fails to measure the uncertainty of rock type distribution and improve the geological interpretation. As presented in Chapter 3, the hierarchical simulation consists of simulating the layout of the rock-type domains and then the chemical grades within each domain conditionally to the grade data inside this domain only. In this research, a total of 20 realizations of chemical grades was produced based on 20 realizations of rock-type domains to capture and assess the risks due to geological uncertainty.

4.2 Research area

4.2.1 General description

Ta Thiet limestone deposit is located 80 km south of Ho Chi Minh City, in the Binh Phuoc province of Vietnam. Figure 4.1 displays the location map of the deposit and the exploratory drill holes. The research area represents a gentle slope downward from West to East, and the agricultural soil covers most of the research area. The deposit consists of four primary rock types, including soil, clay, laterite, and limestone. Currently, the deposit is mined by the Ha Tien cement company, using the open-pit method and supplying raw materials for the Binh Phuoc cement plant, which is situated about 7.5 km far away.

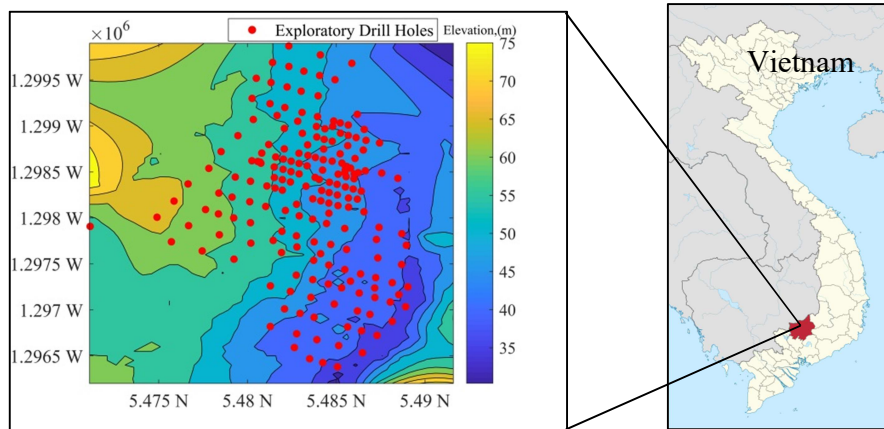


Figure 4.1 Locations of the research area and exploratory drill holes

4.2.2. Data set

Data from 194 exploratory drill holes arranged in a grid with an average spacing of $50\text{ m} \times 50\text{ m}$ to $100\text{ m} \times 100\text{ m}$ were available for this research. Along the drill holes, 3877 samples were obtained and composited into 888 data at a length of 10 m (a minimum length of 2 m), with information on the common rock types and six primary chemical grades, including CaO, SiO₂, Al₂O₃, Fe₂O₃, MgO, and LOI. Figures 4.2 and 4.3 show a perspective view of the rock types and six grades in the research area. Figure 4.4 displays bimodal distributions of the primary chemical grades via histograms, suggesting that the data is a mixture of various populations. CaO, MgO, and LOI are mostly available in the limestone, while SiO₂, Al₂O₃, Fe₂O₃ are in the remaining rock types.

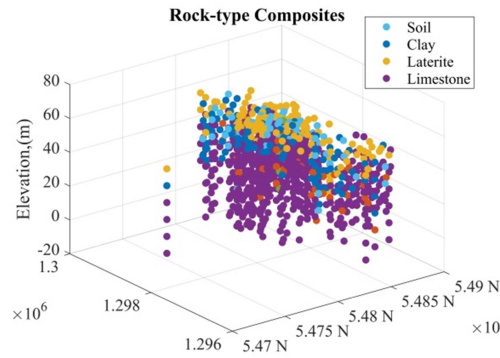


Figure 4.2 A perspective view showing the composites of rock-type composites in the research area

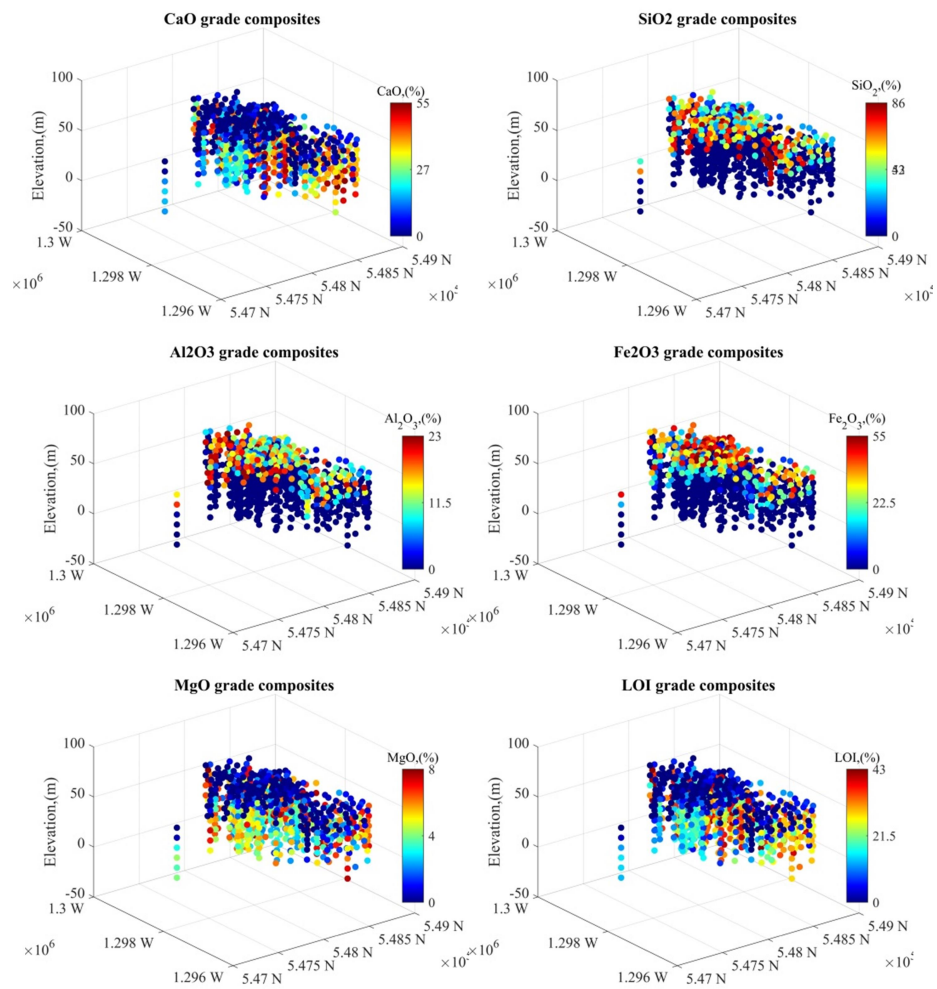


Figure 4.3 A perspective view showing composites of CaO, SiO₂, Al₂O₃, Fe₂O₃, MgO, and LOI grades in the research area

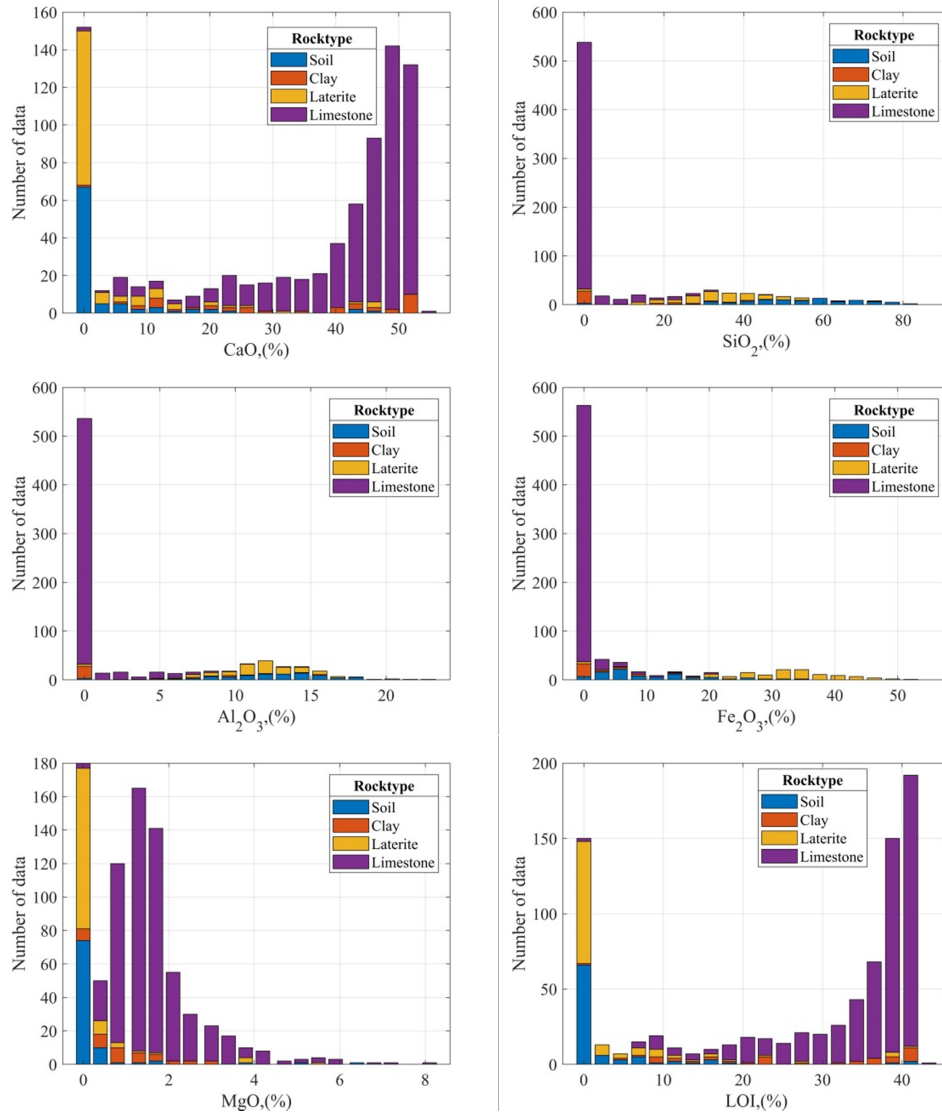


Figure 4.4 Histogram of the six chemical grades

Table 4.1 shows a strong influence of rock types on the average grades. Laterite is the primary source of high grades of Al_2O_3 and Fe_2O_3 , and clay and limestone mainly produce high CaO and SiO_2 , respectively. These facts motivate the resource to a hierarchical simulation approach in which modelling the rock types first can improve grade estimation accuracy.

Table 4.1 Relationships between the rock-type domains and average grades

Rock type	CaO	SiO ₂	Al ₂ O ₃	Fe ₂ O ₃	MgO	LOI
Soil	4.24	55.15	13.3	11.89	0.35	3.73
Clay	34.02	12.48	3.68	3.79	1.23	27.83
Laterite	4.65	35.74	11.87	32.56	0.31	4.11
Limestone	44.03	2.1	0.59	0.75	1.89	36.16

4.3. Application of hierarchical simulation

4.3.1 Rock-type simulation

4.3.1.1 Trend modelling

All rock types in the deposit show clear upward geological trends established by splitting the composited rock type data into cells of the grid used in the simulation and then calculating the proportion of the rock type in each cell. Also, the areal trends were produced by grouping the composited data in different regions of the research area and averaging rock-type proportions in each region. Nevertheless, the indication of the areal trend of rock types was not clear. Hence, only the upward trends were considered for rock-type simulation. Figure 4.5 (right) shows rock-type proportions along the vertical direction, which indicates a trend as the expectation of geologists: more limestone and less soil, laterite, and clay are at the bottom. Matlab Curve Fitting Toolbox [5] was used to fit the upward trend.

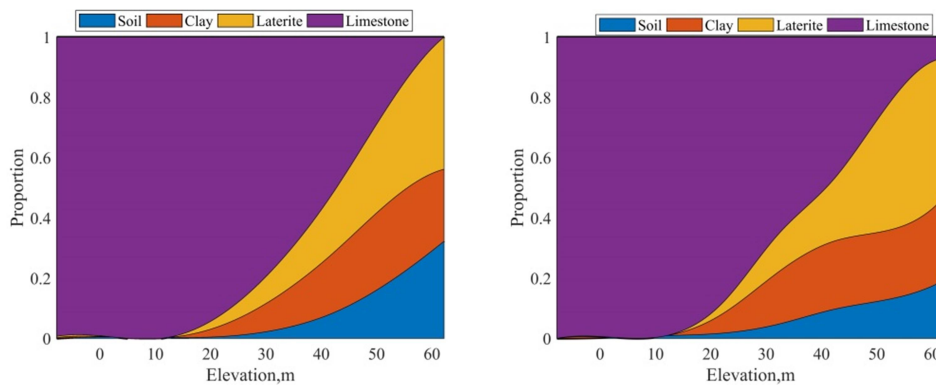


Figure 4.5 Rock-type proportion along the upward direction (right); Example of reproduced trend (right) of rock-type domains on a realization

4.3.1.2 Variogram Analysis

The direct variograms were computed on the codified 0-1 indicator values. First of all, 2D variogram maps, a collection of experimental variogram values, were built to determine major horizontal directions of continuity (Figure 4.6). Two variograms in the horizontal plane and one variogram in the vertical direction were calculated and modelled for each rock type variable. Finally, all experimental variograms were modelled by selecting structure types and correlation ranges for each structure. Figure 4.7 presents the experimental variograms of the rock types and their fitting models in the horizontal and vertical directions.

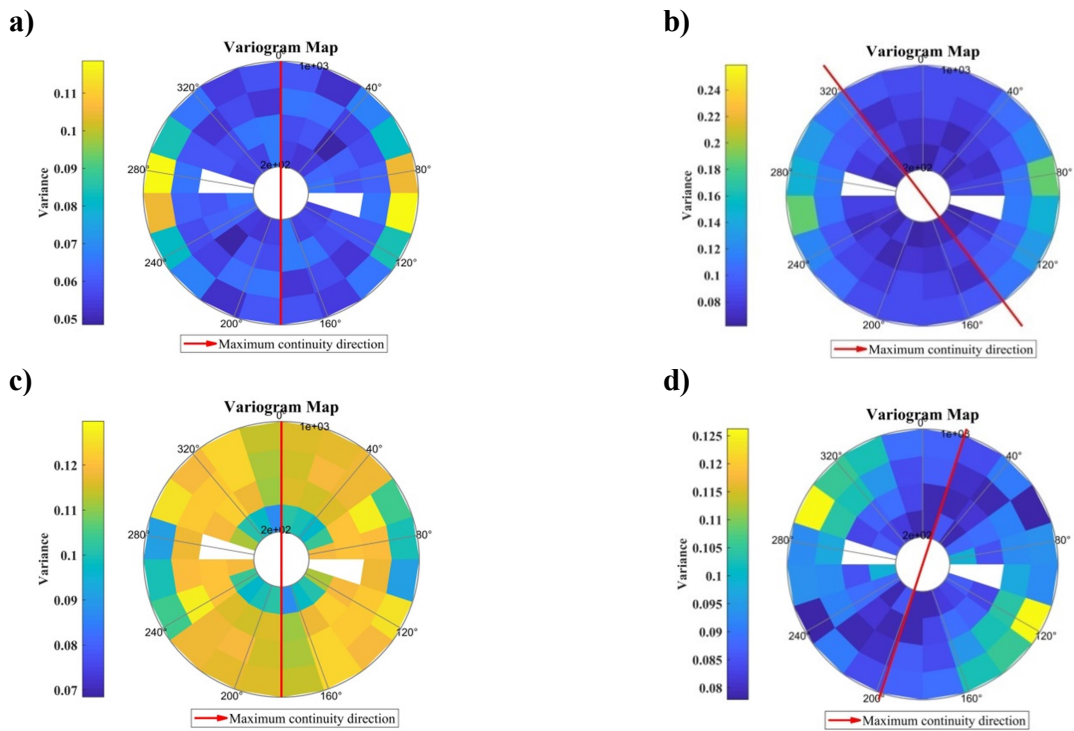


Figure 4.6 Variogram maps of Soil (a), Clay (b), Laterite (c), and Limestone (d). The red lines show the direction of maximum continuity in composited rock-type data

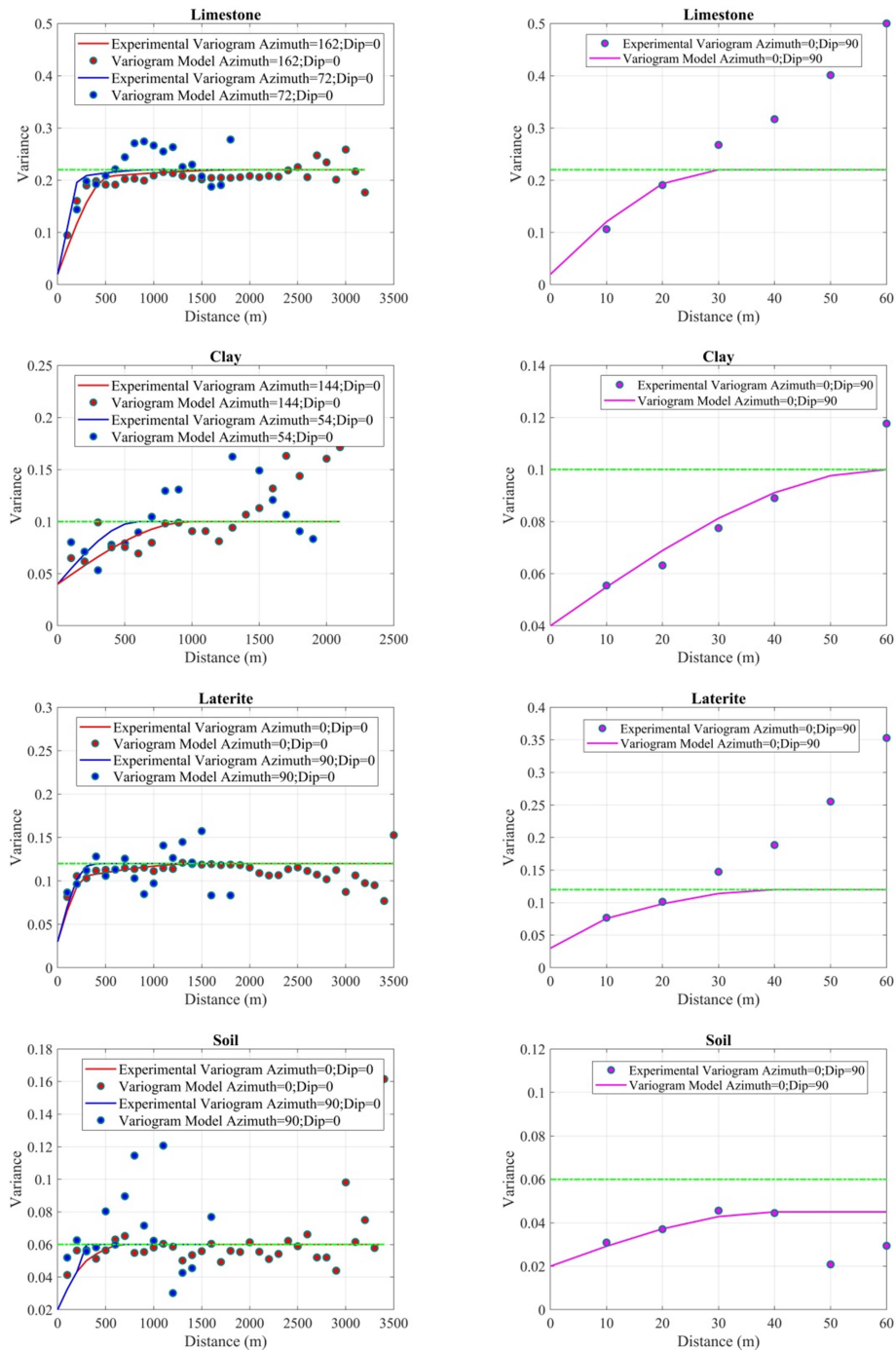


Figure 4.7 Experimental variograms and their suitable models of limestone in the horizontal and vertical directions

Table 4.2 summarises the indicator variogram parameters for each rock type. In all rock types, the variograms have a more extensive range in the horizontal plane than

along the vertical direction, which can be explained by the deposition of rock types in thin layers. The experimental variogram of soil corresponds to zonal anisotropy, where only the horizontal directions contribute fully to the total variance of the phenomenon at that scale. It is because soil mainly appears in a thin layer, so that its data may be insufficient to calculate the total variability. A visual representation of the experimental variograms suggests that the spherical models are reasonably agreed with the data.

Table 4.2 Indicator variogram parameters for each rock type

Rock type	Direction	Nugget	Structure1			Structure2		
			Model	Sill	Range(m)	Model	Sill	Range(m)
Soil	Azimuth 0 ⁰	0.02	Sph.	0.025	700	Sph.	0.015	300
	Azimuth 90 ⁰				300			250
	Vertical				40			∞
Clay	Azimuth 144 ⁰	0.04	Sph.	0.06	1000	-	-	-
	Azimuth 54 ⁰				600			-
	Vertical				60			-
Laterite	Azimuth 0 ⁰	0.03	Sph.	0.07	300	Sph.	0.02	1500
	Azimuth 90 ⁰				300			450
	Vertical				40			10
Limestone	Azimuth 162 ⁰	0.02	Sph.	0.18	550	Sph.	0.02	2000
	Azimuth 72 ⁰				250			1000
	Vertical				30			20

4.3.1.3 Rock-type simulation

Section 4.3.1.1 shows a clear trend of rock-type data along the vertical direction. Hence, constraining SIS to the trend is essential. One can decompose the rock-type data into a residual and a locally variance mean (LVM) and use either of them to incorporate the trend into SIS. However, working with residuals may lead to some problems, including bias in the covariance matrix due to the form of trend function [81]–[83]. In this research, LVM was used as ancillary information that indicates a trend or non-stationary influence of the rock-type variable to simulate rock types. The simulation was performed using the *sisim_lm* program in GSLIB software [6]. Twenty conditional simulations of

rock types were generated on block dimensions of $50 \times 50 \times 10$ m based on the dimension of selective mining unit sizes for future mine planning.

As an illustration, Figure 4.8 displays an example (realization #1) of the spatial distribution of four rock-type domains suggesting that the dominant rock type domain in the research area is limestone. The uncertainty of rock-type distribution can be accessed. For example, Figure 4.9 maps the probabilities of occurrence of four rock types on 3D block models (left), cross-sections (middle), and horizontal sections (right). In these probability maps, the red regions indicate a high possibility for a rock-type occurrence at these locations, while the blue areas are associated with a low chance of finding that rock type at these locations. It is clear that the probability of the existence of limestone increases along with the depth, especially under 20 m, the limestone is very abundant in comparison with other rock types, which mainly concentrate in the upper region. Realizations and occurrence probability of rock types at distinct elevation (32.2 m), as shown in Figure 4.9 (middle and right), respectively, suggest that the distributions of soil, clay, and laterite are not local. They concentrate in small quantities across the section, indicating the difficulty of extracting the raw materials selectively.

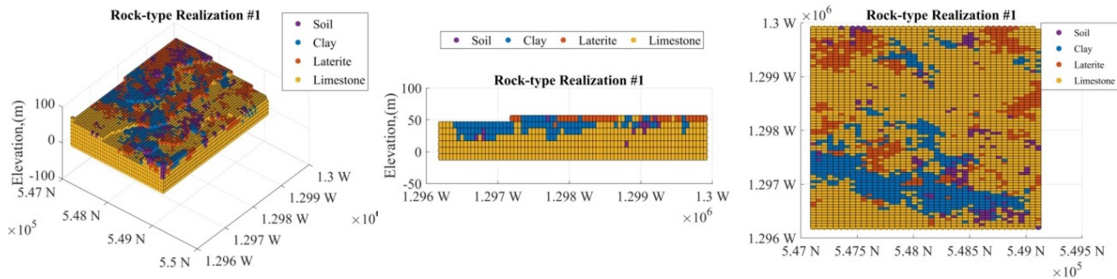


Figure 4.8 Perspective view (left), cross-section (easting = 548110 m) (middle), and horizontal section (elevation= 32.2 m) (right) of rock-type realization #1

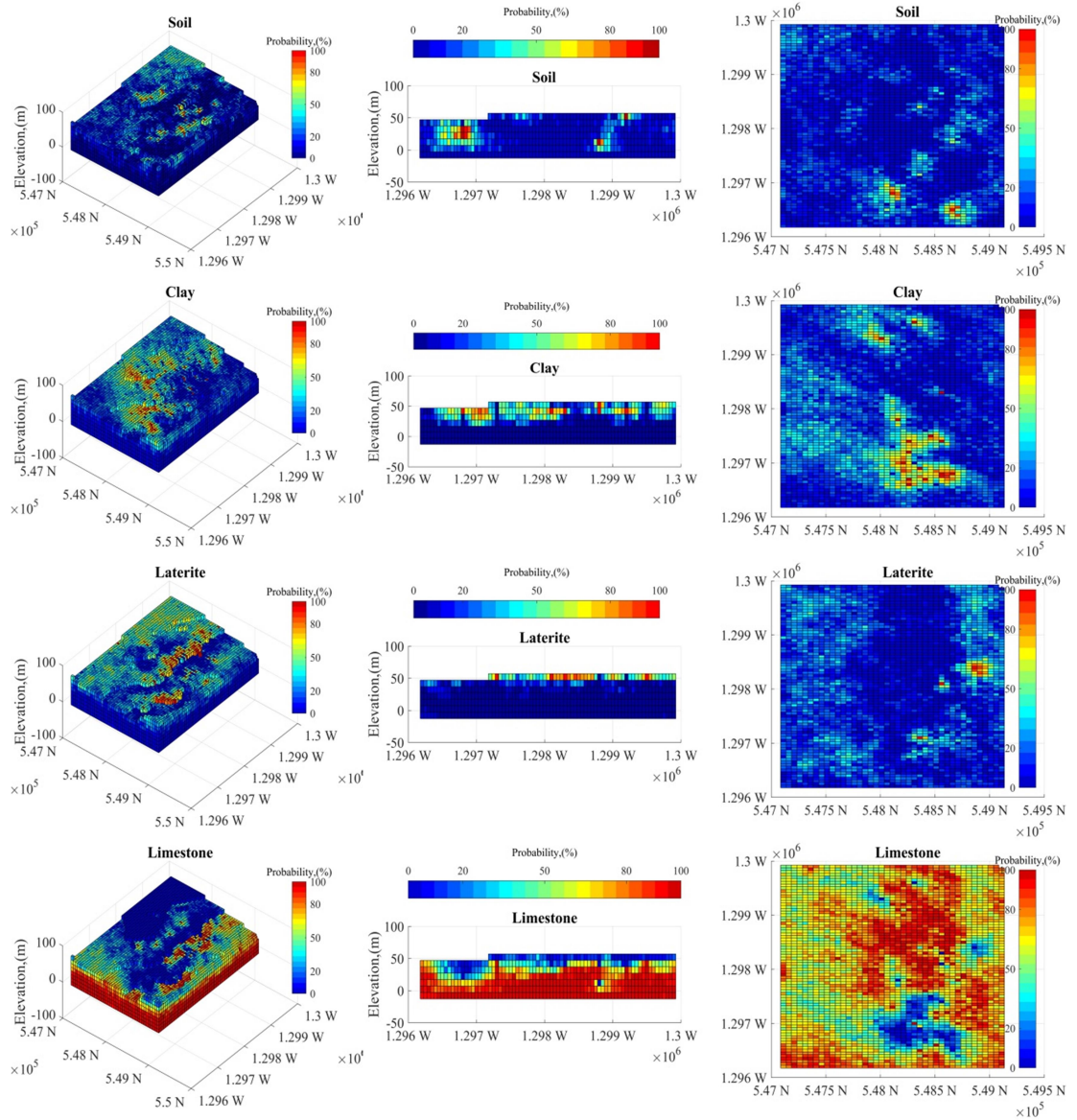


Figure 4.9 Probabilities of occurrence of four rock types, obtained from a set of 20 conditional realizations on 3D block model (left), cross-section (easting = 548110 m) (middle), and horizontal section (elevation= 32.2 m) (right)

4.3.1.4 Validation

A first validation consists of a visual check of histogram and trend reproduction of rock-type domains between the realizations and the composited rock-type data. Each realization should reproduce similar statistical properties and upward trends of the

composited rock-type data. The reproduction of trend and histogram can be seen clearly in Figures 4.5 (right) and 4.10, respectively.

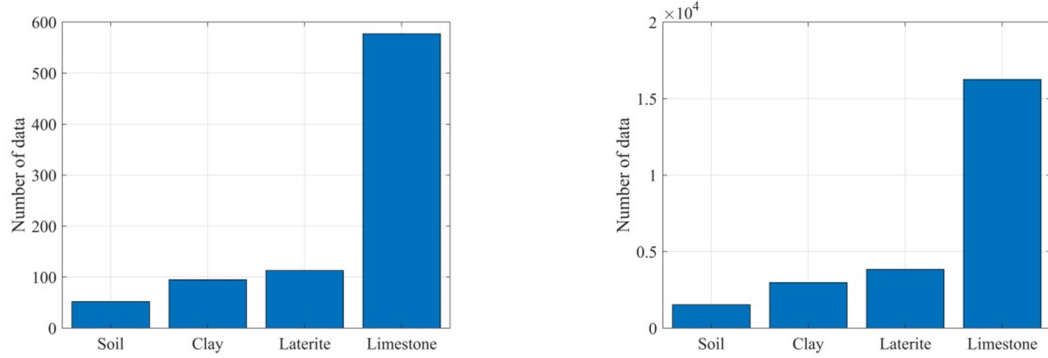


Figure 4.10 Comparison of histograms of rock types between composited data (left) and Realization #1 (right)

A second validation consists of checking the ability of the simulated realizations to preserve the spatial features of the composited rock-type data during the simulation process, which can be done by comparing the fitting variogram models and the variograms on simulated data. The simulated variograms are not as well-behaved and show a higher variance against the model, as shown in Figure 4.11. This limitation of SIS is due to it only accounts for direct indicator variograms and ignores cross-variograms which convey information on the geometry of the domain layouts and their contact relationships as well as higher-order distributional properties. An alternative indicator simulation approach, such as plurigaussian, should be considered in the future.

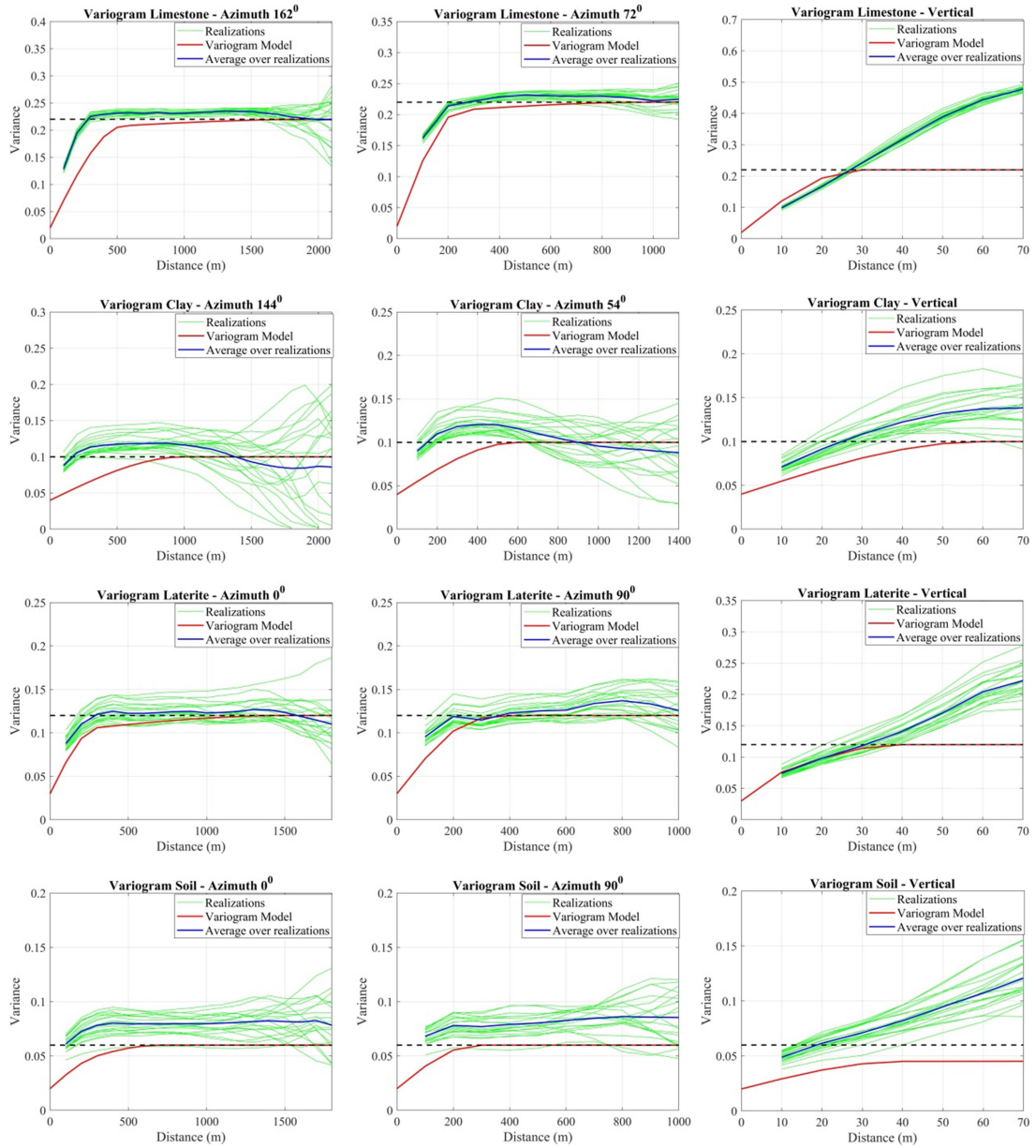


Figure 4.11 Reproduced variograms of four rock types

4.3.2 Grade simulation

Based on the analysis of the data set in Section 4.2.2, one observes that the distribution of the grade variables is consistent with the rock types. Hence, it is reasonable to separate the deposit into two domains for all grade variables before the resource evaluation process: the first consists of soil, clay, and laterite (domain 1); the second consists of limestone (domain 2).

4.3.2.1 Grade simulation

The grade simulation proceeds as follows:

i) Cell declustering: This step is to avoid nonrepresentative sampling in the research area. The application of cell declustering technique to the grade data set in each domain was made by *declus* program in GSLIB [6] using the minimum size of 50 m, the maximum size of 100 m with the number of cell sizes, and the number of origin offsets is 50 and 5, respectively. The changes in mean values of the grades in each domain before and after declustering are shown in Table 4.3.

Table 4.3 Mean value of chemical grades before and after declustering

Domain	Grade	Mean value	Declustered Mean
1	CaO	8.36	7.7
	SiO ₂	40.48	38.35
	Al ₂ O ₃	11.06	10.58
	Fe ₂ O ₃	20.48	18.67
	MgO	0.43	0.39
	LOI	7.04	6.6
2	CaO	43.03	39.41
	SiO ₂	3.13	2.84
	Al ₂ O ₃	0.91	0.81
	Fe ₂ O ₃	1.26	0.98
	MgO	1.84	1.77
	LOI	35.37	32.62

ii) Normal scores transformation: This step transforms the declustering data into Gaussian space or normal score.

iii) Variogram analysis: In this step, 2D variogram maps were generated first to evaluate the existence of spatial anisotropy and determine the direction of maximum continuity of Gaussian grades in each domain (Figures 4.12 and 4.13). Experimental variograms and their fitting models were built to characterize the spatial correlation

structures of Gaussian grades within their controlled domain (Figures 4.14 and 4.15). Tables 4.4 and 4.5 present a summary of the fitting variogram models.

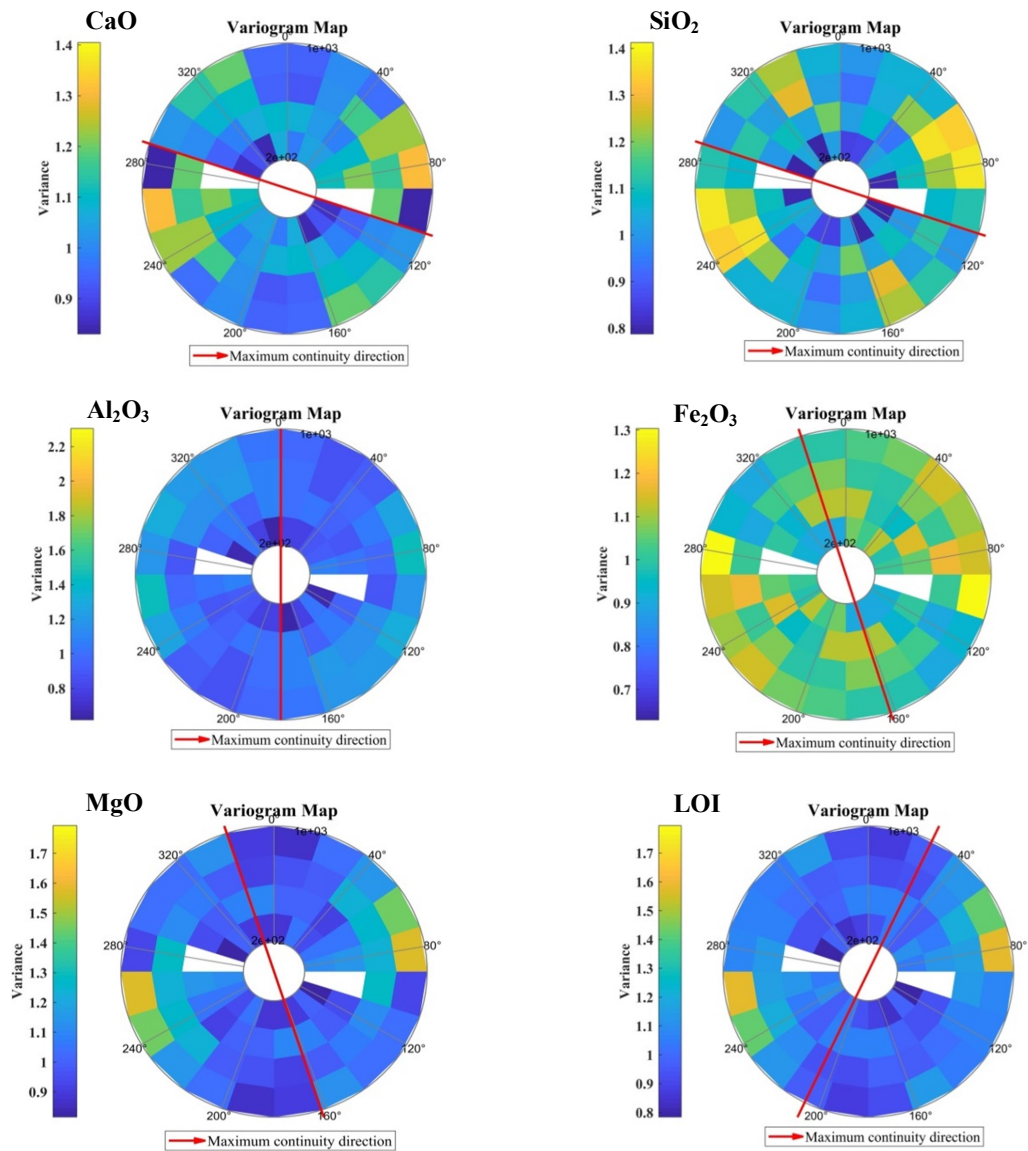


Figure 4.12 Variogram maps of the six chemical grades within domain 1. The red lines show the direction of maximum continuity in composited grade data

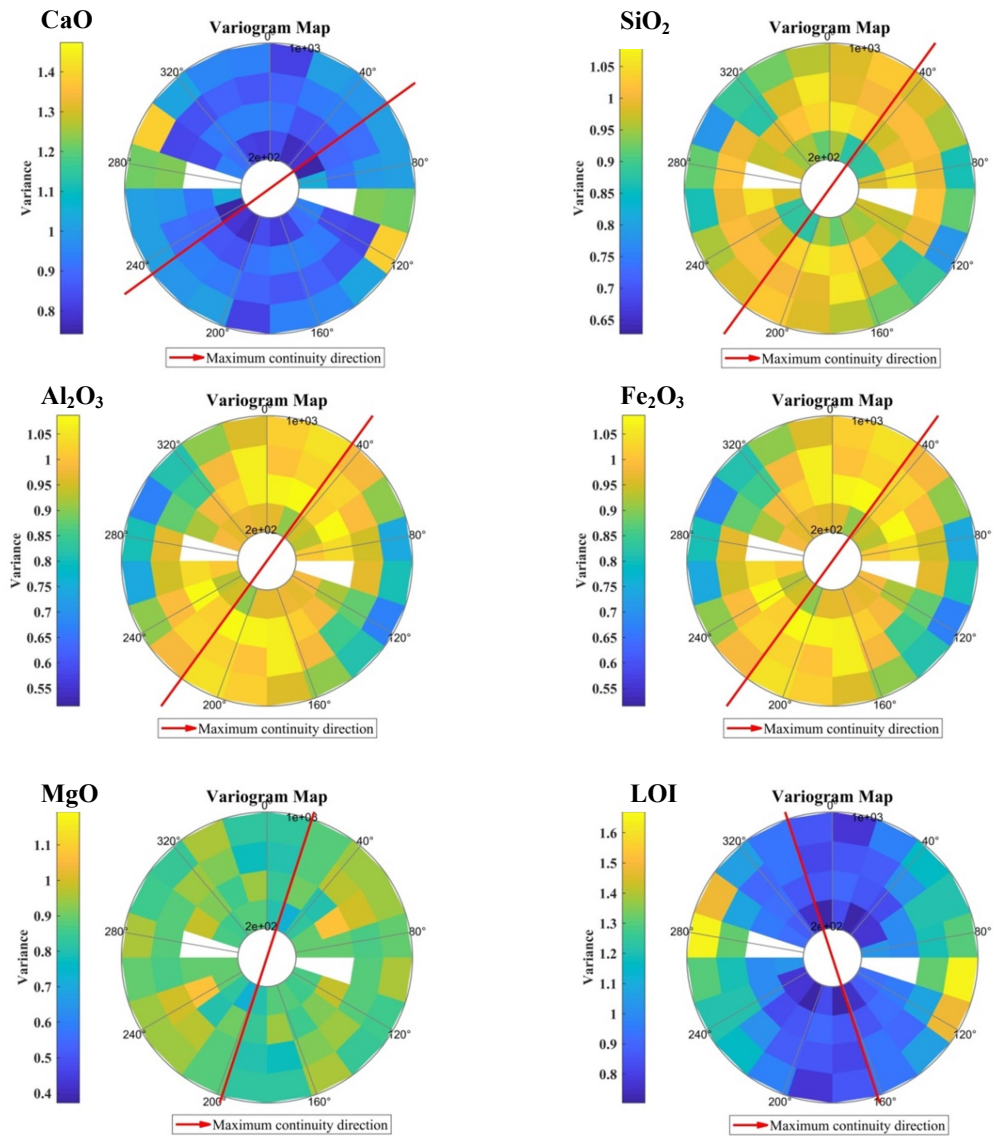


Figure 4.13 Variogram maps of the six chemical grades within domain 2. The red lines show the direction of maximum continuity in composited grade data

Table 4.4 Fitting parameters of variogram models for each Gaussian grades in domain 1
(*Sph* – Spherical; *Exp* – Exponential)

Gaussian Grade	Direction	Nugget	Structure 1			Structure 2		
			Model	Sill	Range(m)	Model	Sill	Range(m)
CaO	Azimuth 108 ⁰	0.2	Sph.	0.8	400	-	-	-
	Azimuth 18 ⁰				200			-
	Vertical				25			-
SiO ₂	Azimuth 108 ⁰	0.1	Sph.	0.7	500	Sph.	0.2	200
	Azimuth 18 ⁰				150			150
	Vertical				20			25
Al ₂ O ₃	Azimuth 0 ⁰	0.1	Sph.	0.35	200	Exp.	0.55	700
	Azimuth 90 ⁰				100			500
	Vertical				20			20
Fe ₂ O ₃	Azimuth 162 ⁰	0.1	Exp.	0.5	300	Sph.	0.4	100
	Azimuth 72 ⁰				160			100
	Vertical				30			15
MgO	Azimuth 162 ⁰	0.1	Exp.	0.7	400	Exp.	0.2	100
	Azimuth 72 ⁰				200			100
	Vertical				27			34
LOI	Azimuth 36 ⁰	0.1	Exp.	0.65	300	Sph.	0.25	100
	Azimuth 126 ⁰				200			100
	Vertical				18			23

iv) Sequential Gaussian Simulation (SGS): SGS was used to construct 20 realizations on a block size of 50 × 50 × 10 meters for each Gaussian grade based on each of 20 rock-type layouts. The entire domains were simulated first at point support of 25×25×5 meters to address the volumetric support of blocks, followed by averaging 20 realizations to obtain block support simulation. Since the simulation was carried out on

Gaussian data, the estimated values were back-transformed to the original unit. Figure 4.16 shows an example of the spatial distribution of SiO₂, CaO, Al₂O₃, Fe₂O₃, and MgO grades generated on rock-type realization #1 through the 3D block model, horizontal and horizontal section of the deposit.

Table 4.5 Fitting parameters of variogram models for each Gaussian grades in domain 1

(Sph – Spherical; Exp – Exponential)

Gaussian Grade	Direction	Nugget	Structure 1			Structure 2		
			Model	Sill	Range(m)	Model	Sill	Range(m)
CaO	Azimuth 54 ⁰	0.05	Exp.	0.4	700	Exp.	0.55	200
	Azimuth 144 ⁰				200			100
	Vertical				74			75
SiO ₂	Azimuth 36 ⁰	0.5	Exp.	0.5	200	-	-	-
	Azimuth 126 ⁰				100			-
	Vertical				27			-
Al ₂ O ₃	Azimuth 36 ⁰	0.5	Exp.	0.5	300	-	-	-
	Azimuth 126 ⁰				110			-
	Vertical				25			-
Fe ₂ O ₃	Azimuth 36 ⁰	0.5	Sph.	0.5	170	-	-	-
	Azimuth 126 ⁰				110			-
	Vertical				23			-
MgO	Azimuth 18 ⁰	0.1	Exp.	0.5	800	Exp.	0.4	200
	Azimuth 108 ⁰				300			200
	Vertical				65			59
LOI	Azimuth 162 ⁰	0.05	Sph.	0.5	100	Exp.	0.55	200
	Azimuth 72 ⁰				200			100
	Vertical				100			81

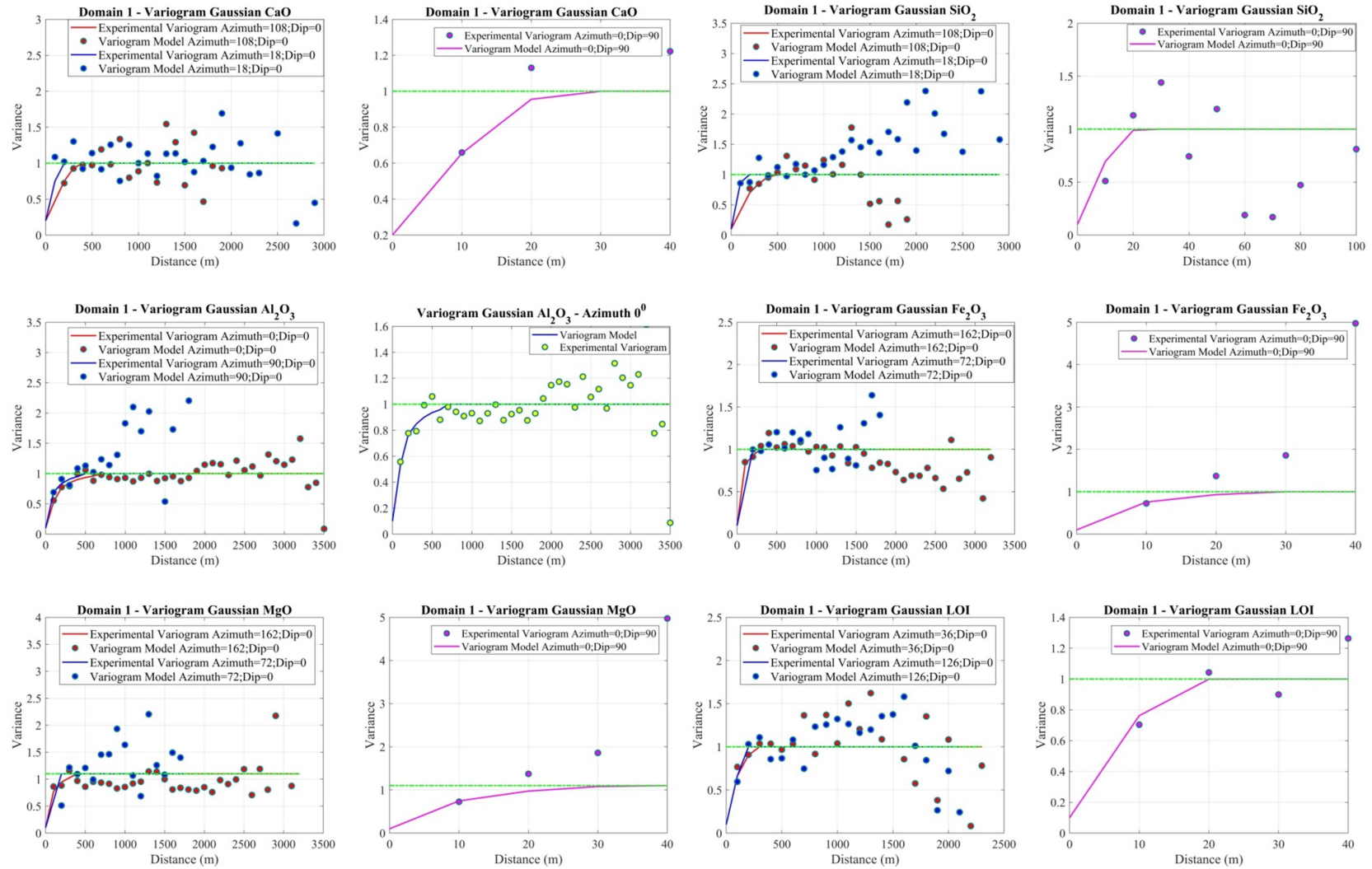


Figure 4.14 Experimental variograms and their fitting models of the six chemical grades in the horizontal plane within domain 1

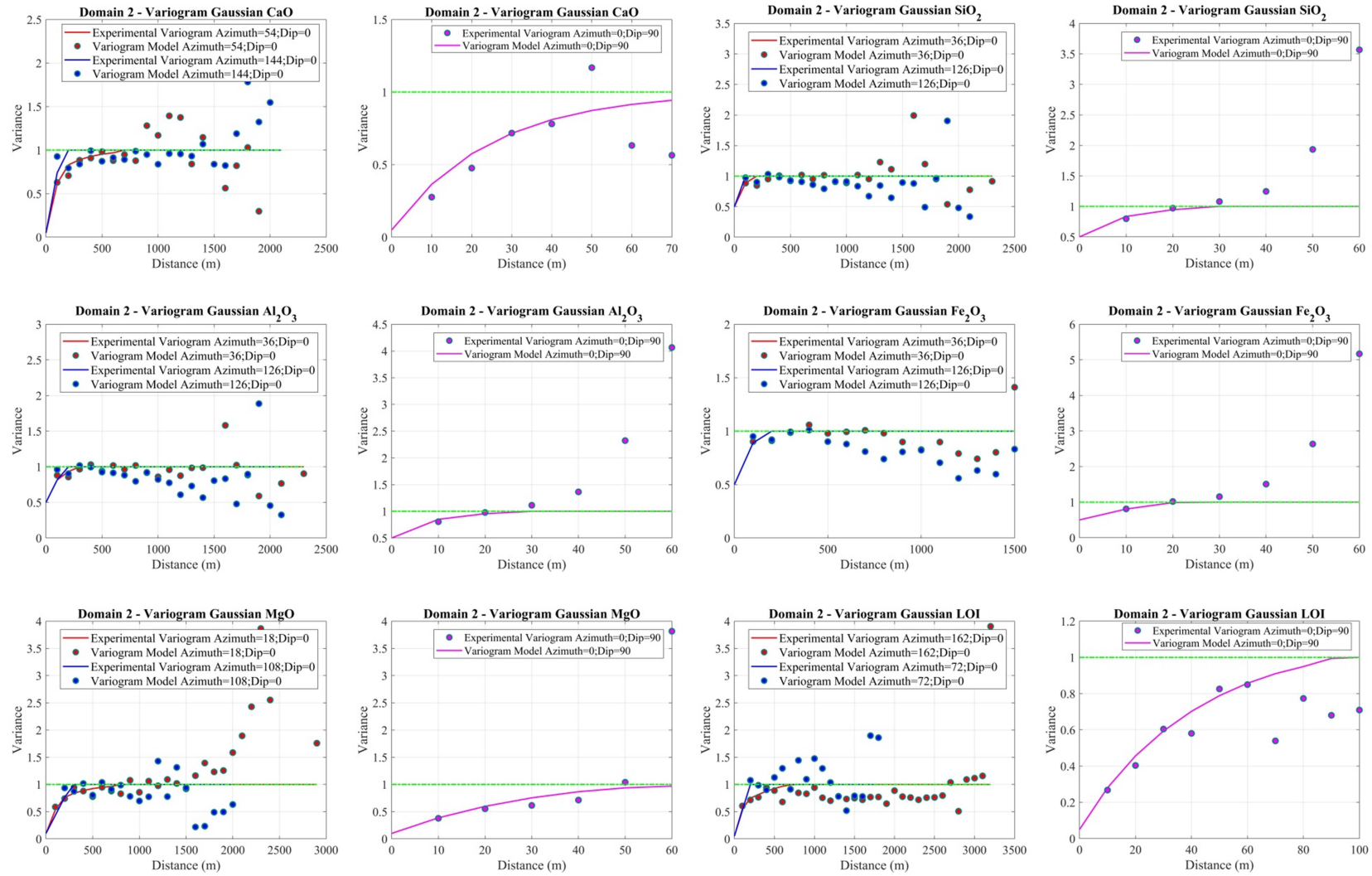


Figure 4.15 Experimental variograms and their fitting models of the six chemical grades in the horizontal plane within domain 2

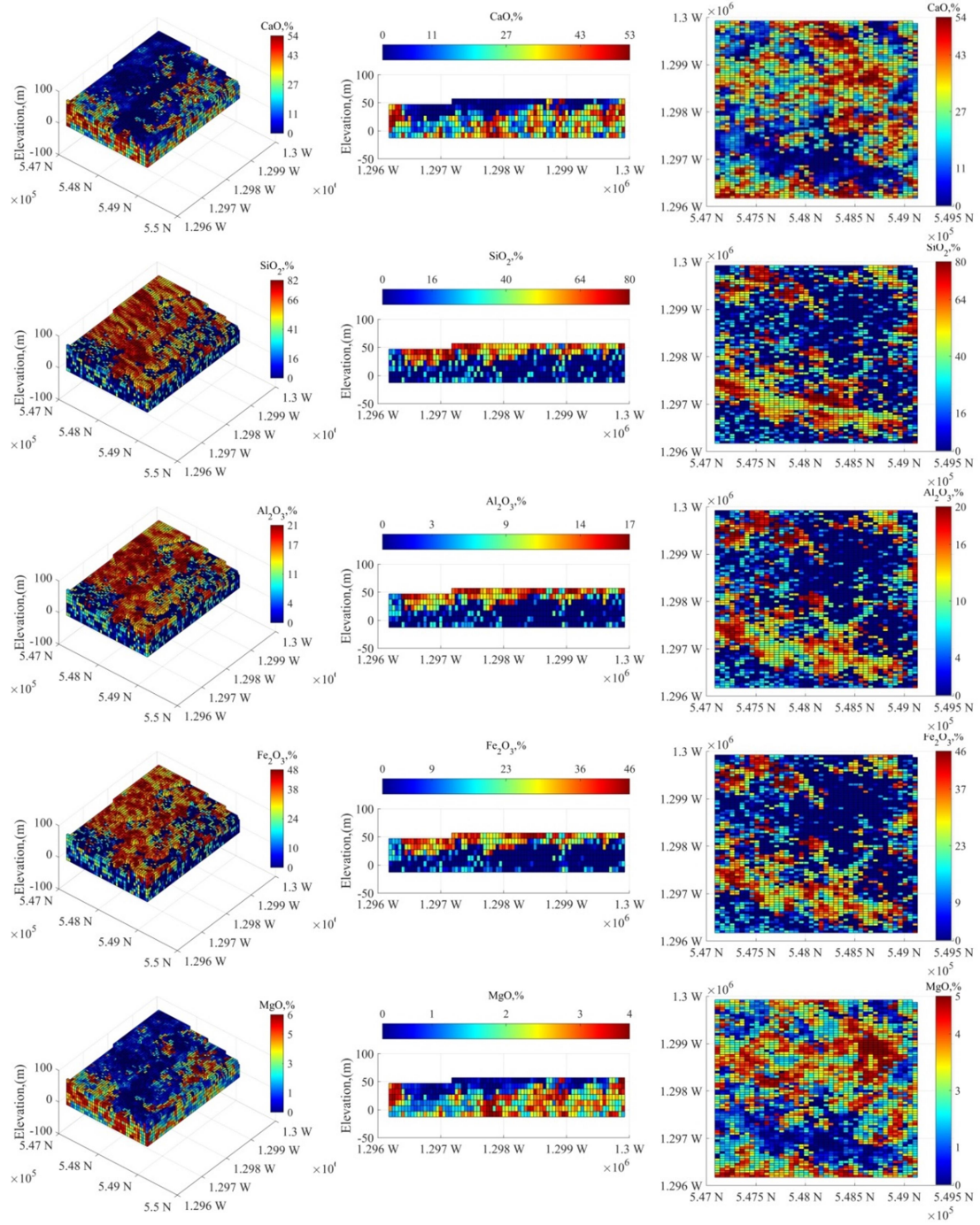


Figure 4.16 Example of the spatial distribution of SiO_2 , CaO , Al_2O_3 , Fe_2O_3 and MgO grades generated on rock-type realization #1 on 3D block model (left), cross-section (easting = 548110 m) (middle), and horizontal section (elevation= 32.2 m) (right)

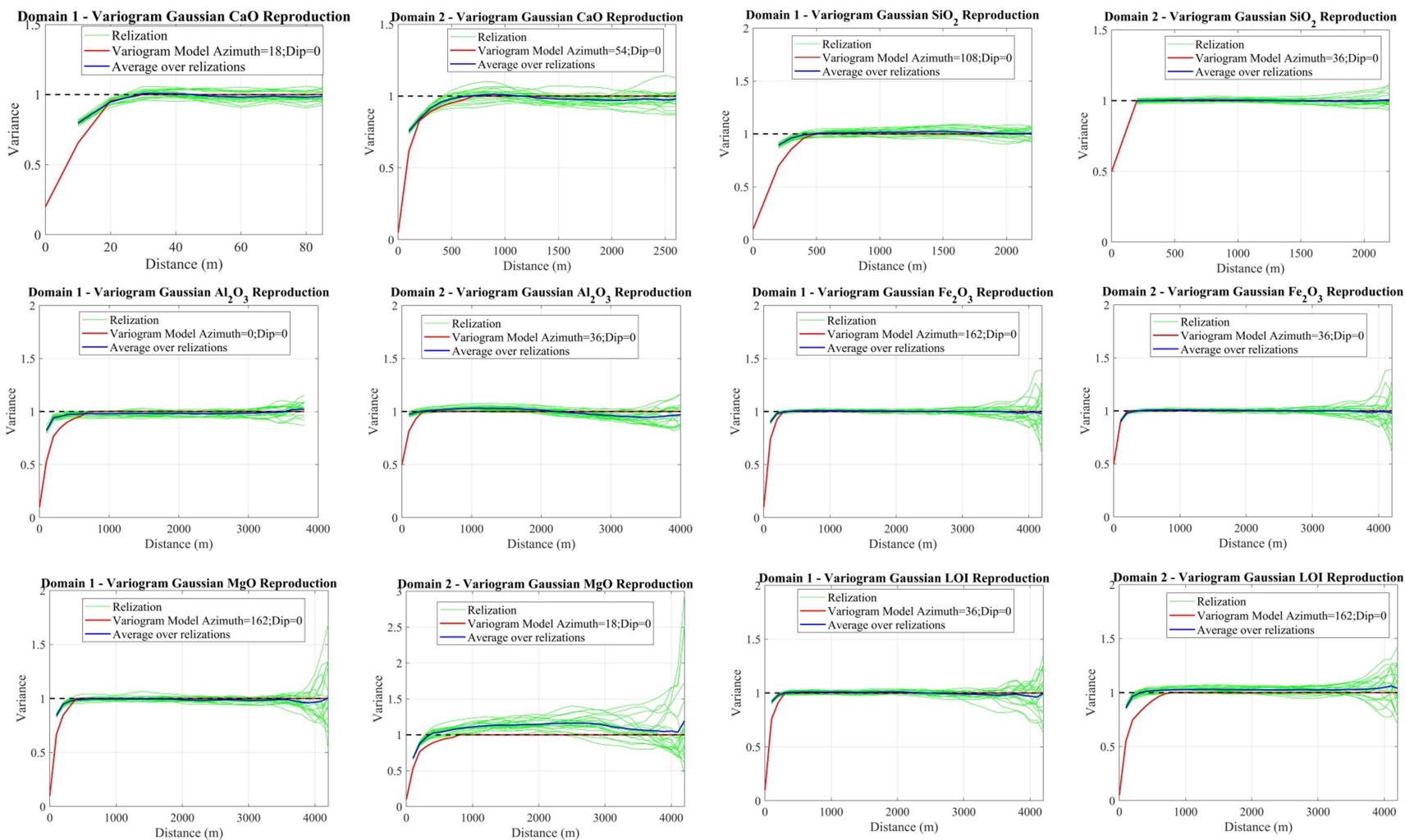


Figure 4.17 Variogram reproduction in the main direction of the six chemical grades within Domain 1 and Domain 2

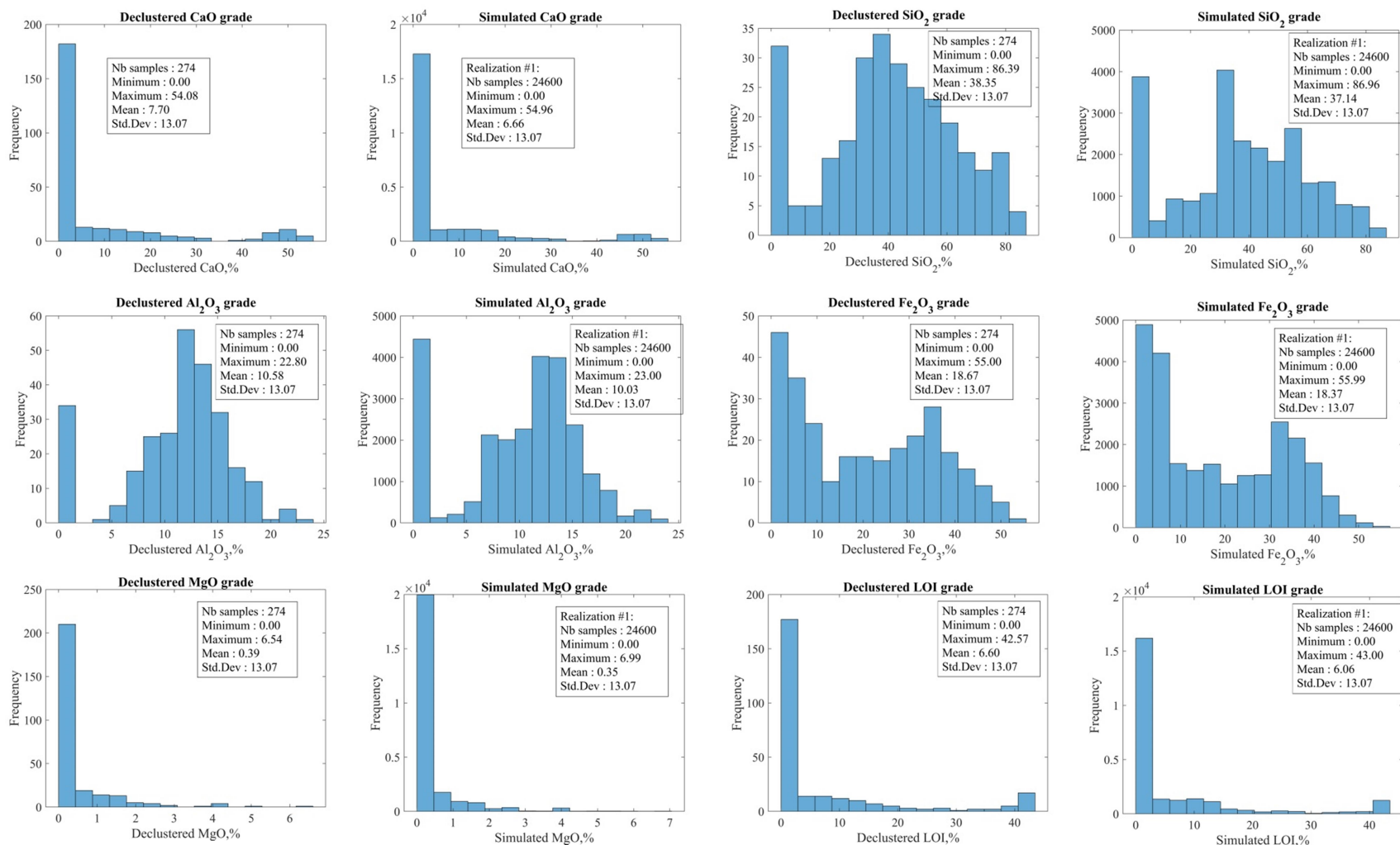


Figure 4.18 Histogram reproductions of the six chemical grades in Domain 1

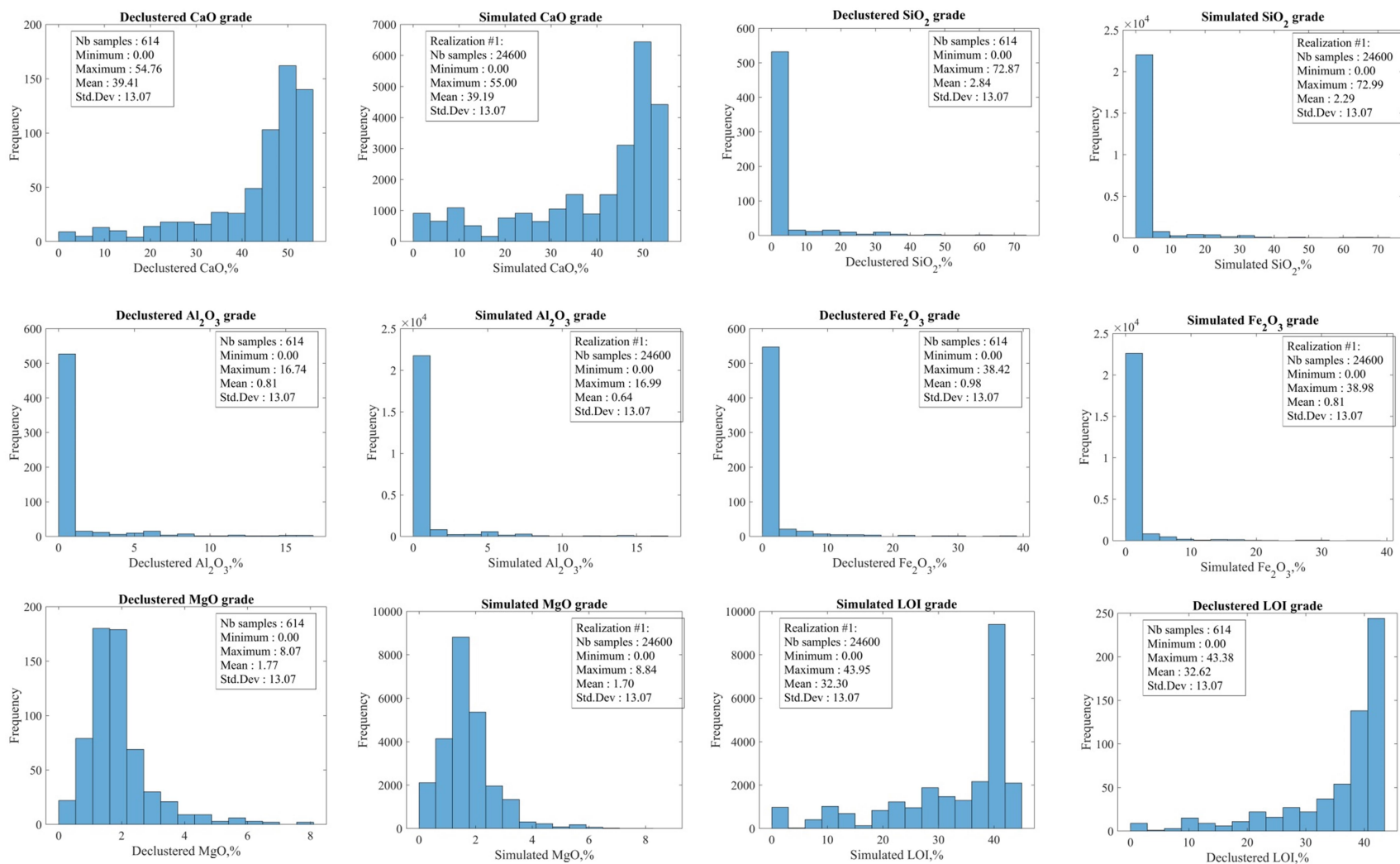


Figure 4.19 Histogram reproductions of the six chemical grades in Domain 2

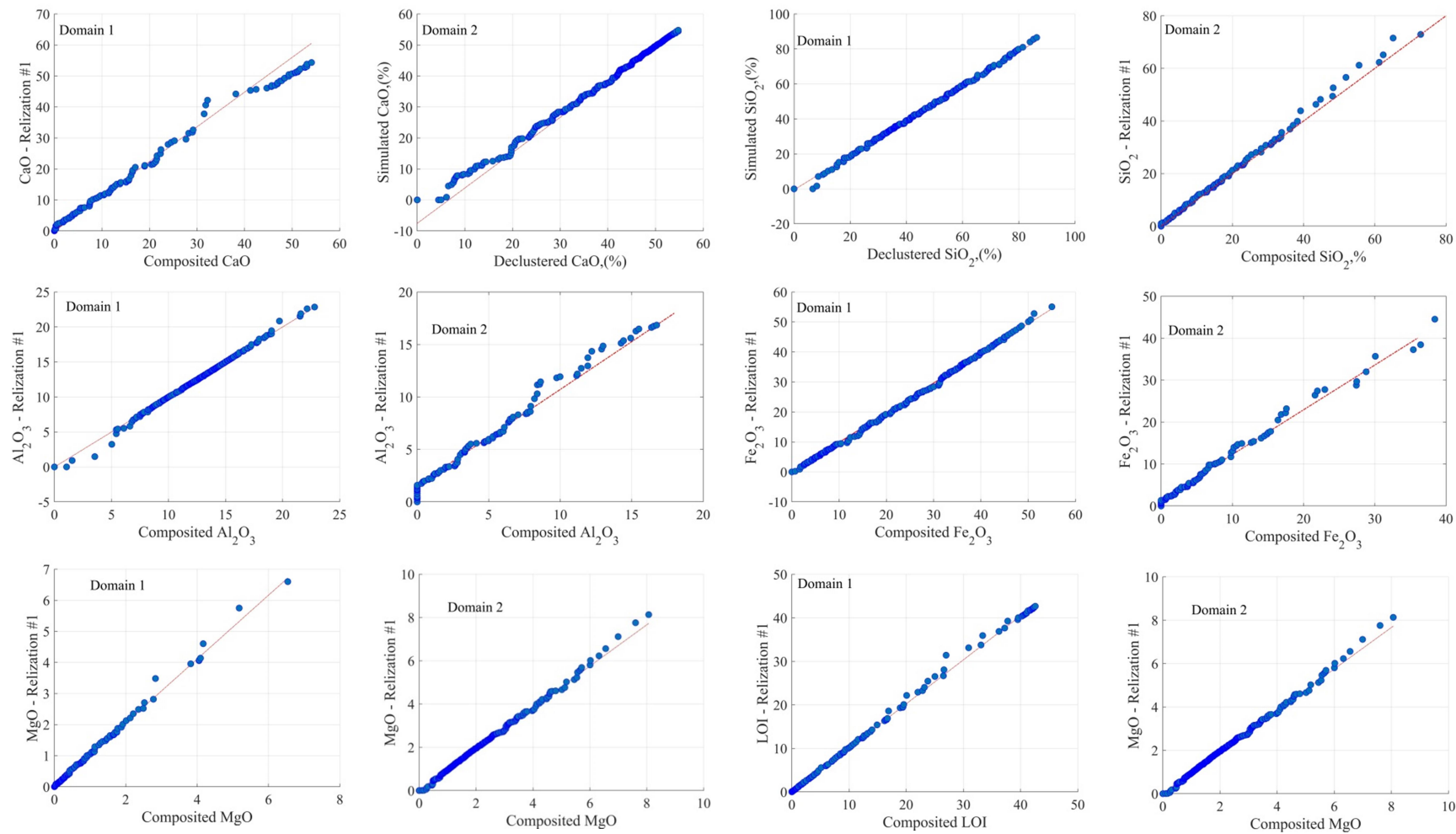


Figure 4.20 Q-Q plot of the six simulated grades versus their declustered data in Domain 1 and 2

4.3.2.2 Validation

Several validation checks were performed to assess the results of the grade simulations. Validation consists of the visual examination of grade distribution consistency with the rock-type domains, the correlation between simulated grades and composited data (after declustering), and verification of histogram, experimental variogram reproduction of composited data characteristics. Figure 4.16 shows the consistency between the chemical grades and the Realization #1 of rock-type domains (Figure 4.9). The grades exhibit spatial continuity within their controlled domain and discontinuities near the boundary between domain 1 and domain 2. The reproduction of simulated data of the six chemical grades on the declustered data is validated in Figure 4.17. Whereas Figures 4.18 and 4.19 present the histograms from the simulated realizations of the grades and then compare them to the histogram of the declustered data. Q-Q plots in Figure 4.20 were prepared for simulated and declustered data of six chemical grades to examine the statistical parameters. All comparisons suggest that the reproduction of the original data characteristics by SGS is excellent.

4.4. Discussion

As indicated in section 4.2, the challenge in modelling the deposit in this research is the complexity in the lithology geometry, where the rock type domain is a significant factor controlling the occurrence and spatial distribution of chemical grade. The construction of the resource model without this relationship can be impractical. Figure 4.21 a, b, and c show the expected CaO grade constructed without rock-type control. The distribution of CaO grade, in this case, is unreasonable. The high CaO grade appears in the regions where soil, clay, and laterite (domain 1) have a high probability of occurrence (see Figure.4.9).

On the contrary, the approach using deterministic rock-type modelling generates the model with the expected CaO grade consistent with the rock-type domain structure (Figure 4.21 d, e, and f). The CaO grade distribution shows clear-cut discontinuities when crossing the boundary between a high-graded domain (domain 2) and a low-graded domain (domain 1). Although this approach relies on an interpretation of the available drill hole data, its limitation is likely to misclassify the real rock type domains due to the dependence on the subjective interpretations of geologists. As a result, errors

in the rock-type modelling impact predicted grades and tonnages. For example, limestone regions (high CaO) can be wrongly assumed to be soil regions (low CaO) or vice versa.

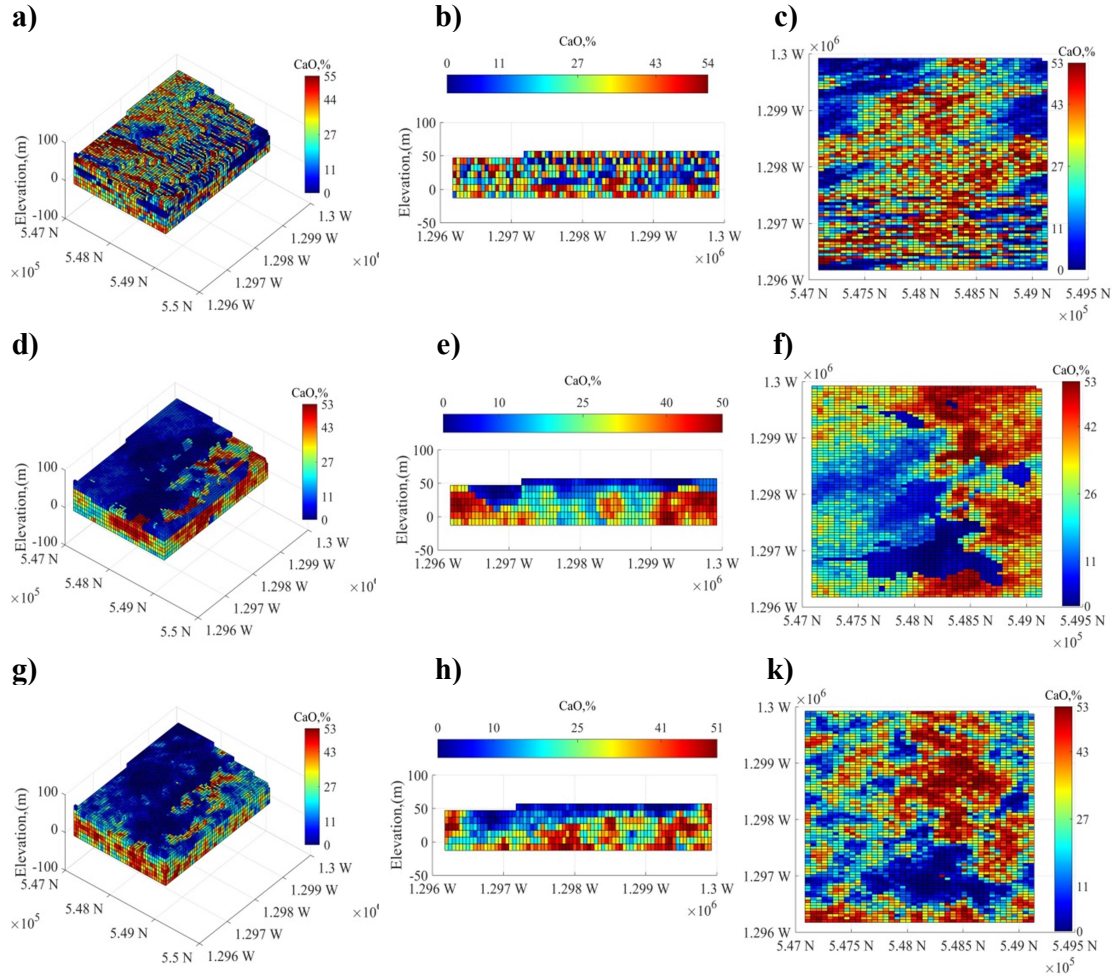


Figure 4.21 Perspective view (left), cross-section (easting = 548110 m) (middle), and horizontal section (elevation= 32.2 m) (right) of the expected CaO grade (calculated by averaging the 20 realizations of chemical grades), obtained without rock-type modeling (a, b, c), with deterministic rock-type modeling (d, e, f), and stochastic rock-type modeling (g, h, k)

In this chapter, a hierarchical simulation method was applied to overcome this challenge, based on the stochastic rock-type modelling and, subsequently, chemical grades in each rock-type domain. SIS, which was constrained with LVM to reproduce the trend of each rock type, was chosen to simulate the uncertainty of the rock-type

domain, which can generate a soft rock-type layout. The case study demonstrated the straightforwardness of this approach in transferring uncertainty in rock-type domains by constructing 20 different numerical realizations, mainly removing the dependence of the grade model on the interpretations of geologists about rock types' boundaries. Despite that, there are some criticisms on SIS, such as unable to impose contact relationships amongst rock types [58] or simulation only based on two-point statistics. Figure 4.21 g, h, and k show the expected models of Cao grade conditioned on such 20 rock-type realizations. The clear-cut discontinuity of the grades no longer apparent and smoother because the grade model accounts for the uncertainty in the spatial extent of rock-type domains. The stochastic rock-type modelling approach accounts for the errors of the misclassification of rock-type domains.

More importantly, these errors can affect the predicted grades and tonnages of raw materials and the future quarry planning in this case. For instance, the box plot in Figure 4.22 compares the distribution of recoverable limestone tonnage above CaO cut-off of 36%. For the deterministic modelling approach using a single layout of rock-type domains, the limestone tonnage fluctuates between about 347 and 400 Mt, with an average of about 370 Mt. Whereas the stochastic modelling approach using 20 realizations of rock-type domains produces a more extensive range of limestone tonnage (between 320 and 400 Mt, with an average of about 373 Mt), which explained because the layout of rock-type domains is uncertain.

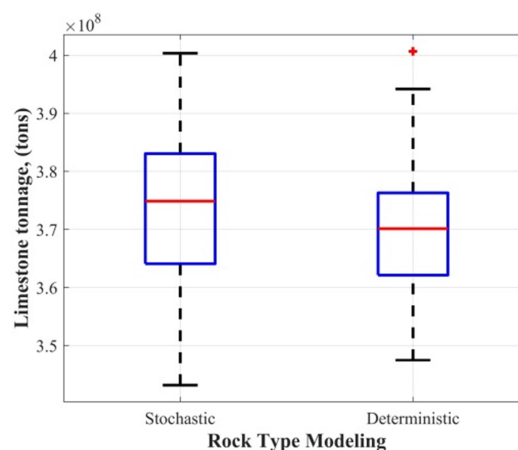


Figure 4.22 Box plot of the limestone tonnage above CaO cut-off of 36%, calculated over 20 realizations using stochastic, and deterministic rock-type modelling approaches

4.5 Conclusion

In the Ta Thiet limestone deposit, the structure of rock-type domains is quite complicated and required to separate from each other in the resource evaluation stage, making it difficult for geologists to interpret their layout. Also, the deterministic modelling approach often fails to qualify the uncertainty in the occurrence of each rock-type domain, which may produce a significant error in grade model construction. The proposed hierarchical approach successfully solved this problem based on probabilistic simulation of the rock types and then combining the rock-type layout simulations with the grade simulation within each rock type. The proposed approach is robust and can account for the available conditioning data at sampling locations, including trends, statistical characteristics, and spatial variability. The simulation results assess the information of geological uncertainty of both rock-type domains of the deposit and grades thoroughly and improve the accuracy of the expected grades. The quarry planning should account for this geological uncertainty and its impact on future cash flows and production targets.

Despite the benefits of this simulation approach in this research, there are still some opportunities for further enhancements. The application of SGS ignores the presence of correlations between variables of interest, such as CaO and LOI. Therefore, future works should investigate the correlation and consider the application of joint or co-simulation techniques to improve the reality of the simulation.

Chapter 5. Application of the stochastic optimization framework

5.1 Introduction

This chapter presents the application and verification of the stochastic optimization framework, as discussed in Chapter 3, on a limestone deposit in Southern Vietnam. The resource models were constructed using geostatistical simulation techniques in Chapter 4 will be employed as inputs for the experiments. Before running the SMIP model, blocks were aggregated into mining cuts to reduce the data scale. The primary capacities of the SMIP model are verified, including (i) optimizing the quarry extraction schedule and (ii) integrating and mitigating the risks due to geological uncertainty. Those capacities are highlighted by comparing the deterministic frameworks using a DMIP model. Finally, the sensitivity of clustering schemes and penalty costs for not meeting the production targets were investigated explicitly. The main results of this chapter were published in [85].

5.2 Implementation of KHRA

The resource model contains 44554 blocks which are difficult to solve in a reasonable timeframe using commercial solvers such as CPLEX. The KHRA was implemented on 20 realizations of the deposit model and eight benches of the quarry, aggregating all blocks into mining cuts to reduce the size of the SMIP formulation. Table 5.1 summarises the input parameters for the algorithm. The created mining cuts aim to have similar grade distribution and rock type patterns with the original block model while producing a minable shape for later extraction. A more detailed sensitivity of clustering input parameters on the optimization results can be found in [48], [71], [72].

Table 5.1 Clustering input parameters

Distance factor weight	Grade factor weight	Rock type penalty	Adjacency threshold (m)	Beneath cluster penalty	Clustering attribute	Num. of shape improvement
1	0.8	0.3	50	0.8	CaO	3

KHRA improves the objective value since it avoids aggregate the low uncertainty blocks with high uncertainty blocks into a mining cut. A different number of mining cuts was generated to investigate its sensitivity to the objective value and

solution time of the SMIP model. The summary results are shown in Table 5.2. Generally speaking, increasing the number of mining cuts can decrease the objective value while increasing the solution time. In the following sections, 952 mining cuts were used as the smallest cost value in our experiment to run the proposed SMIP model. Figure 5.1 illustrates the clustering scheme on bench +32.2 m.

Table 5.2 The sensitivity of the clustering schemes

Maximum cluster size	Number of mining cuts	SMIP run time (s)	SMIP objective value (\$M)
25	251	30522	1860.543
30	489	33133	1683.629
35	748	43072	1585.688
40	952	69579	1442.975

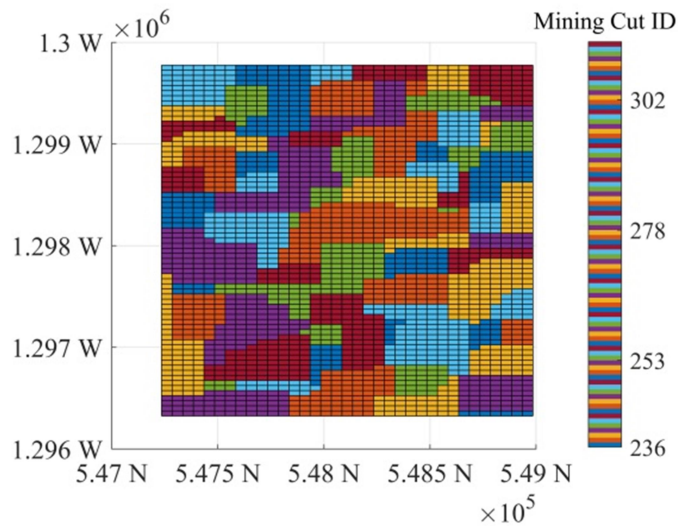


Figure 5.1 Clustering scheme on bench +32.2 m

5.3 Implementation of the SMIP model

The deposit consists of four main rock types, as mentioned in Chapter 4, in which the soil aims to strip and stockpile for use in the rehabilitation of the quarry, although the cement plant can use this material for the raw mix. Hence, a waste dump was considered for disposing of waste. The quarry is extracted using the open-pit method with a bench height of 10 m and an overall slope angle of 20 degrees. A recovery rate of 80% and a discount rate of 8% were applied in the optimization process. The cost for extracting each block depends on their rock type and location. The quality and cost of the additives

are assumed to be known and fixed (Table 5.3). The purchase of additive materials was assumed to be unlimited to understand future agreements with additive suppliers better when the efforts in the quarry extracting process do not help. Therefore, this experiment set the raw mix quality constraints as hard constraints. Also, the penalty costs for violating quarry production (Q_{us}^l / Q_{ls}^l) and raw mix production targets ($Q_{us}^{2l} / Q_{ls}^{2l}$) were selected as 3 and 1 (\$/t), respectively. Table 5.4 summarises the production targets for the implementation of the SMIP model.

Table 5.3 Quality and cost of purchased additive materials

Additive	Cost (\$/t)	CaO (%)	SiO ₂ (%)	Al ₂ O ₃ (%)	Fe ₂ O ₃ (%)	MgO (%)	LOI (%)
Clay	4	5.27	60	2.14	1.5	0.5	30
Laterite	6	0.72	8	47	19.4	1.06	20
High Quality Limestone	4	65	5	1	0.5	1.06	32
Iron Ore	8	1.69	10	1.07	70	1.32	10

Table 5.4 Production target parameters

Description	Value
Num. production periods	10
Mining capacity (Mt)	12 ÷ 15
Raw mix capacity (Mt)	10
CaO (%)	58 ÷ 69
SiO ₂ (%)	14 ÷ 28
Al ₂ O ₃ (%)	4 ÷ 10
Fe ₂ O ₃ (%)	0.5 ÷ 5
MgO (%)	0 ÷ 3
AM = Al ₂ O ₃ / Fe ₂ O ₃	1 ÷ 3
SR = SiO ₂ /(Al ₂ O ₃ + Fe ₂ O ₃)	1 ÷ 3
LSF = CaO/(2.8* SiO ₂ +1.18* Al ₂ O ₃ +0.65* Fe ₂ O ₃)	0.845 ÷ 1

The case study was conducted on a Dell Precision M6800 with a processor of Intel (R) Core [™] i7-4800MQ CPU 2.80 GHz and a RAM of 32.0 GB. The CPLEX solvers used a gap of 5% to terminate the solving process. The resultant schedule was deployed to sequentially apply back to 20 realizations to evaluate the solution of the SMIP model. The results from each run shown as risk profiles represent the possibility of implementing the production schedule in reality and are averaged to get expected results.

5.3.1 Sensitivity of the penalty cost

The proposed SMIP model was tested with different penalty costs of upper/lower deviation from the production targets. The tests generate different risk distributions so that the mine planner can choose a suitable risk distribution. In general, the penalty cost increase results in the decrease of the deviation from the corresponding production targets. It produces a lower risk while raising the total discounted cost for developing the raw mix and purchasing additive materials. However, it should be noted that applying the wrong values for the penalty costs may return impractical solutions. The penalty costs for violating production targets must be higher than the minimum cost to implement those targets. Otherwise, the SMIP model will generate impractical solutions with extreme violations.

Table 5.5 tested the SMIP model with different penalty costs for violating the lower raw mix production target (low_dr) since it is the most critical constraint to guarantee the consistent supply of raw materials in cement projects. All other types of penalty costs are kept constant at 1. As shown in Table 5.5, if the penalty cost for violating low_dr is less than the minimum mining cost of raw material extracted from the quarry (\$2/t for mining clay), the SMIP model can make the raw mix production inactive and high deviations. In schedule S1, the value low_dr is less than \$2/t, and the SMIP model violates the raw mix production target considerably. In schedules S2-S4, where low_dr are higher than \$2/t, the raw mix productions are more practical. However, the more the magnitude of low_dr rises, the more the model extracts raw materials and waste from the quarry and purchase the additives. Therefore, declaring this penalty cost in-approximately can return impractical usage of raw materials. Other types of penalty costs need to be evaluated using this idea.

In the following sections, the schedule S3 is deployed to sequentially apply back to 20 realizations to evaluate the SMIP model's solution. Each result represents the possibility of implementing the production schedule in reality and are averaged to get expected results.

Table 5.5 Summary of four different SMIP schedules with different *low_dr*

<i>low_dr</i> (\$/t)		Period	Quarry Production (Mt)	Waste Production (Mt)	Additive Cost (M\$)	Raw Mix Production (Mt)	Raw Mix Cost (M\$)
S1	1	1	14.873	10.586	2.789	5.197	33.010
		2	14.997	10.777	3.072	5.135	34.500
		3	14.577	10.223	2.729	5.268	29.322
		4	14.764	10.28	2.872	5.32	28.738
		5	14.735	10.315	2.091	5.4	28.084
		6	14.596	10.154	3.474	5.541	24.988
		7	14.589	10.141	3.163	5.534	23.626
		8	14.514	10.361	2.973	5.321	23.631
		9	12.275	8.009	2.005	5.273	18.535
		10	12.27	7.826	2.421	5.581	17.803
Sum		142.19	98.672	27.589	53.57	262.237	
S2	2	1	14.696	6.955	7.615	9.672	36.004
		2	14.802	7.776	9.821	9.661	34.862
		3	14.837	7.611	8.500	9.651	33.314
		4	14.779	7.716	8.171	9.611	30.950
		5	14.785	7.949	8.256	9.382	30.655
		6	13.694	5.853	5.431	9.679	24.403
		7	12.524	5.688	7.364	9.684	23.086
		8	12.727	5.796	6.165	9.471	21.474
		9	13.983	6.730	5.060	9.453	21.460
		10	13.279	6.730	5.893	9.295	20.045
Sum		140.106	68.804	72.277	95.558	276.253	
S3	3	1	14.599	6.64	7.143	9.808	35.452
		2	14.604	7.165	8.798	9.922	36.319
		3	14.264	6.788	7.628	9.872	31.452
		4	14.402	7.113	7.854	9.961	31.593
		5	14.738	7.15	6.804	9.881	27.833
		6	14.365	7.156	6.977	9.863	26.146
		7	14.422	6.975	5.781	9.726	24.242
		8	14.469	7.43	6.067	9.702	23.989
		9	14.482	7.706	6.184	9.747	23.212
		10	14.727	7.717	5.308	9.672	21.968
Sum		145.072	71.84	68.544	98.154	282.206	
S4	10	1	14.689	6.642	6.847	10.003	35.866
		2	14.762	7.455	8.872	10.006	35.574
		3	14.726	7.522	8.984	10.002	33.582
		4	14.798	7.763	8.913	10.000	31.542
		5	14.823	7.205	6.940	10.000	29.112
		6	14.732	7.487	6.498	10.000	26.826
		7	14.786	7.561	6.412	10.000	25.070
		8	14.671	7.557	5.754	10.000	24.371
		9	14.945	8.038	5.722	10.000	23.868
		10	15.011	7.765	5.030	10.000	22.096
Sum		147.944	74.995	69.971	100.011	287.906	

5.3.2 The effectiveness of the SMIP model

The solution demonstrates the ability to supply an average of 98.15 Mt of raw material to the cement plant over ten periods. The hard constraints in Eqs 3.19-3.20 (see Chapter 3) ensure the quality of the raw mix fluctuating within the required ranges, as shown in Table 5.6 and Figure 5.5. The SMIP model uses the realizations to calculate possible blending strategies of raw materials for producing the raw mix with acceptable quality. The stable values across different periods in Table 5.6 are essential to maintain the quality and quantity of raw materials supplied to the cement plant.

Table 5.6 Summary of expected production and quality of the raw mix in each period

Period	Production (Mt)	CaO (%)	SiO ₂ (%)	Al ₂ O ₃ (%)	Fe ₂ O ₃ (%)	MgO (%)	SR	AM	LSF
1	9.81	58.00	17.85	4.39	4.36	2.25	2.06	1.01	1.00
2	9.92	58.09	17.86	4.41	4.40	2.21	2.04	1.00	1.00
3	9.87	58.02	17.87	4.37	4.34	2.17	2.07	1.01	1.00
4	9.96	58.00	17.84	4.42	4.37	2.02	2.05	1.01	1.00
5	9.88	58.00	17.85	4.40	4.34	1.98	2.06	1.02	1.00
6	9.86	58.00	17.95	4.26	4.16	2.02	2.15	1.03	1.00
7	9.73	58.00	17.95	4.28	4.14	2.03	2.15	1.04	1.00
8	9.70	58.00	17.99	4.25	4.01	2.09	2.21	1.09	1.00
9	9.75	58.00	18.04	4.17	3.92	2.10	2.25	1.08	1.00
10	9.67	58.00	18.12	4.13	3.67	2.23	2.35	1.15	1.00
Sum/Mean	98.15	58.01	17.93	4.31	4.17	2.11	2.14	1.04	1.00

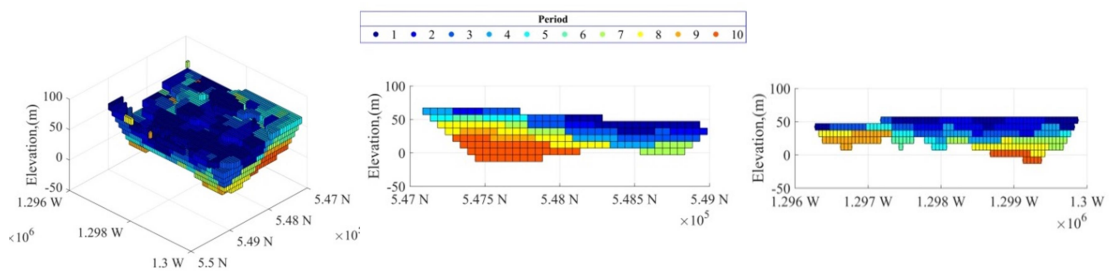


Figure 5.2 Three-dimensional plan view (a), cross-section looking North (b) and West (c) generated by SMIP model

Figure 5.2 shows the applicability of the SMIP model to solve the case study through the 3D plan view and some typical cross-sections. Figure 5.3 presents the expected composition of the raw mix calculated using the average amount of the raw materials extracted from all realizations. In many cases, the quarries often consider limestone as a raw mix component and the other materials as waste. As shown in Figure

5.3, the solution minimises costly additive materials and wastes by adding clay and laterite from the quarry into the raw mix.

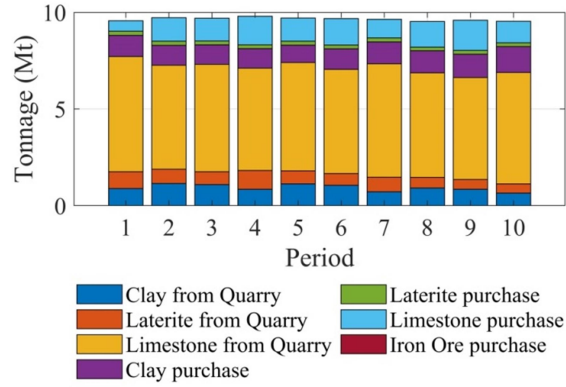


Figure 5.3 Expected composition of the raw mix suggested by SMIP model

One of the significant advantages of the SMIP model in this research is integrating geological uncertainty into the optimization process. Figures 5.4 and 5.5 provide forecasts of deviations of the production targets. For instance, the schedule is most likely able to implement the quarry production target since its deviations in Figure 5.4 (left) (green dots) indicate a slight chance of violating the upper production target over all periods. In Figure 5.4 (right), more dots under the raw mix production target show a higher chance to run below the target of 10 (Mt) per year than over that. Figure 5.5 presents the deviations for the tonnage of materials sent to the waste dump, which gives valuable information for designing the waste dump. Besides, Figure 5.5 forecasts the demand for additive purchases for the cement plant. The need for iron ore purchase, which is the most expensive amongst four additives (see Table 5.3), equals zeros over all periods.

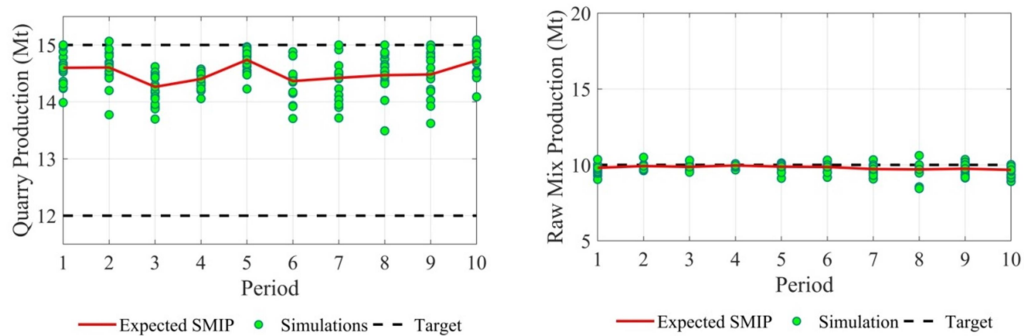


Figure 5.4 Deviations from quarry (left) and raw mix (right) production targets generated by the SMIP model

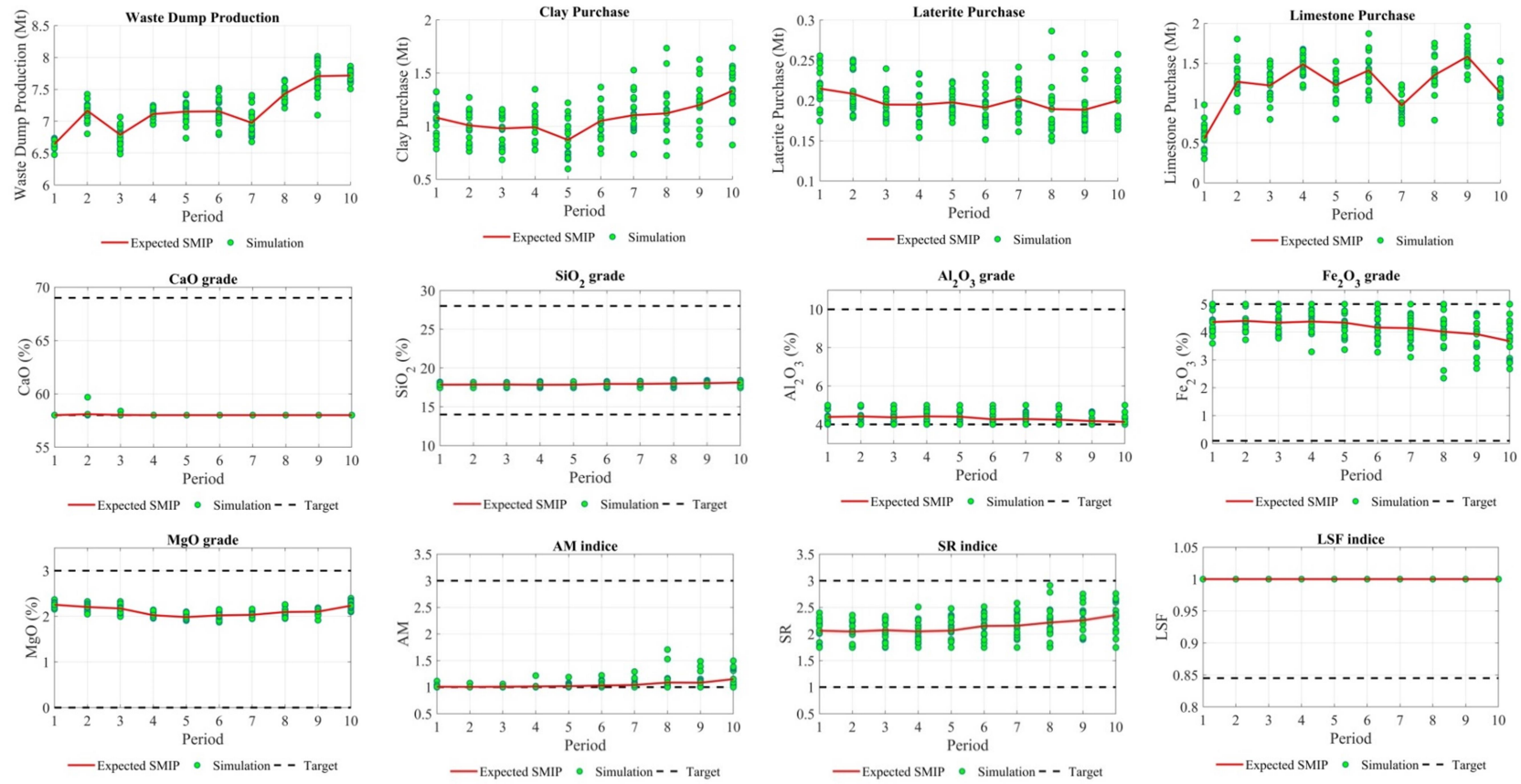


Figure 5.5 Deviations of waste dump production, additive purchases, and raw mix quality targets suggested by the SMIP model

5.4 Risk mitigation

To emphasise the ability of the proposed SMIP model in reducing the geological risk, a DMIP model was formulated using the same clustering scheme, scheduling parameters and the E-type deposit model. The deviations for the production targets of the DMIP model were constructed, as shown in Figures 5.6-5.7, using the same method as the SMIP model. It is clear from the figures that the SMIP model outperforms the DMIP model to mitigate the geological risks. The result of the DMIP schedule illustrates a high chance to operate the quarry under the quarry production target (Figure 5.6 left). In contrast, the SMIP schedule minimises that deviation showing a slight chance to violate the quarry production target (Figure 5.4 left). The decrease in the quarry production forces the DMIP schedule to purchase more additives or decrease its raw mix production. For example, in the first period, the DMIP schedule is expected to buy nearly 3.9 Mt of limestone from outside sources (Figure 5.7), approximately 3.4 (Mt) higher than required by the SMIP schedule. In Figure 5.6 (right), the DMIP schedule shows an unstable supply of raw materials to the cement plant. The SMIP schedule ensures a more stable supply by minimising the deviation of not meeting the raw mix production target. Also, the deviations of raw mix production of the SMIP schedule (the red line) tend to increase towards the later periods (Figure 5.4) while randomly distributed in the DMIP schedule over the production periods (Figure 5.6). As expected in the objective function, the SMIP mitigates the geological risks by delaying mining the quarry's risky parts. However, it should be noticed that the increasing trend of deviations in the SMIP schedule is sometimes not available in subsequent periods because some high uncertainty blocks must be extracted at the earlier period due to slope constraints.

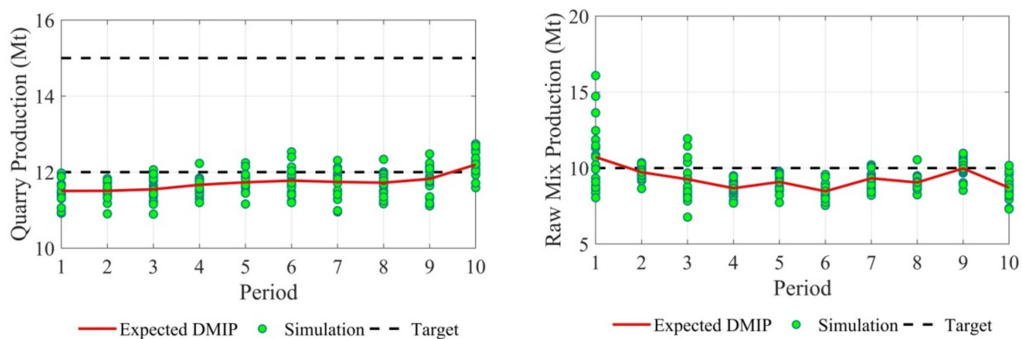


Figure 5.6 Deviations from quarry (left) and raw mix (right) production targets generated by the DMIP mode

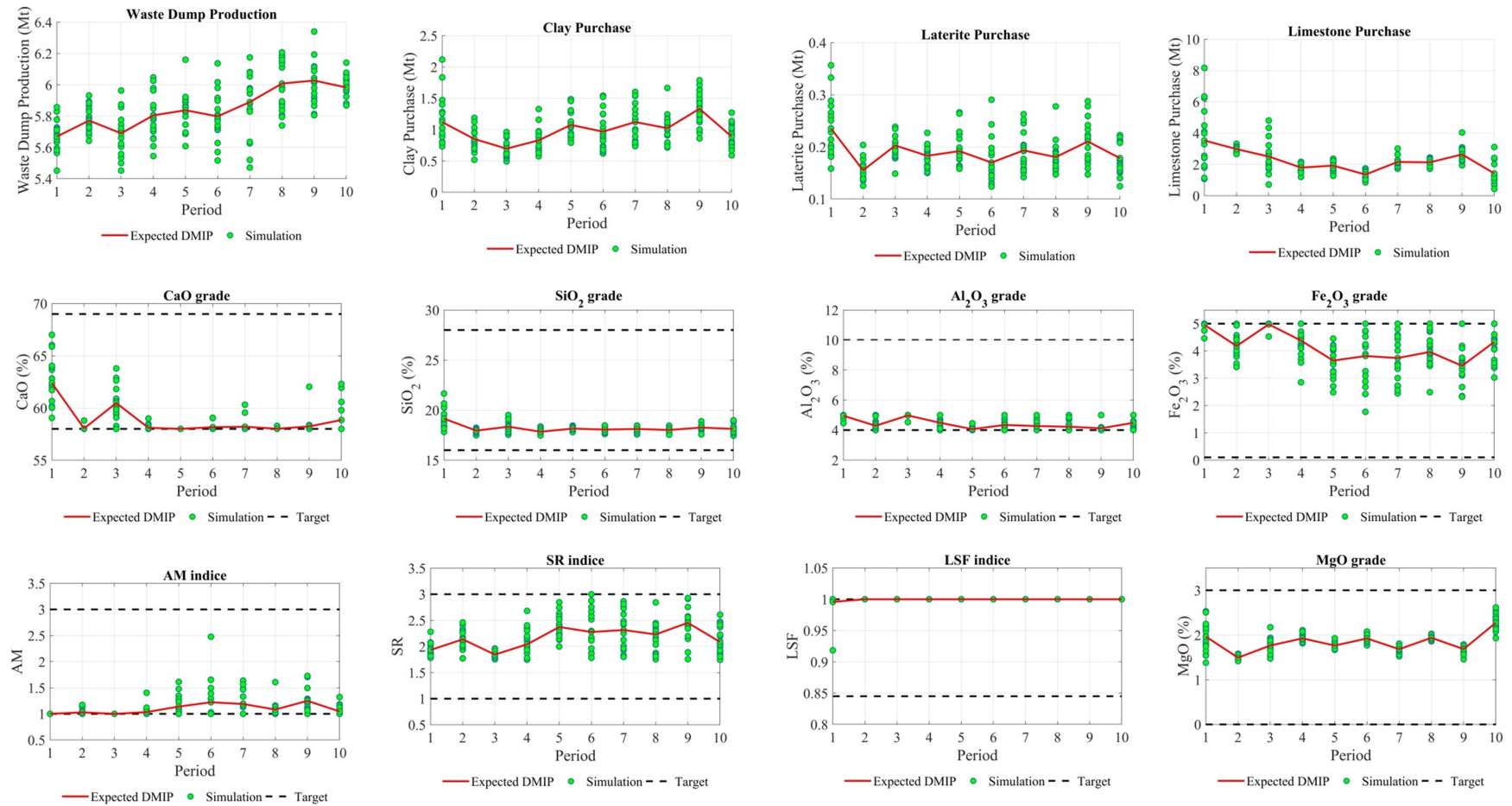


Figure 5.7 Deviations of waste dump production, additive purchases, and raw mix quality targets suggested by the DMIP model

Figure 5.8 compares two models based on two standards: cumulative raw material supply for the cement plant and cumulative cost unit (\$/t). The SMIP schedule supplies an average of 98 Mt of raw materials for the cement plant, nearly 5 Mt higher than the supply from the DMIP schedule. Furthermore, it reduces the unit cost through all the production periods. In total, the SMIP schedule supplies raw materials at the cost of 2.872 \$/t, saving 30.9 % compared to the DMIP schedule. This difference is because of the ability to mitigate the geological risks of the SMIP model.

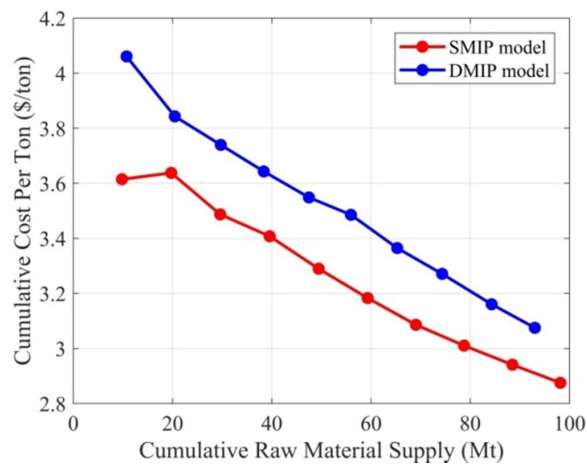


Figure 5.8 Cumulative raw material supply and cost per ton comparison between SMIP and DMIP model

5.5 Conclusion

This chapter verified a risk-based framework, combining the clustering approach KHRA and the SMIP model. First, the KHRA approach uses multiple conditionally simulated deposit models to aggregate the blocks into mining cuts. The SMIP formulation size decreases significantly, allowing generate solutions in a reasonable timeframe on ordinary computers. Solving the LTQPP does not require pit optimization processes such as ultimate pit limit and pushback design. Aggregating blocks into mining cuts provide a simplification as less spending for software and algorithm. This benefit is worth considering in mining cement raw materials when using economic value block models to implement the pit optimization processes are impractical, as discussed in Chapter 2.

By considering mining and blending simultaneously, the SMIP model minimizes the additive purchases to meet blending requirements and the amount of material sent to

the waste dump. Instead of using the traditional methods to respond to the geological risk on raw material supply, the proposed SMIP model addresses it directly, allowing users to assess the risk of deviation from the production targets and mitigate the impact of geological uncertainty on the raw material supply. In this research, the SMIP model is applied efficiently to a limestone deposit in Southern Vietnam, supplying an increase of 5 Mt and a 30 % reduction in unit cost over the DMIP model.

Although the SMIP model proves to be a powerful tool in securing the raw material supply in cement operations, the sensitivity of the number of mining cuts and penalty costs need to be chosen carefully to ensure the practicality and the performance of the SMIP model.

Chapter 6. Conclusions and future works

6.1 Conclusions

Much of cement businesses depend on the reliable supply of raw materials. Failure to obtain the raw materials at expected quantity and quality may adversely impact the financial performance of cement projects. As an initial operation in the cement production process, quarry extraction contributes significantly to ensure the supply of raw materials. While establishing a cement plant or during the operations, proper long-term quarry production planning is the key to handling the raw material issue in cement production. In planning, the quarry planners must meet conflicting business imperatives. They must adhere to the quality and consistent requirements of raw materials to the cement plant while meeting the technical and operational mining requirements of quarry operations. Of course, they must deliver the raw materials at the lowest possible cost. The quarry planning tasks are frequently completed in a spreadsheet or by using mathematical algorithms integrated into software for metallic ore mining, resulting in impractical and not optimal plans. A planning tool to help quarry planners to figure out an effective long-term quarry plan is in need.

In this research, a new stochastic optimization framework and a mathematical model were developed to address this issue. The literature review was conducted first to analyze the raw material management in cement production and established limitations of current mine planning methods. A consistent supply of raw materials to the cement plant is the critical requirement in quarry production planning and sets the difference from metallic ore mining. On the other hand, the significant shortcomings of the current mine planning methods are (i) limitations in dealing with large-size mining problems; (ii) treatment of geological uncertainty using the deterministic framework in optimization processes; (iii) no methodology to address the impacts of geological uncertainty directly. These disadvantages can result in the risks that raw materials cannot be supplied at economical cost or suitable quality.

In general, the development and implementation of the proposed framework were undertaken in three main stages. Geostatistical simulation is employed instead of estimation techniques to generate a set of equally probable resource models in the first stage. This set captures the geological uncertainty and represents the possibilities of the

occurrence of the deposit in reality. In the second stage, the clustering techniques are employed to aggregate blocks into mining cuts. The SMIP model in the third stage takes the generated mining cuts as selective mining units to solve the planning problem with fewer decision variables developing the solution in a reasonable computational time. More specifically, the objective of the SMIP model consists of three main components: (i) minimizing the cost of extracting raw materials from the quarry; (ii) minimizing the cost for purchasing the additive materials from the outside sources; (iii) minimizing the cost for the deviation of production targets due to geological uncertainty. It subjects to various constraints such as mining parameters, production, and blending requirements to ensure the feasibility of the production schedule.

The proposed framework was verified using numerical experiments on a limestone deposit dataset to supply raw materials for a cement plant in southern Vietnam. The case study applied the clustering technique KHRA to schedule 44554 blocks within ten production periods in a practical timeframe using the ordinary computer. In contrast to the manual calculation approach using spreadsheets or guessworks, the implementation of the SMIP model in the case study guaranteed the supply of 98 millions of raw materials to the cement plant at an optimum cost under the conflicting operational and technical constraints. Also, the solution considered the use of lower-grade limestone or other materials within the deposit in the raw mix to eliminate unnecessary and costly additive materials. The risk profiles of the production targets were generated, allowing quarry planners to forecast and provide the information for the project in a feasibility stage. Finally, experiments were implemented to understand the sensitivity of parameters of the clustering scheme and production targets to the optimization results. The results suggest that those parameters need to be chosen carefully to ensure the practicality and the performance of the SMIP model.

One of the outstanding advantages of the SMIP model is the ability to mitigate and control geological risks. The results of the SMIP model showed smaller deviations of production targets in comparison with the DMIP model. The probability of deviations generated by the SMIP model showed better control between production periods. The probability of meeting the production targets was higher at early periods in the SMIP schedule. These differences are mainly due to the ability of the SMIP model to extract the less risk part of the deposit in the earlier periods while postponing the risk part in the

later periods. It makes quarry planners more confident to implement their schedule if assuming that more information would become available in the future. Notably, the SMIP schedule expectedly supplied 5 Mt higher with 30.9% cost unit savings when compared with the DMIP model.

A software application was created using the above concepts and proposed framework, providing a digital tool for quarry planners (see Appendix I). The software can support quarry planners at different levels:

- Understand the characteristics of the deposit. The software allows users to import deposit realizations generated from geostatistical simulation software and visualize qualities inside the deposit in the form of a 3D block model or cross-sections.
- Figure out the long-term quarry extraction plan that is feasible, achievable, and meets the conflicting requirements between mining and blending requirements in cement production.
- Simulate and assess the risk of supplying raw materials to the cement plant. The SMIP model calculates different raw materials production scenarios that the deposit can produce, depending on the quality and other constraints set up by users, including additive materials usage. Simulation results can provide valuable information on the feasibility of the cement project.
- Have a tool to mitigate and control the risk of not supply raw materials at production targets due to geological uncertainty.

6.2 Future works

Although the development of the stochastic framework and optimization model in this thesis has provided a powerful tool for quarry production planning to supply raw materials for cement plants, there is still room for continued improvement and investigation. The current model and framework do not consider multiple quarries such as a limestone quarry and a clay quarry feed raw materials to a single or multiple cement plants. For future research, the proposed framework and model can be extended to deal with this situation.

One of the major shortcomings of the proposed framework is the dependency on geological information or, in other words, the sampling methodologies and modelling techniques. Unrealistic production planning could be generated if there are some errors in these processes. Therefore, one more interesting future work is investigating a mechanism to update the geological database during the mining progress frequently. In this way, the quarry planning could evolve to approximate reality.

References

- [1] Newman AM, Rubio E, Caro R, Weintraub A, Eurek K. A review of operations research in mine planning, *Interfaces* (Providence). Vol. 40, no. 3, pp. 222–245. 2010.
- [2] Dimitrakopoulos R, Farrelly CT, Godoy M. Moving forward from traditional optimization: Grade uncertainty and risk effects in open-pit design. *Mining Technology*. 111(1):82-8. 2022.
- [3] Groeneveld B, Topal E. Flexible open-pit mine design under uncertainty. *Journal of Mining Science*. 47(2):212-26. 2011.
- [4] Vallee M. Mineral resource + engineering, economic and legal feasibility = ore reserve. *CIM bulletin*. 93(1038):53-61. 2000.
- [5] M. Inc., MATLAB (R2007b) Software. Natick, MA, USA, 2007.
- [6] Deutsch CV, Journel AG. *GSLIB : geostatistical software library and user's guide*, 2nd Edition. New York: Oxford University Press. 1998.
- [7] CPLEX, User's Manual for CPLEX, in International Business Machines Corporation. 12th ed., pp. 46(53), 157. 2009.
- [8] Rahman FU. Manufacture of Cement Materials and Manufacturing Process of Portland Cement. 2019.[Online].
Available:<https://theconstructor.org/building/manufactuofcement/13709/>. [Accessed: 29-Jan-2020].
- [9] Labahn, Otto. *Cement Engineer's Handbook* Cement Engineer's Handbook. Bauverlag. 1983.
- [10] Pawel Kawalec, Cornelis Bockemühl. Block model based cement quarry optimization. *Cement Building Material Review*. vol. 53. pp. 70–77. 2018.
- [11] LafargeHolcim. Annual Report. 2007.
- [12] Austin GT. *Shreve's chemical process industries*. 5th edition. McGraw Hill Book Company New York. 1984.
- [13] Carr DD. *Industrial minerals and rocks*. 6th edition. Society of Mining, Metallurgy, and Exploration. Inc., Littleton, Colorado. 1994.
- [14] Rehman SU, Asad MW. A mixed-integer linear programming (milp) model for short-range production scheduling of cement quarry operations, *Asia-Pacific journal of operational research*. Vol. 27. no. 03. pp. 315–333. 2010.

- [15] Asad MW. Multi-period quarry production planning through sequencing techniques and sequencing algorithm. *Journal of Mining Science*. 44(2):206-17. 2008.
- [16] Asad MW. A heuristic approach to long-range production planning of cement quarry operations. *Production Planning & Control*. 22(4):353-64. 2011.
- [17] Joshi D, Chatterjee S, Equeenuddin SM. Limestone quarry production planning for consistent supply of raw materials to cement plant: A case study from Indian cement industry with a captive quarry. *Journal of Mining Science*. 51(5):980-92. 2015.
- [18] Dagdelen K. Open pit optimization-strategies for improving economics of mining projects through mine planning. In 17th International Mining Congress and Exhibition of Turkey . pp. 117-121. 2001.
- [19] Whittle J. Beyond optimization in open pit design. in *Canadian Conference on Computer Applications in the Mineral Industries*. pp. 331–337. 1988.
- [20] Osanloo M, Gholamnejad J, Karimi B. Long-term open pit mine production planning: a review of models and algorithms. *International Journal of Mining, Reclamation and Environment*. 22(1):3-5. 2008.
- [21] Hochbaum DS, Chen A. Performance analysis and best implementations of old and new algorithms for the open-pit mining problem. *Operations Research*. 48(6):894-914. 2000.
- [22] Lerchs H., Grossmann L. Optimum design of open-pit mines, *Transactions of CIM*. pp. 17-24. 1965.
- [23] Zhao Y. Algorithms for optimum design and planning of open-pit mines, 1992.
- [24] Hochbaum DS. The pseudoflow algorithm: A new algorithm for the maximum-flow problem. *Operations research*. 56(4):992-1009, 2008.
- [25] Picard JC. Maximal closure of a graph and applications to combinatorial problems. *Management Science*. 22(11):1268-72, 1976.
- [26] Underwood R, Tolwinski B. A mathematical programming viewpoint for solving the ultimate pit problem. *European Journal of Operational Research*. 107(1):96-107, 1998.
- [27] Seymour F. Pit limit parameterization from modified 3D Lerchs-Grossmann algorithm. *SME. Preprint*. 1995(95-96).
- [28] Ramazan S, Dagdelen K. A new push back design algorithm in open pit mining. In *Proceedings of 17th MPES conference, Calgary, Canada*. pp. 119-124, 1998.

- [29] Dagdelen K. Optimum open pit mine production scheduling by Lagrangian parameterization. Proc. of the 19th APCOM. 1986:127-42.
- [30] Meagher C, Dimitrakopoulos R, Vidal V. A new approach to constrained open pit pushback design using dynamic cut-off grades. Journal of Mining Science. 50(4):733-44, 2014.
- [31] Johnson TB. Optimum open pit mine production scheduling. California Univ Berkeley Operations Research Center. 1968.
- [32] Gurobi, Gurobi Optimisation. 2016.
- [33] Lamghari A, Dimitrakopoulos R, Ferland JA. A hybrid method based on linear programming and variable neighborhood descent for scheduling production in open-pit mines. Journal of Global Optimization. 63(3):555-82, 2015.
- [34] Espinoza D, Goycoolea M, Moreno E, Newman A. MineLib: a library of open pit mining problems. Annals of Operations Research. 206(1):93-114, 2013.
- [35] Ramazan S, Dagdelen K, Johnson TB. Fundamental tree algorithm in optimising production scheduling for open pit mine design. Mining Technology. 114(1):45-54, 2005.
- [36] Caccetta L, Giannini LM. An application of discrete mathematics in the design of an open pit mine. Discrete Applied Mathematics. 21(1):1-9, 1988.
- [37] Chicoisne R, Espinoza D, Goycoolea M, Moreno E, Rubio E. A new algorithm for the open-pit mine production scheduling problem. Operations Research. 60(3):517-28, 2012.
- [38] Gershon M. Heuristic approaches for mine planning and production scheduling. International Journal of Mining and Geological Engineering. 5(1):1-3, 1987.
- [39] Ramazan S, Dimitrakopoulos R. Recent applications of operations research and efficient MIP formulations in open pit mining. SME Transactions. 2004.
- [40] M. P. Ltd. MineMax Scheduler. Minemax Pty Ltd, West Perth, Western Australia.
- [41] D. S. C. S. Inc. "MineSched." Vancouver. BC, Canada, 2016.
- [42] Ramazan S. Large-scale production scheduling with the fundamental tree algorithm: Model, case study and comparisons. Orebody modelling and strategic mine planning, 2nd edn. The Australasian Institute of Mining and Metallurgy, Melbourne. 2007:121-7.
- [43] Askari-Nasab H, Pourrahimian Y, Ben-Awuah E, Kalantari S. Mixed integer linear

programming formulations for open pit production scheduling. *Journal of Mining Science*. 47(3):338-59, 2011.

[44] G. S. International. Whittle strategic mine planning software. Gemcom Software International, Vancouver, B.C.

[45] Stone P, Froyland G, Menabde M, Law B, Pasyar R, Monkhouse P. Blasor-blended iron-ore mine planning optimisation at Yandi. In *Orebody Modelling and Strategic Mine Planning*", Proceedings of the International Symposium, AIMM, pp. 285-288. 2004.

[46] Whittle G. Global asset optimisation. *Orebody modelling and strategic mine planning*. 2007.

[47] Lamghari A, Dimitrakopoulos R. A diversified Tabu search approach for the open-pit mine production scheduling problem with metal uncertainty. *European Journal of Operational Research*. 222(3):642-52.2012.

[48] Tabesh M, Askari-Nasab H. Two-stage clustering algorithm for block aggregation in open pit mines. *Mining Technology*. 120(3):158-69. 2011.

[49] Godoy M, Dimitrakopoulos R. Managing risk and waste mining in long-term production scheduling of open-pit mines. *SME transactions*. 2004.

[50] Goodfellow R. Unified modelling and simultaneous optimization of open pit mining complexes with supply uncertainty (Doctoral dissertation, McGill University Libraries).

[51] Denby B, Schofield D. Open-pit design and scheduling by use of genetic algorithms. *Transactions of the Institution of Mining and Metallurgy. Section A. Mining Industry*. 1994.

[52] Sattarvand J, Niemann-Delius C. Perspective of metaheuristic optimization methods in open pit production planning. *Gospodarka Surowcami Mineralnymi*. 24(4):143-56. 2008.

[53] Baker CK, Giacomo SM. Resource and reserves: their uses and abuses by the equity markets. In *Ore reserves and finance: a joint seminar between Australasian Institute of Mining and Metallurgy (AusIMM) and Australian Securities Exchange (ASX)*, Sydney. 1998.

[54] Vann J, Bertoli O, Jackson S. An overview of geostatistical simulation for quantifying risk. In *Proceedings of Geostatistical Association of Australasia Symposium" Quantifying Risk and Error*. Vol. 1, pp. 1. 2002.

[55] Chiles JP, Delfiner P. *Geostatistics: modeling spatial uncertainty*. John Wiley &

Sons. 2009.

- [56] Jones P, Douglas I, Jewbali A. Modeling combined geological and grade uncertainty: application of multiple-point simulation at the Apensu gold deposit, Ghana. *Mathematical geosciences*. 45(8):949-65. 2013.
- [57] Roldão D, Ribeiro D, Cunha E, Noronha R, Madsen A, Masetti L. Combined use of lithological and grade simulations for risk analysis in iron ore, Brazil. In *Geostatistics Oslo*. pp. 423-434. Springer, Dordrecht. 2012.
- [58] Talebi H, Sabeti EH, Azadi M, Emery X. Risk quantification with combined use of lithological and grade simulations: Application to a porphyry copper deposit. *Ore Geology Reviews*. 75:42-51. 2016.
- [59] Mery N, Emery X, Cáceres A, Ribeiro D, Cunha E. Geostatistical modeling of the geological uncertainty in an iron ore deposit. *Ore Geology Reviews*. 88:336-51. 2017.
- [60] Dowd PA. Risk assessment in reserve estimation and open-pit planning. *Transactions of the Institution of Mining and Metallurgy (Section A: Mining Industry)*. 1994.
- [61] Ravenscroft PJ. Risk analysis for mine scheduling by conditional simulation. *Transactions of the Institution of Mining and Metallurgy. Section A. Mining Industry*. 1992.
- [62] Smith M, Dimitrakopoulos R. The influence of deposit uncertainty on mine production scheduling. *International Journal of Surface Mining, Reclamation and Environment*. 13(4):173-8. 1999.
- [63] Godoy M, Dimitrakopoulos R. Managing risk and waste mining in long-term production scheduling of open-pit mines. *SME transactions*. 316(3). 2004.
- [64] Leite A, Dimitrakopoulos R. Stochastic optimization of mine production scheduling with uncertain ore/metal/waste supply. *International Journal of Mining Science and Technology*. 24(6):755-62. 2014.
- [65] Ramazan S, Dimitrakopoulos R. Stochastic optimisation of long-term production scheduling for open pit mines with a new integer programming formulation. In *Advances in applied strategic mine planning*. pp. 139-153. Springer, Cham. 2018.
- [66] Benndorf J, Dimitrakopoulos R. Stochastic long-term production scheduling of iron ore deposits: integrating joint multi-element geological uncertainty. *Journal of Mining Science*. 49(1):68-81. 2013.

- [67] Dimitrakopoulos R, Ramazan S. Stochastic integer programming for optimising long term production schedules of open pit mines: methods, application and value of stochastic solutions. *Mining Technology*. 117(4):155-60. 2008.
- [68] Mai NL, Topalt E, Ertent O. A new open-pit mine planning optimization method using block aggregation and integer programming. *Journal of the Southern African Institute of Mining and Metallurgy*. 118(7):705-14.2018.
- [69] Leite A, Dimitrakopoulos R. Stochastic optimisation model for open pit mine planning: application and risk analysis at copper deposit. *Mining Technology*. 116(3):109-18. 2007.
- [70] Lamghari A, Dimitrakopoulos R, Ferland JA. A variable neighbourhood descent algorithm for the open-pit mine production scheduling problem with metal uncertainty. *Journal of the Operational Research Society*. 65(9):1305-14. 2014.
- [71] Tabesh M, Askari-Nasab H. Automatic creation of mining polygons using hierarchical clustering techniques. *Journal of Mining Science*. 49(3):426-40. 2013.
- [72] Tabesh M, Askari-Nasab H. Clustering mining blocks in presence of geological uncertainty. *Mining Technology*. 2019.
- [73] Azimi Y, Osanloo M, Esfahanipour A. An uncertainty based multi-criteria ranking system for open pit mining cut-off grade strategy selection. *Resources Policy*. 38(2):212-23. 2013.
- [74] Dimitrakopoulos R. Conditional simulation algorithms for modelling orebody uncertainty in open pit optimisation. *International journal of surface mining, reclamation and environment*. 12(4):173-9. 1998.
- [75] Dowd PA. Risk assessment in reserve estimation and open-pit planning. *Transactions of the Institution of Mining and Metallurgy (Section A: Mining Industry)*. 1994.
- [76] Journel AG. Modeling uncertainty: some conceptual thoughts. In *Geostatistics for the next century*. pp. 30-43. Springer, Dordrecht. 1994.
- [77] Tabesh M, Mieth C, Askari-Nasab H. A multi-step approach to long-term open-pit production planning. *International Journal of Mining and Mineral Engineering*. 5(4):273-98. 2014.
- [78] Askari-Nasab H, Awuah-Offei K, Eivazy H. Large-scale open pit production scheduling using mixed integer linear programming. *International Journal of Mining and*

Mineral Engineering. 2(3):185-214. 2010.

[79] Koushavand B, Askari-Nasab H, Deutsch CV. Transfer geological uncertainty through mine planning. In MPES (MPES-International Symposium of Mine Planning/Equipment Selection). 2009.

[80] Vu T, Drebenstedt C, Bao T. Assessing geological uncertainty of a cement raw material deposit, southern Vietnam, based on hierarchical simulation. International Journal of Mining Science and Technology. 30(6):819-37. 2020.

[81] Beckers F, Bogaert P. Nonstationarity of the mean and unbiased variogram estimation: extension of the weighted least-squares method. Mathematical geology. 30(2):223-40. 1998.

[82] Cressie N. Statistics for spatial data. John Wiley & Sons. 2015.

[83] Kitanidis PK. Generalized covariance functions in estimation. Mathematical Geology. 25(5):525-40. 1993.

[84] Geovia. Minesched. 2011.

[85] Vu T, Bao T, Drebenstedt C, Pham H, Nguyen H, Nguyen D. Optimisation of long-term quarry production scheduling under geological uncertainty to supply raw materials to a cement plant. Mining Technology. 2021.

[86] Bao TD, Thang HH, Vu T. An Introduction of New Simulation and Optimization Software Application for Long-Term Limestone Quarry Production Planning. Inżynieria Mineralna. 2020.

Appendix I. Software Application

A.I.1 Introduction

In line with the development of the SMIP framework in this research, this research aims to create new digital software for quarry planners to generate robust and practical quarry plans to meet production targets in the long term. The main functions of this software were published in [86]. The software was built through the application development program (GUIDE) in Matlab and can be used as a standalone application. The workflow of the software represents the stochastic framework in this research, as shown in Figure A.I.1.

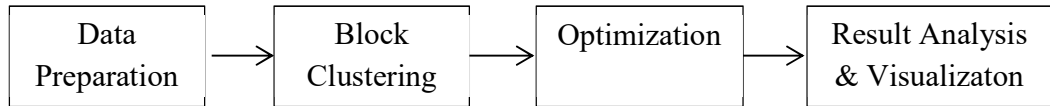


Figure A.0.1 The workflow of the developed software

The software design illustrated in Figure A.I.2 consists of three main menus: Input, Optimization, and Visualization. These menus can be chosen using the pop-up menu (the red rectangle).

QUARRY PRODUCTION OPTIMIZATION

Input

1. Import Block Model

Import

Import Block Model

Simulation ID

Select coordinates

x y z

Select block size

x y z

Topography

Import Topography

Remove

Materials & Final Pit Slope

Specific gravity

Rock type ID

Rocktype

Final Pit Slope 45

Apply Cancel

2. Cost

Import from block model

Choose

Cost Assignment

Reference Mining Cost 1 tonne

Mining Recovery 1

Mining Dilution Fraction 1

Block Mining Cost Adjustment Factors

Factor Range

Rocktype Details

Choose

Rock IDs	Calculation	Factor	Mining Recovery Fraction	Mining Dilution F

Remove

Apply Cancel

3. Size Reduction

Choose Method Block Clustering

Import Save

Block Clustering

Clustering Parameters

Num. shape improvement 1

Maximum cluster size 1 Distance factor weight 1

Grade weight factor 0 Rock type penalty 0

Adjacency Threshold 1 Clustering attribute Pop-up Menu

Beneath Cluster Penalty 0.8 Minimum cluster size 1

Clustering results

	Average grade CV (%)	Average rock unity (%)	Cluster size CV (%)
1			
2			

Apply Cancel

(a)

QUARRY PRODUCTION OPTIMIZATION

Optimization

4. Destination

Material for Destination

Type	Name	Constraint	Minimum	Maximum	Rehandling
<input type="text"/>					

Targets

Destination: Maximum:

Quality	Minimum	Maximum
<input type="text"/>		

Quality	Equation	Minimum	Maximum
<input type="text"/>			

5. Additive

Additive purchase

Name	Min Purchase	Max Purchase	Unit Cost
<input type="text"/>			

Additive's quality

Property	Value
<input type="text"/>	

6. Production Capacity

Location	From Period	To Period	Minimum	Maximum
<input type="text"/>				

7. Pit Slopes

Min X	Max X	Min Y	Max Y	Min Z	Max Z	Slope Angle
<input type="text"/>						

8. Optimization

Uncertainty Cost

Factor	Deficient Cost/Excess Cost
<input type="text"/>	

Running Option

Choose CPLEX solver

Discount Rate (%) 8 Relative Gap 0.0001

Absolute Integer Gap 0.000001 Solving Time(s) 999999999

Num. Fraction of Mining Cut 2

(b)

QUARRY PRODUCTION OPTIMIZATION

Visualization

Block Model

Simulation:

Attribute:

Show surface: ☐

Colormap:

Colorbar: ☐

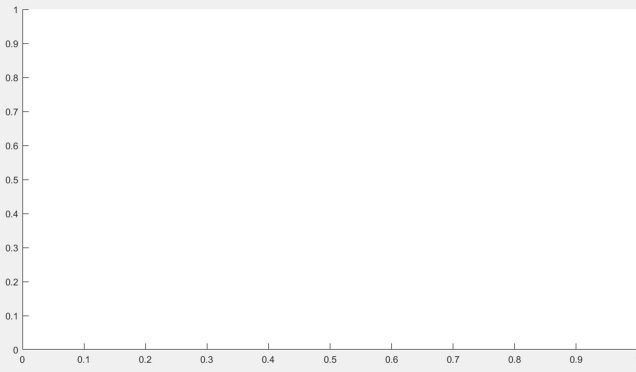
Filtering:

Attribute	Min	Max
<input type="text"/>		

Charts

Location:

Chart:



(c)

Figure A.0.2 Three main menus of the developed software

(a – Input; b – Optimization; c – Visualization)

A.I.2 Input preparation

A.I.2.1 Format of block model input

The block model input contains a series of realizations of deposit generated by any geostatistical software. Users can store the realizations in Excel files (.xlsx) or text files (.txt) in which the first row is the header, and the remaining rows are the block data. Each column in input files provides the information of blocks within the realization of

the deposit, such as location, grade, or rock types. Fig.A.I.3 shows an example of the block model input stored in an excel file.

	A	B	C	D	E	F	G	H	I	J	K
1	x	y	z	Density	Rocktype	CaO	SiO2	Al2O3	Fe2O3	MgO	LOI
2	548860	1296450	2.2	1.51	Soil	1.208890841	38.57033313	11.9287011	13.52385717	0.044509668	1.100307463
3	548910	1296450	2.2	1.51	Soil	2.807043275	39.27415423	11.97925203	21.23480707	0.131121373	2.790483984
4	548910	1296500	2.2	1.51	Soil	0.756097396	53.26165047	13.03883143	23.28679783	0.135229691	2.180760375
5	548810	1296550	2.2	1.51	Soil	4.827968402	47.83241606	14.53268071	23.29102468	0.102589058	2.7494099
6	548860	1296550	2.2	1.51	Soil	9.732575038	58.91754865	16.2508513	33.61565168	0.416093972	7.704398988
7	548960	1296550	2.2	1.51	Soil	0.41457797	52.0639162	11.73754785	13.70824511	0.037933387	0.547205905
8	548610	1296650	2.2	1.51	Soil	12.94220202	70.45375444	15.82387642	30.23841338	0.390881296	6.631864729
9	548810	1296650	2.2	1.51	Soil	20.07664132	77.88332282	19.43543002	38.92498001	0.799485456	13.05173281
10	548860	1296650	2.2	1.51	Soil	35.17749074	98.10656552	25.61464648	57.75333897	2.543949842	28.89176261
11	548860	1296400	2.2	1.78	Laterite	21.74139818	9.045388464	3.07794564	2.499698199	1.936144389	11.9767268
12	548410	1299750	2.2	1.51	Soil	0	5.120718875	1.953686588	1.350443188	0	0
13	548810	1296300	12.2	1.51	Soil	0	19.4344995	7.2871607	6.251103613	0.000624334	0
14	548760	1296350	12.2	1.51	Soil	0.010235097	25.86363113	9.655704638	7.284087963	0.000625	0
15	548660	1296450	12.2	1.51	Soil	0.000375	29.06770838	8.62614295	5.88873694	0.000203362	0
16	548510	1296500	12.2	1.51	Soil	17.67015881	46.72345612	16.55251852	31.36784422	1.125877897	12.04673111
17	548610	1296500	12.2	1.51	Soil	3.371511056	35.34245229	10.96328089	19.84768307	0.143437156	2.391383051
18	548710	1296500	12.2	1.51	Soil	0.010298061	43.41277762	10.43560258	19.55329605	0.039485083	1.092585863
19	548810	1296500	12.2	1.51	Soil	5.031903342	59.76288831	14.61022452	33.37853729	0.410616674	8.051410454
20	548610	1296550	12.2	1.51	Soil	11.30589734	57.65663264	15.83059642	33.08278607	0.495670033	8.439878113
21	548710	1296550	12.2	1.51	Soil	0.332444321	48.26516208	12.30602607	24.64024906	0.098700953	2.461012311

Figure A.0.3 Example of block model input

A.I.2.2 Import block model input

1. Click the button **Import Block Model** and specify the folder directory used to store block model files. The software uses this folder to store the results after finishing the optimization process.
2. Specify the columns in the block model containing the location information x,y, and z.
3. Specify the block size, including length (x), width (y), and height (z).
4. Choose the topography file (.xlsx or .txt) using the button **Import Topography** and specify the columns containing the location information. Users can tick the box **Remove air blocks** to remove the air or extracted blocks.
5. In the box **Material & Final Pit Slope**, users can specify the specific gravity and rock type column in the block model file. Also, users can choose the final pit slope to remove the blocks outside the ultimate pit limit of the quarry.

1. Import Block Model

Import

1 Import Block Model

	Simulation	ID
1	Realization1LOI	1
2	Realization2LOI	2
3	Realization3LOI	3
4	Realization4LOI	4
5	Realization5LOI	5
6	Realization6LOI	6
7	Realization7LOI	7
8	Realization8LOI	8
9	Realization9LOI	9
10	Realization10LOI	10
11	Realization11LOI	11
12	Realization12LOI	12
13	Realization13LOI	13
14	Realization14LOI	14
15	Realization15LOI	15

2 Select coordinates

x x
y y
z z

3 Select block size

x 50
y 50
z 10

4 Topography

Import Topography

x x
y y
z z

☒ Remove air blocks

5 Materials & Final Pit Slope

Specific gravity Density
Rocktype Rocktype
Final Pit Slope 45

Rock type	ID
Clay	1
Laterite	2
Limestone	3
Soil	4

Apply **Cancel**

Figure A.0.4 Import block model menu

All the steps above are illustrated in Figure A.I.4. When users click **Apply**, the block model input will be evaluated and stored in the memory. Each rock type is assigned an ID so that users can use it to specify the rock type in the downstream steps. Using the visualization menu, users can view and analyze the input model (Figure A.I.5).

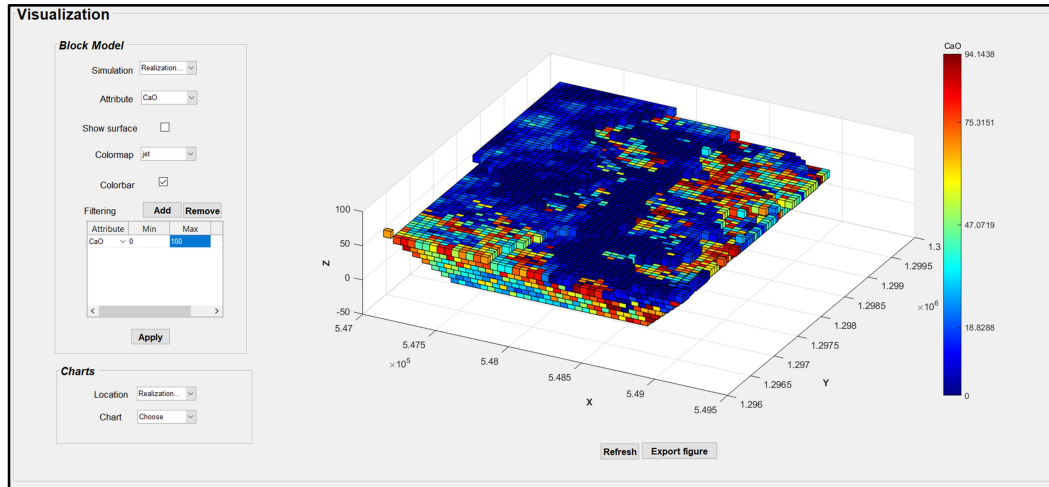


Figure A.0.5 An example of visualization of the block model input

A.I.2.2 Cost assignment

In this section, the software provides various methods to define the cost for each block.

- Method 1: Import from block model file

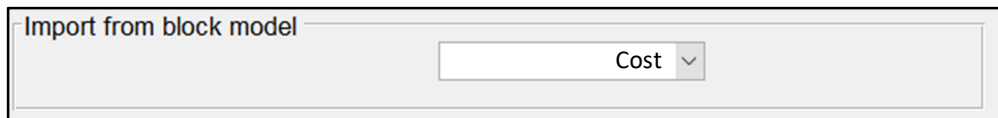


Figure A.0.6 Import from block model file

Users can construct the cost for each block and add it to the block model input file. The pop-up menu in this section allows users to specify the column of block mining cost (Figure A.I.6).

- Method 2: Using mining cost adjustment factor (MCAF)

This method allows users to import the mining cost using a range function or equation of MCAF. For instance, users can build up the distribution of mining costs following the z -direction of the model, like in Table A.I.1.

As a range function, users can build up a range function using the format:

MCAF, level, MCAF, level, ..., MCAF, level, for example (Figure A.I.7):

1,80,1.03,60,...,1.2, 0

Table A.0.1 An example of mining cost and MCAF distribution

z	Mining Cost	MCAF
80	1.50	1
70	1.55	1.03
60	1.61	1.07
50	1.65	1.1
40	1.70	1.13
30	1.76	1.17
20	1.80	1.2
10	1.85	1.23
0	1.95	1.3

The screenshot shows a software interface for importing mining costs. It includes the following fields and controls:

- Reference Mining Cost:** A text input field containing the value "1.5".
- Unit:** A dropdown menu currently set to "tonne".
- Mining Recovery:** A text input field containing the value "1".
- Mining Dilution Fraction:** A text input field containing the value "1".
- Block Mining Cost Adjustment Factors:** A section containing a dropdown menu set to "Range" and a large text input field with the following comma-separated values: "1,80,1.03,70,1.07,60,1.1,50,1.13,40,1.17,30,1.2,20,1.23,10,1.2,0".

Figure A.0.7 An example of mining cost import using MCAF by a range function

As an equation, users use the equation to describe how the MCAF is used to assign the mining cost. For example, users can create the best fit with the linear data in Table.A.I.1 using Excel (Figure A.I.8) and then import the parametric equation to assign the mining costs into the software, as shown in Figure A.I.9.

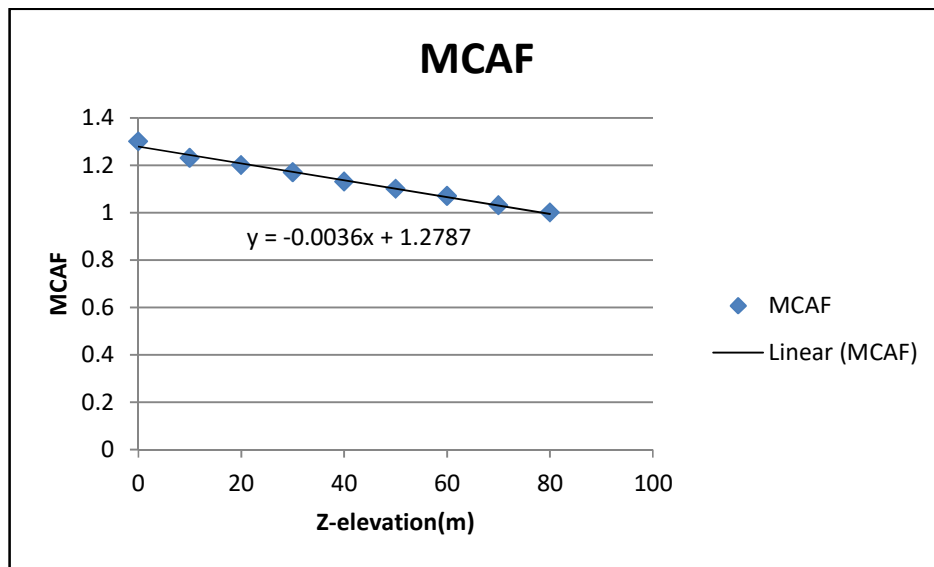


Figure A.0.8 An example of using the line of best fit with the equation

The screenshot shows a software interface for configuring mining cost parameters. It includes the following fields and settings:

- Reference Mining Cost:** 1.5 (unit: tonne)
- Mining Recovery:** 1
- Mining Dilution Fraction:** 1
- Block Mining Cost Adjustment Factors:**
 - Factor:** Equation
 - Equation:** $-0.0036z + 1.2787$

Figure A.0.9 An example of mining cost import using MCAF by a range equation

- Method 3: Using block attribute

Users can use the same methods (range and equation), as described above, but with two attributes available in the block model. Figure A.I.10 illustrates an example to import the mining cost using rock type classification and elevation.

Choose Rocktype					
Rock IDs	Calculation	Factor	Minin...	Mining...	M
1	Range	z	1	1 1,-7.8;1,2.2;1,12.2;1,22.2;1,3	
2	Range	z	1	1 2,-7.8;2,2.2;2,12.2;2,22.2;2,3	
3	Range	z	1	1 2.5,-7.8;2.5,2.2;2.5,12.2;2.5,4	
4	Range	z	1	1 0.5,-7.8;0.5,2.2;0.5,12.2;0.5,4	

Figure A.0.10 An example of mining cost import using rock type and elevation

A.I.2.3 Size reduction

Two size reduction techniques are available in the software: reblocking and clustering. Users can specify the pop-up menu to opt for the methods.

A.I.2.3.1 Reblocking technique

In this menu, users can specify larger block sizes to reduce the number of blocks within the model and decrease the solution time when running the optimization. The block sizes can be set, as shown below, in Figure A.I.11.

3.Size Reduction

Choose Method
Reblocking
Import
Save

Reblocking

User Block Size

x = 50
y = 50
z = 10

New Block Size

x = 100
y = 100
z = 10

New Block Summary

Total No. Blocks
Storage Efficiency %

Figure A.0.11 An example of the definition of block sizes using the reblocking technique

A.I.2.3.2. Block clustering

The menu in Figure A.I.12 allows entering all necessary parameters for the clustering process and viewing the results. Users can use the **Import** button to import the clustering scheme, which is saved from the previous run or the **Save** button to save the current result. Also, the visualization of the clustering scheme can be shown in the **Visualization** menu (Figure A.I.13).

3.Size Reduction

Choose Method: Block Clustering

Block Clustering

Clustering Parameters

Num. shape improvement: 3

Maximum cluster size: 35 Distance factor weight: 1

Grade factor weight: 0.80 Rock type penalty: 0.3

Adjacency Threshold: 50 Clustering attribute: CaO

Beneath Cluster Penalty: 0.8 Minimum cluster size: 5

Clustering results

	Average grade CV (%)	Average rock unity (%)	Cluster size CV (
1	64.1200	80.7850	63.6% ^
2			^
< >			

Figure A.0.12 Block clustering menu

Parameters for the clustering technique can be explained as follows:

- Minimum cluster size is the minimum number of blocks in each cluster. The cluster can be broken into individual blocks in the shape refinement process if its size is smaller than the minimum cluster size.
- Maximum cluster size is the maximum number of blocks in each cluster.
- Distance weight factor is applied to distance measure to calculate the distance similarity between blocks (W_d in Equations 3.27 and 3.28).
- Grade weight factor is the value applied to the primary grade difference to calculate the grade similarity between blocks. It should be noted that if the clustering attribute is not the grade attribute, then this grade weight factor is not be used (W_g in Equation 3.22).
- Rock-type penalty is the penalty value for blocks that are different in the rock-type attribute.
- Adjacency threshold is the limit value to determine the adjacency between blocks to avoid forming fragmented clusters (AD_{ij} in Equation 3.27).
- Clustering attribute is the attribute of blocks that are selected to be used in the clustering process. A pop-up menu allows users to choose the attribute.
- Beneath cluster penalty is the penalty value for the blocks located above the different clusters (B_{ij} in Equation 3.28).

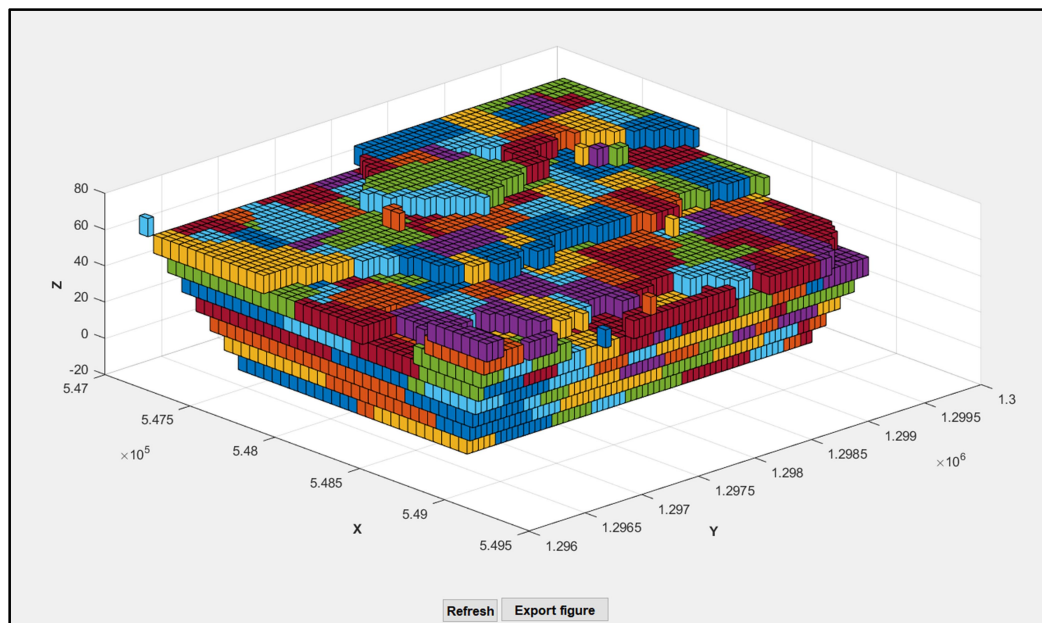


Figure A.0.13 An example of visualization of a clustering scheme

A.I.3. Optimization

A.I.3.1 Destination

4. Destination

Material for Destination

	Type	Name	Constraint	Minimum	Maximum	Rehandling
1	Dump	Waste Dump	Rocktype ▾ 1	1	4	1
2	Process	Cement Plant	Rocktype ▾ 1	3		1

< >

Dump **Stockpile** **Process** **Remove** **Apply**

Targets

Destination Cement Plant ▾ Maximum 12000000

Add **Remove**

	Quality	Minimum	Maximum
1	CaO ▾	58	69
2	SiO2 ▾	14	28
3	Al2O3 ▾	4	10
4	Fe2O3 ▾	0.5	5
5	MgO ▾	0	3

Add User's Equation **Remove**

	Quality	Equation	Minimum	Maximum
1	AM	al2o3/fe2o3	1	3
2	SR	sio2/(al2o3+fe2o3)	1	3
3	LSF	cao/(2.8*sio2+1.18*al2o3+...	0.845	1

< >

Apply

Figure A.0.14 Definition of destinations

A common desire in mine planning is to define the destinations for the extracted materials. Therefore, the software provides a menu where users can specify the destinations for the quarry materials based on the attributes of blocks. Users also can give the name for the defined destination.

In Figure A.I.14, the optimization employs two destinations: a waste dump and a cement plant. The quarry materials are specified to those destinations based on four rock types, as indicated by the ID values when importing the block model (see Figure A.I.4). The quality targets are defined for each destination, including attributes originated from the block models or calculated by the user.

A.I.3.2 Production capacity

The table in Figure A.I.15 is used to set up the production capacity for each destination through the production periods. Users also can specify the production for a specific period in the period columns.

5. Production Capacity

	Location	From Period	To Period	Minimum	Maximum
1	Quarry	1	10	15000000	15000000
2	Cement Plant	1	10	10000000	10000000
3	Waste Dump	1	10	0	15000000

Add Location **Remove** **Apply**

Figure A.0.15 Production capacity set up

A.I.3.3 Additive purchase

This panel is used to define the typical purchase of additive materials in cement production. Users define the allowable amount of additives and their purchase costs before specifying the quality for each additive material. An example of additive purchase input can be seen in Figure A.I.16.

6. Additive

Additive purchase

Name	Min Purchase	Max Purchase	Unit Cost
Clay	0	1000000	4
Laterite	0	1000000	6
Limestone	0	1000000	4
Iron Ore	0	1000000	8

Add **Remove**

Additive's quality

Quality	Clay	Laterite	Limestone	Iron Ore
CaO	5.27	0.72	80	1.69
SiO2	80	5	5	10
Al2O3	2.14	80	2	1.07
Fe2O3	1.5	1.74	0.5	70

Add **Remove**

Apply

Figure A.0.16 An example of additive purchase input

A.I.3.4 Pit slopes

In the pit slope panel, users can specify the slope for regions defined by the blocks' coordinates. In the example below, the slope angle of 20 degrees is fixed for all interested regions.

7. Pit Slopes

	Min X	Max X	Min Y	Max Y	Min Z	Max Z	Slope Angle
1	547110	549110	1296200	1299900	-7.8	62.2	20

Add Remove Apply

Figure A.0.17 Pit slope input

A.I.3.5 Optimization

In this panel, users can define the penalty costs of not meeting the production targets set in previous sections. Notice that if users do not set the penalty costs, the optimization model is similar to the deterministic model. Users have to specify the installed CPLEX solver's location in their computer and choose parameters for it. Notably, the software allows selecting the number of fractions of a mining cut mined through the production periods to make the schedule more practical [77]. Figure A.I.18 presents an example of optimization input.

8. Optimization

Uncertainty Cost

	Factor	Deficient Cost	Excess Cost
1	Quarry P	1	1
2	Cement F	3	3

Add Remove

Running Option

Choose CPLEX solver

Discount Rate (%) 8 Relative Gap 0.00001

Absolute Integer Gap 0.0000001 Solving Time(s) 72000

Num. Fraction of Mining Cut 10

Run CPLEX

Figure A.0.18 Optimization input parameters

A.I.4 Visualization of optimization results

There are two methods to analyze the results of the optimization process. First, the software prints the results into an Excel file in which the results are recorded in various sheets (Figure A.I.19). Secondly, the software visualizes the results using the visualization menu. The visualization consists of two panels: the block model and charts.

	A	B	C	D	E	F	G	H	I	J	K
1	Production										
2		Period	Realization1LOI	Realization2LOI	Realization3LOI	Realization4LOI	Realization5LOI	Realization6LOI	Realization7LOI	Realization8LOI	Realization9LOI
3		1	10011148.28	9985768.174	10000000	10011148.28	9808771.712	9291019.177	9953933.854	9639301.438	9041498.192
4		2	10018034.46	10000000	9619959.636	10018034.46	10000000	10000000	10000000	9703901.09	9702169.618
5		3	10000000	10000000	9731999.878	10000000	9906967.855	10000000	10000000	9628451.354	9881488.976
6		4	10000000	10000000	10000000	10000000	9863883.992	9670956.607	10000000	10000000	9998826.021
7		5	10000000	10123567.23	10000000	10000000	9119221.05	9846555.494	9878527.851	10000000	10000000
8		6	10000000	10221022.14	10000000	10000000	9182017.623	10000000	9536560.933	9930022.974	10000000
9		7	10000000	10336003.81	9617566.514	10000000	9102490.799	10000000	9580228.676	9504687.901	9759748.64
10		8	10000000	10617345.71	9480400.835	10000000	8553646.036	10000000	9469760.48	10000000	10000000
11		9	10000000	10356492.75	9568323.961	10000000	9350690.002	10180343.08	9945862.206	10000000	9852927.407
12		10	10000000	10000000	9218901.104	10000000	8907595.641	9942294.116	9164676.255	9791078.571	10000000
13	Excess_Production										
14		Period	Realization1LOI	Realization2LOI	Realization3LOI	Realization4LOI	Realization5LOI	Realization6LOI	Realization7LOI	Realization8LOI	Realization9LOI
15		1	11148.28012	0	0	11148.28012	0	0	0	0	0
16		2	18034.46202	0	0	18034.46202	0	0	0	0	0
17		3	0	0	0	0	0	0	0	0	0
18		4	0	0	0	0	0	0	0	0	0

Figure A.0.19 Numerical results of optimization results recorded in an Excel file

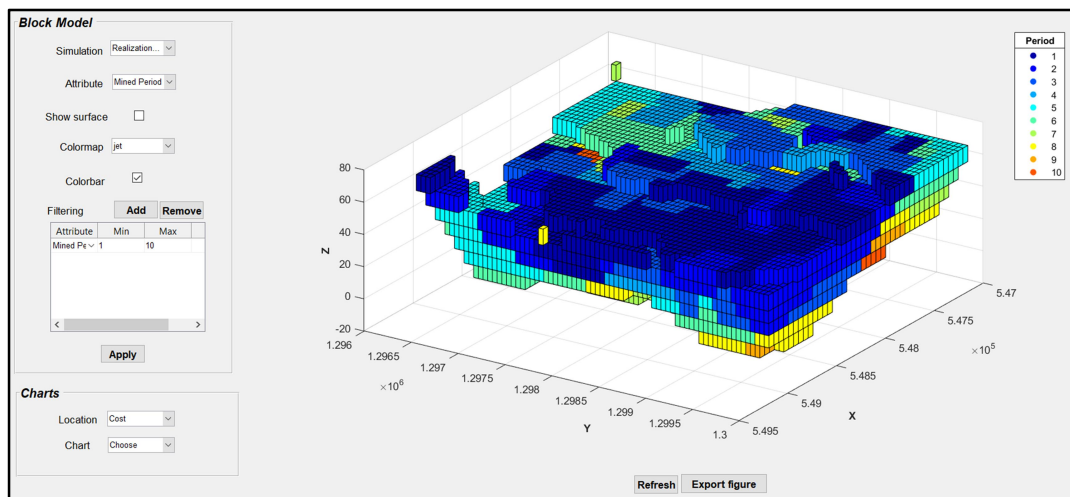


Figure A.0.20 Example of 3D quarry extraction schedule

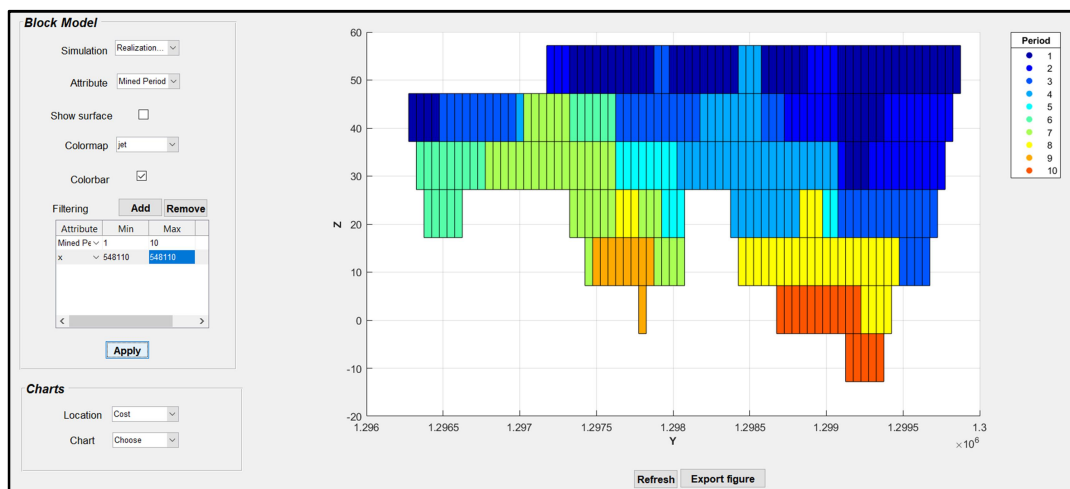


Figure A.0.21 Example of a 3D quarry extraction schedule on a cross-section

In the block model panel, users can animate the quarry extraction schedule in 3D (Figure A.I.20) or sections (Figure A.I.21). Various attributes within the block model can be used to present the resultant schedule. Also, users can view the ultimate topography after finishing all mining periods by using the tick box *Show surface* (Figure A.I.22).

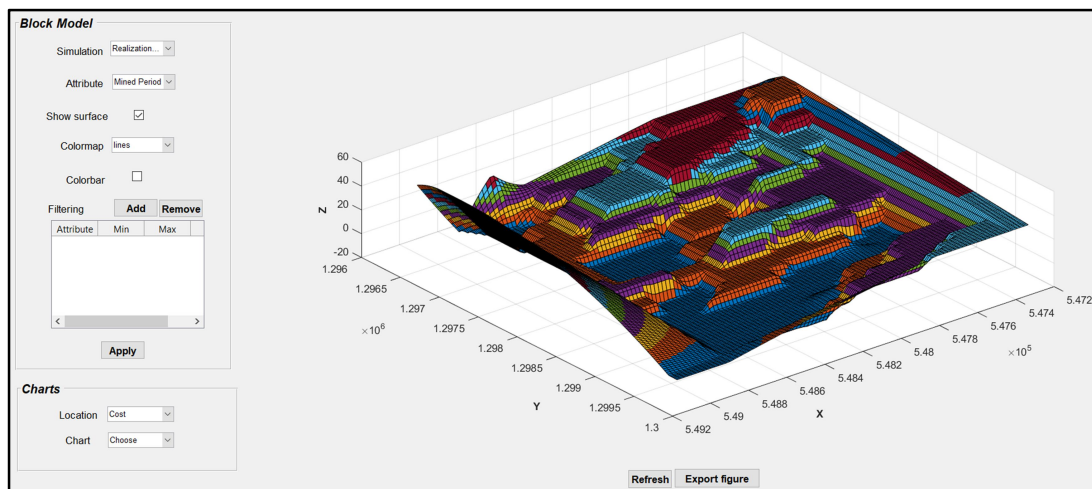


Figure A.0.22 An example of ultimate topography after finishing all mining periods

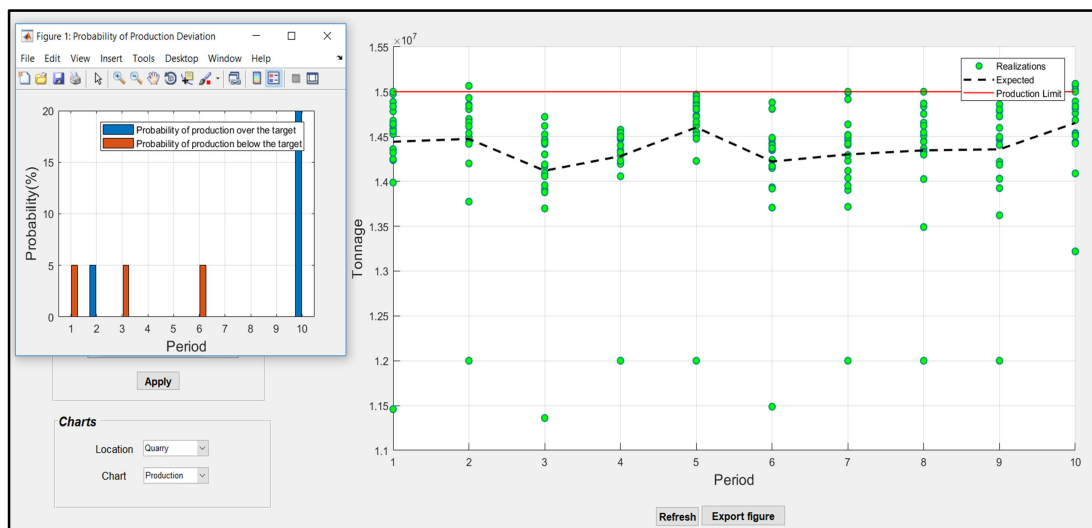


Figure A.0.23 Deviations of the quarry production target along with their probability

The charts panel aims to analyze the results of the resultant schedule at each destination. For instance, Figure A.I.23 presents the deviations of the production target at the quarry. The probability of these deviations in each production period also is calculated in the same visualization.